Proceedings

THE TWELFTH SYMPOSIUM
ON THE
ART OF GLASSBLOWING

1967

THE

AMERICAN SCIENTIFIC GLASSBLOWERS SOCIETY

Proceedings

THE TWELFTH SYMPOSIUM
ON THE
ART OF GLASSBLOWING

Sponsored by

THE AMERICAN SCIENTIFIC
GLASSBLOWERS SOCIETY

DINKLER PLAZA HOTEL
ATLANTA, GEORGIA

JUNE 28, 29, 30, 1967

THE AMERICAN SCIENTIFIC GLASSBLOWERS SOCIETY
309 Georgetown Avenue, Gwinhurst
Wilmington, Delaware 19809

CONTENTS

OFFICERS AND DIRECTORS OF THE AMERICAN SCIENTIFIC GLASSBLOWERS SOCIETY FOR 1966-67

OFFICERS

President—ALFRED H. WALROD
Varian Associates, Palo Alto, California

President Elect—RICHARD W. POOLE
Union Carbide Nuclear Company, Oak Ridge, Tennessee

Secretary—WERNER H. HAAK
Purdue University, Lafayette, Indiana

Treasurer—PAUL W. UTHMAN
Alcoa Research Laboratory, New Kensington, Pennsylvania

President Emeritus—J. ALLEN ALEXANDER
20 Merwood Drive, Upper Darby, Pennsylvania

DIRECTORS-AT-LARGE

J. ALLEN ALEXANDER
AUSTIN MASON
RANDOLPH H. SEARLE
JONATHAN W. SECKMAN
WILLIAM A. WILT

SECTIONAL DIRECTORS

JOHN F. BELZ, JR.
RUFUS T. DIXON
OLIN E. HINES
ROBERT R. STRASBURGER
CHARLES M. LITZ
LOUIS E. GRAY, JR.
TONY A. ZUREK
JOHN BALKWILL
WILLIAM A. GILHOOLEY
JOSEPH WEST
JAMES T. BLASI
KARL H. WALTHER
HENRY L. CHRISTIE

EXECUTIVE SECRETARY

GEORGE A. SITES
American Scientific Glassblowers Society
309 Georgetown Avenue
Wilmington, Delaware 19809
Phone 302 798-4498

TWELFTH SYMPOSIUM COMMITTEE

General Chairman ..... Richard W. Poole
Union Carbide Nuclear Company

Exhibits Chairman ..... Howard L. Epperson
University of Georgia

Technical Papers Chairman ..... Donald E. Lillie
Georgia Institute of Technology

Workshops Chairman ..... Randolph H. Searle
E. I. du Pont de Nemours

Publicity Chairman ..... Edward A. Robinson
Illumination Industries, Inc.

National Technical Papers Screening Chairman ..... Jules E. Benbenek
R.C.A. Laboratories

National Symposium Sites Chairman ..... Karl H. Walther
Brookhaven National Laboratories

MODERATORS

Tony A. Zurek
Chemstrand Research Center, Inc.

Carlton E. Nelson
Auburn University

Austin Mason
U.S.D.A. Southern Regional Labs

Thomas A. Henson
Duke University

Owen J. Kingsbury, Jr.
Vanderbilt University

Elmer W. Mattson
Oglethorpe College

THE PROCESSING OF RZ-2 GLASS

DUANE H. GROWEG
Materials Development Section, Research Department
Consumer and Technical Products Division
Owens-Illinois, Inc.
Toledo, Ohio

ABSTRACT:

Since Owens-Illinois introduced RZ-2 Glass in 1966, several developments have been made in equipment and in technique for processing powder seals. The construction and design of a R.F. induction-heated atmosphere furnace will be discussed. The preparation of powdered RZ-2 Glass seals will be described in detail. Properties will be discussed and uses of RZ-2 Glass in sealing and decorating will be described.

INTRODUCTION

RZ-2 Glass is a copper-aluminosilicate glass which has a coefficient of thermal expansion comparable to that of fused silica; that is, 5 x 10^{-7} in/in/°C over the temperature range from 0 to 300°C. It has a softening point of 1607°F. (875°C.), and an annealing point of 1058°F. (570°C.). Fused silica parts can be sealed using RZ-2 Glass at temperatures much lower than required to make direct fused silica seals; however, special precautions and techniques are required.

THE R.F. ATMOSPHERE FURNACE

In order to retard the formation of higher oxides, an inert atmosphere furnace is required to make RZ-2 Glass powder seals. The furnace must be capable of producing temperatures in the range from 2200°F. to 2400°F. (1204°C. to 1316°C.). A furnace that is powered by a R.F. generator is such a device.

Since most glasses are not subject to direct R.F. induction heating, an alternate technique must be used. This technique uses the load coil of the R.F. generator to set up eddy currents in a carbon susceptor which will heat up to 3000°F. (1649°C.) or higher. The radiation from the susceptor in turn heats the fused silica RZ-2 Glass assembly that is to be sealed.

There are two major design considerations. The first is the power output of the R.F. generator that will power the furnace. Care must be exercised so that the power requirement of the furnace does not exceed the power output of the generator. The ideal situation provides the ability to maintain the furnace at 2400°F. (1316°C.), using only 80 to 85 percent of the power available. This condition will provide faster heating rates of the furnace than will an under powered system. The R.F. generator output will determine the maximum furnace size that can be built.

The second design consideration concerns the physical size of the parts to be sealed in the furnace. They must clear the inside walls of the susceptor. In small furnaces, one-eighth inch on all sides is sufficient clearance; however, larger furnaces require one inch or more on all sides.

Property Data (typical values) for low expansion Copper Glass RZ-2

(Data on Fused Silica is Given For Comparison)

THERMAL PROPERTIES:	RZ-2 GLASS	FUSED SILICA†
Coefficient of Thermal Expansion		
oc x 10^7/°C (0 - 300°C)	5.0	5.5
oc x 10^7/°C (0 - 38°C)	1.5	-
Specific Heat, cal/g/°C	0.182	0.18
Thermal Conductivity, cal/cm/sec/°C	0.003	0.0033
Thermal Diffusivity, cm^2/sec	0.0061	0.0082
Thermal Shock - ΔT to ice water (cane sample)	500°C (932°F)	980°C (1800°F)
Max. Service Temperature - continuous	520°C (968°F)	1000°C (1830°F)
- short term	725°C (1337°F)	1300°C (2370°F)
MECHANICAL PROPERTIES:		
Density, g/cc	2.7*	2.20
Hardness, Knoop (100 g loading)	490	670
Young's Modulus, psi	11.5×10^6	10.5×10^6
Rigidity Modulus, psi	5.0×10^6	4.3×10^6
Bulk Modulus, psi	7.3×10^6	5.3×10^6
Poisson's Ratio	0.2	0.14
OPTICAL PROPERTIES:		
Index of Refraction - N_D	1.563	1.459
ELECTRICAL PROPERTIES:		
Dielectric Constant, 25°C, 100 cps	7.1 (Est.)**	-
25°C, 1mc	6.2	3.85
Dissipation Factor, 25°C, 100 cps	0.045 (Est.)**	<0.0009
25°C, 1mc	0.0125	<0.0009
Volume Resistivity, ohm-cm, 25°C	10^{13}**	10^{18}
250°C	10^7 **	10^{12}
350°C	10^5 **	10^9
WORKING PROPERTIES:		
Softening Point	875°C ± 25°C*	1667°C
Annealing Point	570°C ± 10°C*	1140°C
Strain Point	525°C ± 5°C*	1070°C
Seal Stress to Fused Silica - Annealed	1200 psi	-
CHEMICAL DURABILITY		
ACID TEST - 0.02N H_2SO_4 90°C 4 Hrs., Crushed sample		
% CuO Dissolved (Std. Titration)	0.020	
% CuO Dissolved (Chemical Analysis)	0.017	
WATER TEST - 90°C 4 Hrs., Crushed sample		
% CuO Dissolved (Std. Titration)	0.00025	
% CuO Dissolved (Chemical Analysis)	0.0005	
ALKALI TEST - 90°C 5% NaOH 6 Hrs.		
% CuO Dissolved (Chemical Analysis)	0.24	
Weight Loss - mg/gm	17	

* May vary slightly due to slight differences in oxidation state of copper ions in bulk glass. Function of glass melting conditions.

** Properties controlled by oxidation state of copper ions in glass surface layers. May vary over wide range, depending on thermal/ambient atmosphere history and use conditions.

† Data on fused silica obtained from manufacturers published literature.

The R.F. atmosphere furnace has four major parts: the carbon susceptor, the atmosphere introduction and control system, the R.F. load coil and the framework to contain the furnace as a unit. The parts of the furnace will be discussed in the order given. Exact design parameters cannot be given, since they vary with the R.F. generator used and the size of the sample to be fired. To illustrate the technique and construction principles, a cylindrical tube-type furnace will be considered.

THE CARBON SUSCEPTOR

The R.F. load coil induces eddy currents in the carbon susceptor, causing the susceptor to heat up and become the radiating source of the furnace. Carbon can be heated by induction to temperatures higher than 3000°F. (1649°C.) in an inert atmosphere without appreciable deterioration. A desirable property of carbon is its gettering action for oxygen when heated. This effect aids in maintaining an inert atmosphere.

The grade of carbon used for the susceptor is not critical. The inside diameter and length are determined by the size of the parts to be fired. The part should clear the side walls by one-eighth inch on all sides in a small furnace. In a large furnace, the part clearance should be one inch or more. The susceptor should extend beyond the part length at each end at least 25 percent of the inside diameter. This factor is not critical. The desired result is end heating of the part. The wall weight of the carbon cylinder depends on the size of the furnace. In the small furnace, one-sixteenth inch wall thickness will provide sufficient physical strength, but a large furnace may require one-fourth inch or more. The surface finish should be fairly uniform and smooth.

THE ATMOSPHERE RETAINING CHAMBER AND INTRODUCTION SYSTEM

The furnace shell is constructed from fused silica and transite board. The fused silica selected may be either the clear or translucent type. Fused silica with its exterior surface exposed to air will allow heating the carbon susceptor to temperatures higher than 3000°F. (1649°.), without deformation. A clearance of one-sixteenth inch to one-eighth inch between the inner surface of the fused silica and the exterior surface of the carbon susceptor is necessary to allow the atmosphere gas to circulate between the carbon and fused silica. This clearance also allows for expansion of the carbon during the heat-up cycle. The fused silica tube length is dependent on the size of the furnace. In a small furnace, three-eighths inch added beyond each end of the susceptor is sufficient to prevent destruction of the transite end caps; however, two and one-half inches to four inches may be required in larger furnaces.

The next step after the selection of the fused silica tube is the design and construction of the end caps. Transite board, usually three-fourths inch thick, is used for this purpose. The end caps are machined to be approximately three-fourths inch larger in diameter than the selected tube size. A groove is machined into one surface, one-fourth inch deep, one-eighth inch larger in diameter than the outside of the fused silica tube, and one-eighth inch less in diameter than the inside of the fused silica

tube selected. These dimensions allow adequate room for alignment and expansion when the furnace is heated. The bottom of the groove is then lined with a soft, insulating material, such as asbestos rope or cord. This soft liner will re-form to irregularities in the end of the tube making a semi-gas-tight seal. It is suggested that one end cap be equipped with a fused silica viewing port.

Both end caps are equipped with gas inlet ports. These ports can be made by boring into the transite, making sure the hole clears the bottom of the groove. The outer end of the bore is tapped to accept threaded tubing. From the inside of the end caps, a series of small holes are drilled into the cross bore to spread the gas entering the furnace chamber. The end cap inlets are connected to a single gas feed hose.

In the end cap not used for the viewing port, the thermocouple protection tube is installed near the inside wall of the carbon susceptor. A platinum, platinum-rhodium thermocouple is used to measure the sample temperature. The end of the tubing outside of the furnace is sealed with asbestos papier-mâché made from asbestos paper and water.

THE R.F. LOAD COIL

Copper tubing is used to wind the load coil for the furnace. The tubing diameter should be compatible with the R.F. generator output connections. The coil inside diameter should clear the outside of the silica tube by one-sixteenth inch in the case of a small furnace, and by one to one and one-half inches in large furnaces. In larger furnaces, the heat losses will cause excessive heating of the generator cooling water if the coil is too close.

The coil length is dependent on the type of generator used. In general, the length can be equal to or slightly longer than the susceptor length.

FURNACE FRAME

Since the furnace described may be operated in either a vertical or horizontal position, the general support of the furnace must be designed accordingly. For vertical operation, ceramic supports must be added to the lower end cap to hold the susceptor in the proper area of the coil. When operated horizontally, provisions must be made to hold the end caps in place. The general support, therefore, is left to the builder. The materials used for the support should be electrically insulated, because of the R.F. field present, and be able to withstand the radiated heat.

R.F. ATMOSPHERE FURNACE—SUMMARY

In summary, the furnace described has extremely rapid heat-up rates. A small furnace will heat from room temperature to a sample temperature of 2400°F. (1613°C.) in about sixty seconds; a large one will take three to four minutes. Similarly, the cooling rates are rapid because of designed-in heat losses. A small furnace can cool from 2400°F. (1316°C.) to 500°F. (260°C.) in about two minutes, without damage to the furnace. Larger furnaces take fifteen to thirty minutes to cool.

Temperature control and stability are very good. When the generator power is increased or decreased, corresponding furnace temperature changes are almost instantaneous. Heat-up cycles and temperatures are reproducible.

The tube-type furnace has been discussed; however, a box-type furnace can be constructed by using similar techniques and principles. In some applications, the box-type furnace may be more desirable.

CONDITIONING OF THE R.F. ATMOSPHERE FURNACE FOR SEALING RZ-2 GLASS

Before the furnace can be used for making RZ-2 seals, it must be heated to 2500°F. (1371°C.) for three to four minutes using a nitrogen atmosphere, and then cooled. The heating-cooling cycle is repeated four or five times to burn out the binder and/or oil residue in the carbon susceptor. The bake-out operation tends to force water out of the fused silica shell and the transite end caps. At this point, the furnace is ready to make RZ-2 seals, the preparation of which will be discussed next.

THE TECHNIQUE OF MAKING RZ-2 GLASS POWDER SEALS

The procedures indicated here are applicable to nearly any type or shape of seal. Examples of seal geometries are: tubing to tubing, cane to cane, flat plate to tubing, and plates assembled into square or rectangular cells or tanks. Various combinations of the above are possible. Optical distortion of fused silica plates, such as those used for viewing ports in scientific apparatus, is minimized by using RZ-2 Glass for a seal. RZ-2 Glass is available in can and powder form, in commercial development quantities. Inquiries for other forms, such as solid cast blanks, fibers and capillary tubing, are solicited.

RZ-2 POWDER

In this paper, the discussion will be concerned with the powder form of RZ-2. The glass is ground by the ball mill technique; however, other equally well known techniques may be used, providing the copper glass does not become contaminated.

After the RZ-2 Glass has been ground, it is advisable to select, by standard screening procedures, a particle size that will pass a 40-mesh screen (420 microns), but will not pass through a 325-mesh screen (44 microns). The particle size of the powder is not critical; however, for certain application processes, a more selective sizing may be desirable, such as minus 100 mesh plus 200 mesh size product.

BINDER CONSIDERATIONS

A binder must be mixed with the powdered RZ-2 Glass for handling purposes. Nitrocellulose dissolved in amyl-acetate is a suitable binder for the material. The binder selection is of great importance. A binder burn-out temperature of about 600°F. (316°C.) is desirable. After burn-out, the ash and/or carbon residue content should be very low. For this particular glass, the binder must be neutral chemically. A binder that has

highly oxidizing or reducing characteristics is not usable with RZ-2 copper glass. Distilled water may be used as a binder; however, the green strength of the assembly is poor. Such an assembly cannot be allowed to air dry before firing.

The ratio of powdered RZ-2 Glass to the binder is unimportant. The viscosity of the mixture must be compatible with the application technique. For general hand application, the powder and binder are mixed in a ratio that will result in a moist paste which can be applied to the seal area.

FUSED SILICA PART PREPARATION

The preparation of the fused silica is dependent upon dimensional tolerances and the quality of the end product. Parts to be sealed can be shaped by cutting with a carborundum saw, ultrasonic machining, and/or by grinding techniques. The surfaces that are to be sealed may be ground and polished, if desired, but polishing is not mandatory for making a good seal. The surface quality resulting from grinding with 240 grit and water is satisfactory. A combination of a ground surface and a ground and polished surface can be sealed successfully with RZ-2 Glass. For instance, a fused silica optical window may be sealed between the ground and polished face and a mating ground opening. The quality of the physical match between the surfaces to be sealed will determine the uniformity of the resulting seal. Gross mismating should be discouraged.

Upon completion of the physical cutting and/or shaping procedure, the fused silica parts should be cleaned to remove grinding grit, fingerprints and grease. The cleaning procedure must be such that the fused silica is not etched or damaged or optical properties destroyed. The parts are washed in detergent and tap water, followed by distilled water rinsing. Acetone may be used as a final rinse to dry the parts and complete the cleaning. No surface residue should remain. Handling of the parts after cleaning should be done with white cotton gloves or tongs.

RZ-2 GLASS APPLICATION

After cleaning, the fused silica parts are ready for the application of the copper glass binder mixture. The mixture can be applied to one or both surfaces that are to be sealed. The volume of the mixture will diminish as firing occurs, hence material must be added to compensate for shrinkage. Amounts of RZ-2 and binder to be added for shrinkage are dependent upon the seal area and shape. After application, the glass-binder mixture is air dried until the mixture surface loses its glossy or "wet" appearance. Before the mixture is completely dry, the fused silica parts are mated, making sure that the entire seal area is in contact with the RZ-2 Glass and binder. The mated parts are then allowed to air dry completely. An infrared heat lamp can be used to speed the drying process.

When the assembly is dry (brown tan color), it may be cleaned to remove excess or undesired material. Using a cotton swab and light pressure, the excess sealing glass can be loosened. The loosened material is easily removed from the seal area with the aid of a mild air stream. Any binder residue left is removed by a cotton swab dampened with acetone, with care being taken not to rewet the RZ-2 powder joint. The assemblies are now ready for firing.

SEAL FIRING TEMPERATURE AND TIME REQUIREMENTS

The furnace requirements for sealing powdered RZ-2 Glass should be re-emphasized. These parameters are applicable to a conventional atposphere furnace or to a R.F. powdered furnace as described in this paper.

The copper glass powders are subject to air oxidation at elevated temperatures; therefore, the furnace must be capable of operation with an inert atmosphere. Nitrogen or argon is acceptable, with nitrogen preferred because of lower cost. The furnace must be able to operate at 2200°F. to 2400°F. (1204°C. to 1316°C.).

The assembled parts do not require a preheat cycle; however, in resistance heated furnace operation, it may be desirable to preheat the samples in an area adjacent to the furnace hot zone to prevent shocking the furnace. The preheating and firing *must be done* in an inert atmosphere, being careful that at no time are the seals exposed to air at elevated temperatures. The use of two furnaces with an air transfer between them is prohibited.

The time-temperature cycle is not critical, but is dependent upon the seal size and the furnace. The firing is done at temperatures between 2200°F. and 2400°F. (1204°C. and 1316°C.). The time normally can range from two to ten minutes; but a large assembly may have to soak at 2400°F. (1316°C.) for an extended time.

By the proper selection of the RZ-2 powder particle size, temperature and time, seals can be sintered to be porous or melted into a solid glass.

SEAL HOLDERS

It may be desirable to construct a holder to keep the parts aligned during handling and sealing. The materials used must be able to stand the time, temperature and atmospheric conditions required for sealing. Holders should not be in contact with the sealing glass. It is desirable to exert pressure on the parts during sealing to cause the seal to fillet.

ANNEALING

The sealed articles are annealed at the annealing temperature indicated for the RZ-2 Glass. Annealing is done preferably in a nitrogen atmosphere to prevent oxidation of the exposed RZ-2 sealing glass.

RZ-2 GLASS APPLICATIONS

Powdered RZ-2 Glass can be used to fabricate cells and tanks from fused silica and seal fused silica windows with a minimum amount of window distortion. By using the techniques indicated here, complex fused silica units can be constructed without deformation of the parts. A spectrophotometer cell is one example of this application of RZ-2 Glass. The application of the RZ-2 Glass binder mixture by the silk screen method will allow the seal shape and thickness to be controlled closely. This technique is applicable to cells requiring a very narrow or thin cross section.

RZ-2 powder may also be used for decorating fused silica. By using

silk screen methods, any design or decoration may be applied. Identification marks such as various styles or types of graduated scales can be permanently applied to fused silica.

Preliminary investigations indicate that RZ-2 Glass powder may be sintered into porous or dense parts by using controlled temperature and an inert atmosphere.

Until now, we have been concerned primarily with the powdered form of RZ-2 Glass. The cane form that is available may be utilized by employing conventional lampworking procedures to effect a fused silica seal while minimizing distortion of the fused silica parts. The flameworking method involves beading the area to be sealed with the RZ-2 cane, then mating the parts to complete the seal. The cane may also be reformed and ground to make preforms for special sealing applications. While on the subject of RZ-2 preforms, solid RZ-2 Glass may be cut into thin sections and then cut ultrasonically to a desired configuration. Preforms prepared by these methods are then sealed by the furnace technique. Preforms have been used to make an optical wedge cell and fluid amplifiers which require an intricately shaped passage.

Solid RZ-2 Glass has decorative features. By using special heat treating cycles, the outer polished surface will become reflective and, with modified heat treatment, a very thin copper metal layer can be produced on the surface. Parts or all of the coatings can be removed by chemical methods, thus producing the decorative effect. Thin sections of solid RZ-2 Glass can be used as optical filters or as substrates.

CONCLUSION

Possible applications and techniques for using the new, unique RZ-2 Glass have been discussed in this paper. Inquiries on other possible applications are invited by Owens-Illinois, Inc.

HIGH POWER CARBON DIOXIDE LASERS

L. A. WEAVER
Westinghouse Research Laboratories
Pittsburgh, Pennsylvania 15235

ABSTRACT

Solid state and gaseous laser systems of current interest are described, with special emphasis directed towards recent developments in high power carbon dioxide lasers. The principles of operation are outlined, and promising applications to the cutting and fusing of materials such as metals, plastics and quartz are presented.

INTRODUCTION

During its brief and fast-paced history, the laser has characterized itself as a precocious and fickle child of modern technology. From its conception in 1958 by Schawlow and Townes,[1] breakthroughs have followed rapidly upon one another, each one holding even greater promise of potential usefulness in both military and commercial applications. In a manner which appears to be distinctive of contemporary scientific development, the laser has emerged as a concept and device which rivals the transistor in technological impact and potential widespread utilization. Indeed, it now appears evident that the laser will soon find itself as thoroughly entrenched in our everyday lives as the transistor is today.

The first laser oscillation was observed by Maiman[2] in 1960 in ruby on a pulsed basis, followed in 1961 by the discovery of continuous laser action in a He-Ne gaseous discharge by Javan, Bennett and Herriott.[3] These early developments were succeeded by a flurry of activity in which a large variety of materials were made to "lase" at wavelengths extending from the near ultraviolet to the infrared. Semiconductor[4] and liquid[5] lasers emerged from the laboratory, and the novel applications of a burgeoning laser technology began to fill the scientific literature. However, these early devices were typically of low average power capability. It remained for a second generation of techniques and devices to extend wavelength and power output ranges to the point where the original optimistic promises of the laser could begin to be realized.

Improvements in optical pumping and crystal-growing techniques have resulted in the pulsed operation of solid state materials at gigawatt levels. These devices can also be pumped continuously, yielding cw power outputs approaching several watts. However, it was the noble-gas ion lasers, notably the argon ion laser,[6] which first demonstrated high continuout power levels in the visible part of the spectrum. Currently these devices are capable of providing some tens of watts of cw power. At about the same time lasers utilizing molecular gases began to push the oscillation wavelength into the submillimeter region (676μ in ICN)[7] previously approached using only microwave techniques. Moreover, it was discovered that molecular gas lasers were capable of extremely high continuous power levels; laser action at 10.6μ in carbon dioxide[8] was pushed from the milliwatt level to the kilowatt level in the space of about one year.

At present optically folded discharge tubes 190 feet in length[9] have been constructed which can produce several kilowatts of continuous power output from carbon dioxide mixtures.

The development of lasers has now reached the point where reliable units may be purchased commercially at constantly decreasing prices. As these devices become available to laboratory and industrial users, new applications and techniques become evident. Laser holography[10] and interferometry[11] are examples of very active new fields which have been opened up by the advent of the laser. Even more familiar is the use of inexpensive ($\sim$\$300) He-Ne lasers in laboratories for purpose of optical alignment. Ironically enough, much of this alignment is performed on new laboratory laser systems. Both pulsed Nd^{3+} and continuous CO_2 lasers are finding application in optical range-finding and materials operations such as cutting, drilling and welding.

As lasers become more indispensable as laboratory and industrial tools, the more it is necessary that users understand their limitations and peculiarities. Glassblowers have long been familiar with the construction of various laser systems, for many lasers were actually born within the laboratory glass shop. Both optical pumping lamps and gaseous discharge tubes have drawn upon the skills of the glassblower, and there is no doubt that in such complex designs as the argon ion laser the quality of his workmanship was crucial to successful operation of the laser. Nor does this intimate association with lasers end here, however, for it appears that high power lasers might find use in the cutting and fusing of certain glasses. It is entirely possible that the laser might become a familiar and indispensable tool for these purposes within the glass shop in years to come. In order to describe such a possibility, the general theory of laser action will be reviewed, followed by a description of the more familiar conventional solid state and gaseous laser systems. Emphasis will then be placed upon the high power carbon dioxide laser, including its principles of operation, its performance characteristics, and its effects upon various materials. Several applications to industrial material cutting and welding operations will be outlined.

PRINCIPLES OF LASER OPERATION

The term "laser" is an acronym for the phrase "Light Amplification by Stimulated Emission of Radiation." This means that light is actually generated through an internal amplification process in which "stimulated emission" plays the dominant role. This may be understood by considering the three fundamental mechanisms by which an electron occupying a certain energy level within an atom may change this energy in a simple two-level system. These processes are illustrated in Fig. 1. Of course, in a typical atom there exist many such energy levels, but only two such levels are considered here for simplicity. The first process is that of absorption, in which light of a frequency v corresponding exactly to the energy difference E of the levels.....

$$E = hv$$

is incident upon the system. Here h is Planck's constant. Atoms residing in the lower energy level will resonantly absorb this energy and use it to jump into the upper level, thereby increasing the atom's energy at the

Figure 1
Interactions of radiation with matter.

expense of the incident light photons. This is analogous to the resonant "singing" of a taut guitar string as it absorbs acoustic energy from incident sound waves corresponding to the string's resonant frequency. In an actual material this absorption constitutes a decrease in light intensity as the light propagates through the material. Once the atom is in the excited state, however, it does not remain there long. In the absence of any light energy at all, it is capable of jumping down to the lower energy level, converting its energy E to a photon of light at frequency $v = E/h$ which propagates away from the atom in various directions. This is like stating that a wobbly domino stood on edge will fall over of its own accord in some certain average time, giving up its energy to a sound wave which emanates from the scene of the crash. Such a process in an atom is called spontaneous emission, since a photon of light is emitted without any external provocation. The average time required for spontaneous emission to occur is extremely short, however: on the order of 10^{-9} seconds in most gases. But just as the domino can be tumbled over prematurely by an adroit flick of the wrist, so can an excited atom be induced to give up its stored energy when it is set upon by a photon of light having exactly the proper frequency $v = E/h$. In this process, designated as stimulated emission, the photon released during the jump to the lower state has precisely the same frequency, phase and direction of propagation as the

original light wave. Thus, the light is actually increased in intensity due to the atom's contribution.

In ordinary matter, each of these three processes occurs with great frequency as light passes through the material. Typically many more atoms reside in the lower-lying energy levels, so that absorption occurs more frequently than stimulated emission. Thus under ordinary circumstances light propagating through matter suffers a net absorption rather than an amplification. Moreover, spontaneous re-emission of excitation energy tends to randomize the direction of propagation of re-emitted

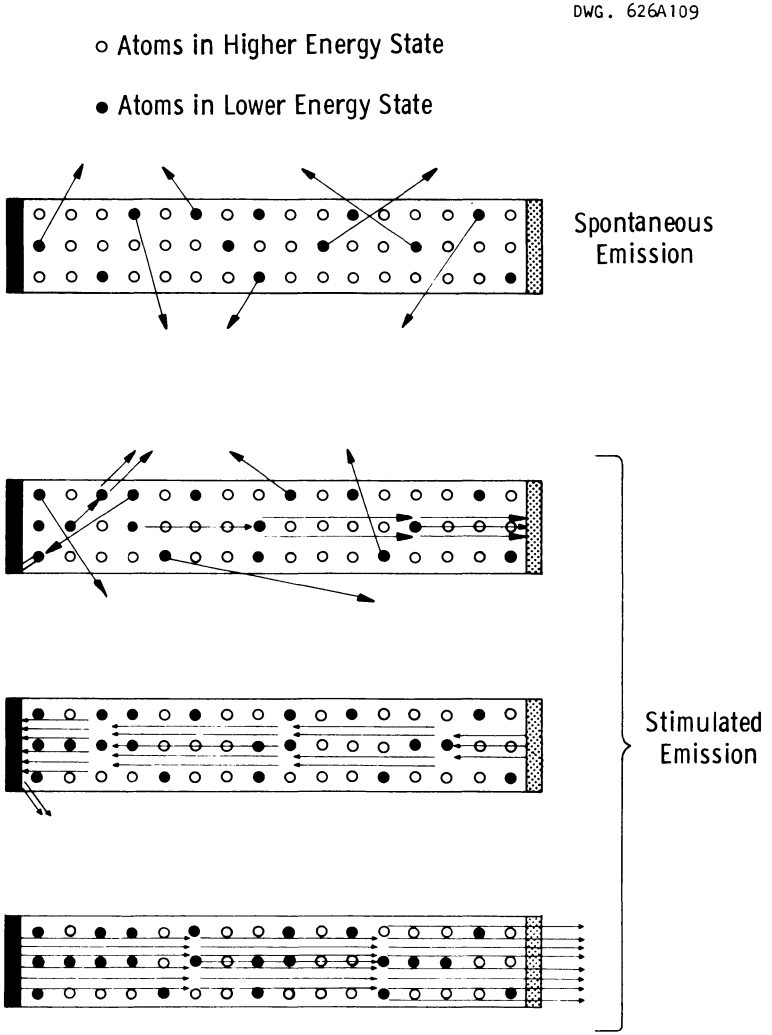

Figure 2
Amplification of light wave by stimulated emission.

light, further tending to decrease light intensity in a specific direction. However, in laser materials the opposite situation applies. By various means of pumping, a so-called population inversion is created in which more atoms reside in the upper energy level than in the lower. Thus light of the proper frequency will experience more stimulated emission than absorption during passage through the laser material, resulting in an increased light intensity, as shown in Fig. 2. Just as a line of dominos stood on end will all tumble over in succession if the first one is nudged, so do the excited atoms in a laser on the average contribute to a net amplification of the light in the direction of propagation.

If mirrors are placed at each end of the material perpendicular to the direction of this amplification, the process will be repeated many times over as the constantly increasing light bundle reflects back and forth through the laser medium. Eventually a steady-state level is reached where the light intensity remains constant, and a small percentage allowed to leak out of one of the mirrors constitutes the actual laser light output.

The light which is produced by a laser is quite different from the light emanating from ordinary sources such as an incandescent lamp. Because of the nature of the stimulated emission process, the radiation is monochromatic at a frequency $v = E/h$ determined by the atomic transition within the active medium. Furthermore, each atom is stimulated to emit its radiation with a very definite phase relationship to the incident radiation, with the result that the light emission is coherent. Coupled with the inherent directivity of the process, the resultant laser light is a tightly bundled, monochromatic beam capable of remaining intact during propagation over large distances.

There are several methods of guaranteeing a population inversion in an active medium; optical pumping and gas discharge collisional pumping are among the most prominent of these. In an optically pumped system, as illustrated in Fig. 3, intense incoherent light from a flash tube is

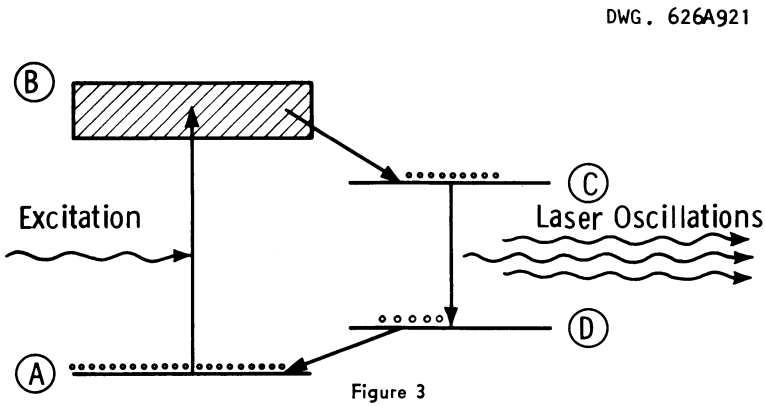

Figure 3
Laser oscillations in a fluorescent system.

focussed upon the active laser medium, and through an absorption process excites the material from the ground state A to a high energy band B.

Figure 4
High energy coaxial flash lamp.

Subsequent relaxation to the upper laser level C occurs quite rapidly, and the actual laser oscillations occur during the stimulated transition from C to D. The lower level is depopulated through spontaneous emission or lattice vibrations to the ground state to complete the laser cycle. It is this

Figure 5
Nd^{3+}-doped laser rods of barium crown silicate glass.

type of optical excitation scheme which is used in the familiar ruby laser, where bluish incoherent pump light is re-radiated as an intense red laser output at 6943Å. Similarly, Nd^{3+} ions are optically pumped in solid hosts such as YAG (yttrium aluminum garnet) and glass to lase at 1.06μ Fig. 4 shows a unique coaxial optical pumping geometry in which a high energy pulsed xenon discharge surrounds an axially located Nd^{3+}-doped glass rod, several of which are shown in Fig. 5. It is seen that carefully formed glass constitutes an integral part of both the pump lamp and the active laser medium.

A second pumping method used to create inverted populations is that of collisional excitation within gaseous discharges. In this case, shrewd advantage is taken for Mother's Nature's natural preference towards certain electronic excitation and collisional transfer processes. This will be illustrated in complete detail during discussion of the high power carbon dioxide laser. The familiar He-Ne laser depends upon a selective near-resonant energy transfer from long-lived helium metastable states into certain neon energy levels during an atomic collision. This transfer is quite efficient and selective, and insures the population inversion which gives rise to the continuous red 6328Å laser radiation from neon. In the argon ion laser, the process is somewhat more complex, depending upon certain electronic excitation preferences in both the neutral argon atom and in the ion. For this purpose very large current densities are required, which places a severe strain upon the properties of the glass discharge tube enclosure. Fig. 6 illustrates an argon ion laser tube constructed of quartz

Figure 6
DC excited argon ion laser tube, showing water jacket and cataphoresis loop.

which typically conducts dc currents of hundreds of amperes. The discharge portion is enclosed by a water-cooling jacket, and an internal coiled gas feedback loop serves to recirculate gaseous constituents which have been drawn preferentially to one of the electrodes. This design represents one of the more complex and sophisticated tubes which the glassblower has been called upon to fabricate.

THE CARBON DIOXIDE LASER

Of all the developments in the field of laser technology since the

initial discoveries, perhaps none has excited the imagination more than the introduction of the high power carbon dioxide laser.[8] Even during its earliest days, the 10.6μ laser oscillation in CO_2 attracted the attention of many investigators because of its promise of high power output and efficiency. With increasing developmental work, it was demonstrated that the addition of nitrogen gas to the carbon dioxide greatly enhanced the laser performance,[12] permitting continuous power outputs and efficiencies previously unheard of. Excitement was further heightened at the discovery that the addition of helium produced a threefold improvement in the CO_2 performance.[13] In a very short time cw power levels in excess of 100 watts were reported, at tube efficiencies of around 15%. In a rapid succession of efforts in which parameters were optimized and larger units constructed, these figures were soon pushed up to 500 and 1000 watts cw at 17% efficiency. The most recent reports indicate that power levels in excess of 2300 watts at 25% have been obtained in a flowing $CO_2 : N_2 : He$ mixture at 10.6μ, utilizing an optically folded discharge tube 190 feet in length.[9]. There appears to be every indication at present that even greater power levels are within reach.

Type of Gas Laser	Continuous Power Output	Tube Efficiency	Wavelength
CO_2:N_2:He	2300 w	25%	10.6 μ
Ar II Ion	10 w	~0.2%	4880 Å
He-Ne	100 mw	~0.1%	6328 Å

Figure 7
Comparion of gas laser performance.

Figure 7 compares some of the other cw laser systems currently in use to the CO_2 laser. It is seen that the CO_2 laser far outstrips all competitors in both efficiency and continuous power capability. Furthermore, 10.6μ is a wavelength at which the atmosphere is quite transparent. There does exist a limitation in detector capability at this wavelength, however, compared to the visible. For purposes of material cutting and welding this is no restriction.

Why is the CO_2 laser so efficient and powerful compared to other types of lasers? The reason lies in the nature of the CO_2 energy level structure, and a fortuitous combination of physical properties. Molecular gases such as CO_2 differ from monatomic gases like Ne and Ar in that the constituent atoms are free to vibrate in various modes with respect to one another. Figure 8 illustrates the three independent modes of vibration for a CO_2 molecule in which energy can be stored. In addition, the molecule is free to rotate en masse, which constitutes still another way in which the molecular gas can store energy. In the CO_2 laser, it is primarily the vibrational storage mechanisms which are of interest, since the 10.6μ

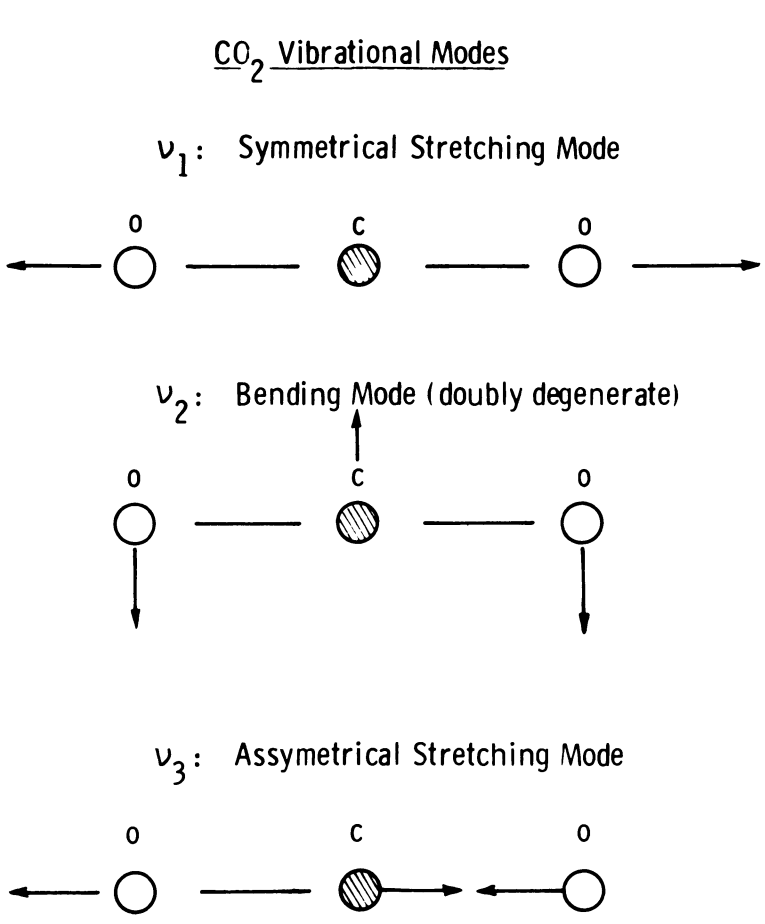

Figure 8
Vibration modes within a carbon dioxide molecule.

laser oscillation corresponds to the difference in energy between the asymmetrical and the symmetrical stretching modes of vibration. Figure 9 illustrates these vibrational energy levels in CO_2, along with a similar level in nitrogen. In the $CO_2 : N_2 : He$ laser, electrons in the discharge collide with ground state N_2 molecules and excite them to higher lying vibrational levels. The lowest level, which has a very long lifetime, lies in almost perfect energy coincidence with the 00°1 vibrational level in CO_2. Thus through collisions with excited N_2 molecules, the ground state CO_2 molecules receive resonant transfer of this energy, which preferentially populates the 00°1 level in CO_2. This devious method of excitation, although complex, turns out to be remarkably efficient, and very large excesses of 00°1 molecules accumulate as compared to CO_2 molecules in the 10°0 vibrational mode. Furthermore, the various vibrational lifetimes happen to be in the proper ratio, a situation which is greatly improved by

the addition of He. Thus conditions are established in CO_2 which create a population inversion due to a selective collisional transfer process from N_2 and a net stimulated emission occurs at 10.6μ as the CO_2 molecule alters its vibrational mode, thereafter decaying spontaneously to the ground state to complete the laser cycle. But what distinguishes the CO_2 laser from noble gas lasers is that besides having a remarkably effective population inversion mechanism, very little of the energy supplied to the upper 00°1 laser level is wasted during the laser cycle. Some 41% of this energy is converted into the light photon at 10.6μ during stimulated emission, since all of the levels lie so very close to the ground state. In monatomic gases, however, which cannot vibrate, about 100 times as much

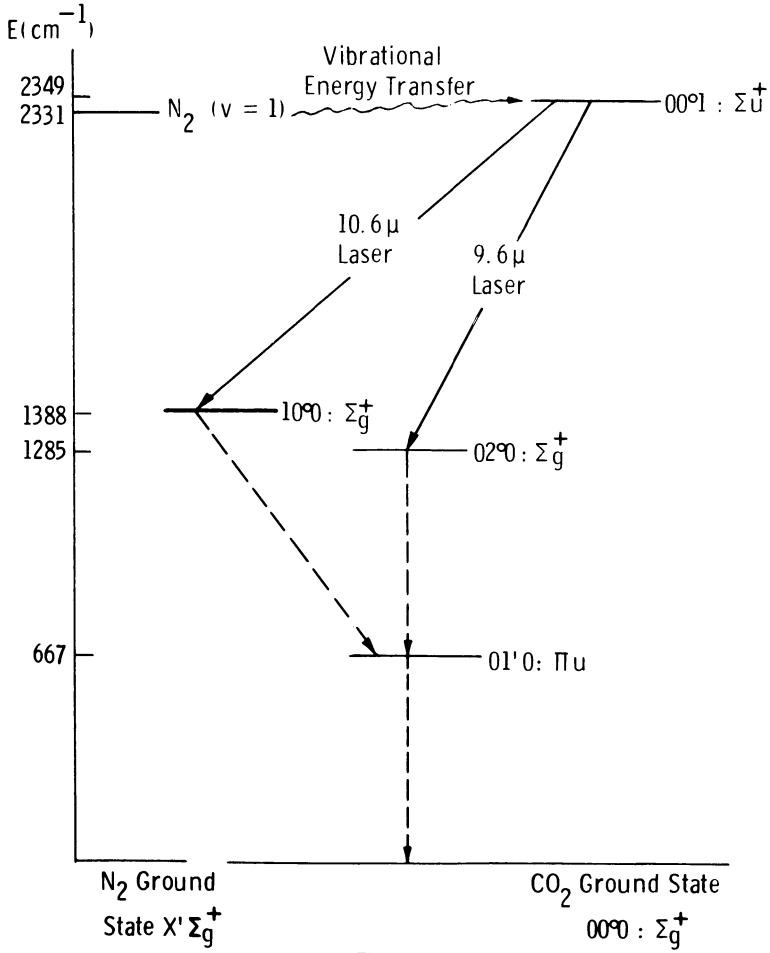

Figure 9
Energy level diagram of the carbon dioxide and nitrogen molecules.

energy must be expended to reach even the lowest electronic energy level. Of this energy, typically less than 10% is extracted in the form of laser light output, the remainder being wasted. Moreover, in gaseous discharges the excitation of high lying electronic levels in gases can be accomplished by only a very small proportion of the electrons in the discharge. Thus the CO_2 laser, with N_2 and He additives, utilizes much more of the energy expended to create the discharge, and wastes much less in releasing the laser radiation. This accounts for the remarkable efficiency of the CO_2 laser system, and other molecular gas laser systems as well.

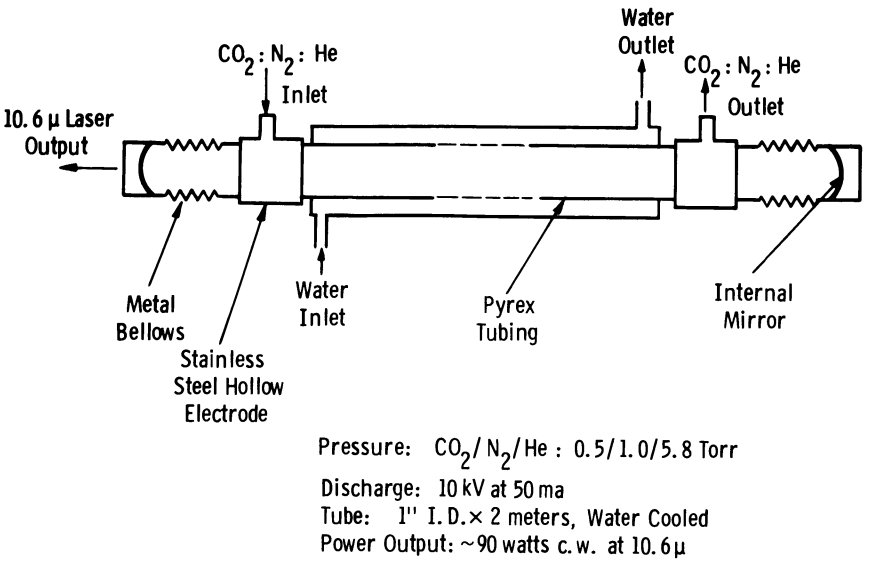

Figure 10
Schematic diagram of a flowing gas $CO_2 : N_2 : He$ laser.

Figure 10 is a schematic representation of a typical gas-flow CO_2 laser. The mixed gases are pumped continuously through the water-cooled discharge tube so that contaminants caused by chemical decomposition of the molecular gases cannot interfere with the laser action. A dc discharge is maintained between the hollow electrodes, and adjustable mirrors on either end of the tube are peaked for maximum laser power output. Typically the laser energy is extracted through a partially transmitting dielectric mirror, or through a hole placed in the center of one of the mirrors. Figure 11 shows a laboratory model of such a laser, utilizing a 1-in. diameter, 6-foot length of standard pyrex pipe with a 2-in. diameter water jacket surrounding it. This unit, using gold-coated internal mirrors, is capable of about 90 watts continuous power at 10.6μ, with tube efficiencies of $\sim$12%.

Recent work with such units has attempted to condense their length by folding the optical path and zig-zagging the beam back and forth several times through the discharge. For this purpose, a 90° reflector has been

Figure 11
Laboratory model of the CO_2 : N_2 : He power gas laser.

Figure 12
Right-angle optical fold using a ball and socket joint.

designed which incorporates a reflective mirror mounted upon a modified ball and socket joint, as shown in Fig. 12. A teflon-seated pyrex ball joint is used, and the mechanical adjustments are made with a three-point spring-loaded screw drive.

APPLICATIONS

Perhaps the most interesting aspect of recent laser development is the variety of novel uses to which its output beam can be turned. In many cases laser radiation can perform remote cutting and welding operations which are impractical or impossible using conventional techniques. For example, the welding of a damaged electron gun support through the glass envelope, shown in Fig. 13, utilizes the unique absorption properties

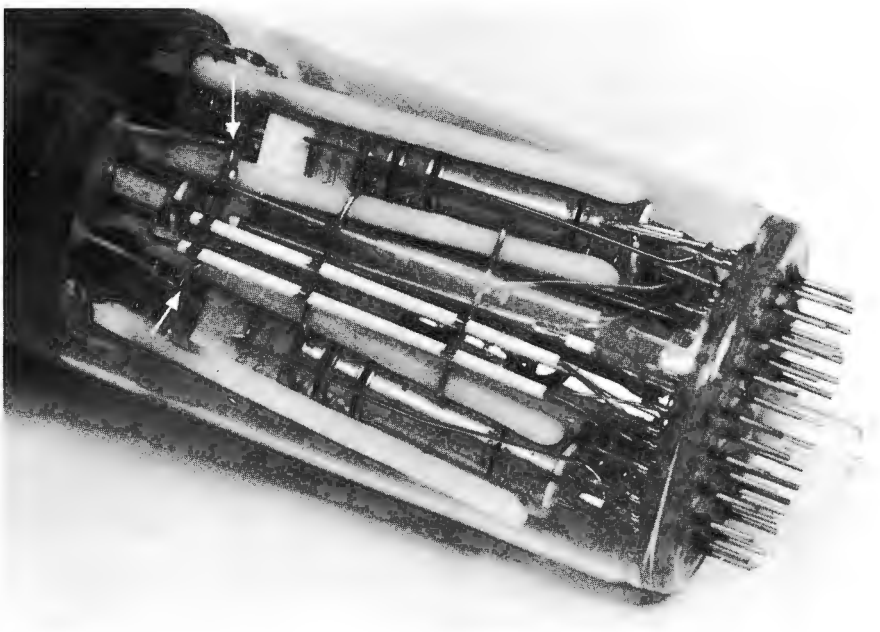

Figure 13
Welding of an electron gun support through the glass envelope.

of a focussed 6943Å pulsed ruby laser. Microcircuitry can be welded, and very small holes drilled using such techniques. The CO_2 laser, operating continuously at about 80 watts, is very effective in cutting organic materials which are strongly absorbent at 10.6μ. This includes most wood, rubber, plastic and fibrous material. Most metals, on the other hand, are highly reflective at 10.6μ, and little of the incident energy is absorbed. Thus the CO_2 radiation is very effective in cutting materials such as

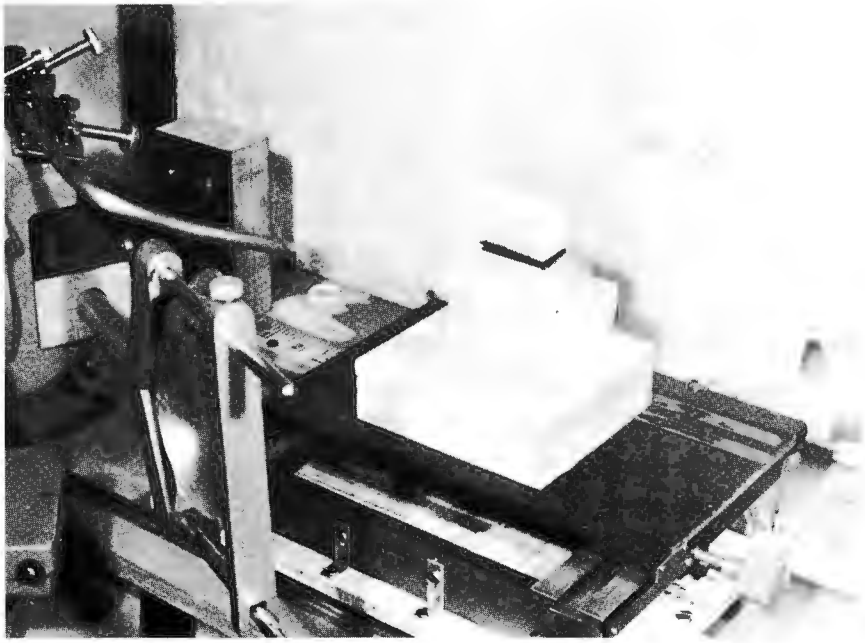

Figure 14
A ¾" thickness of wood being cut by the focussed output of a CO_2 laser.

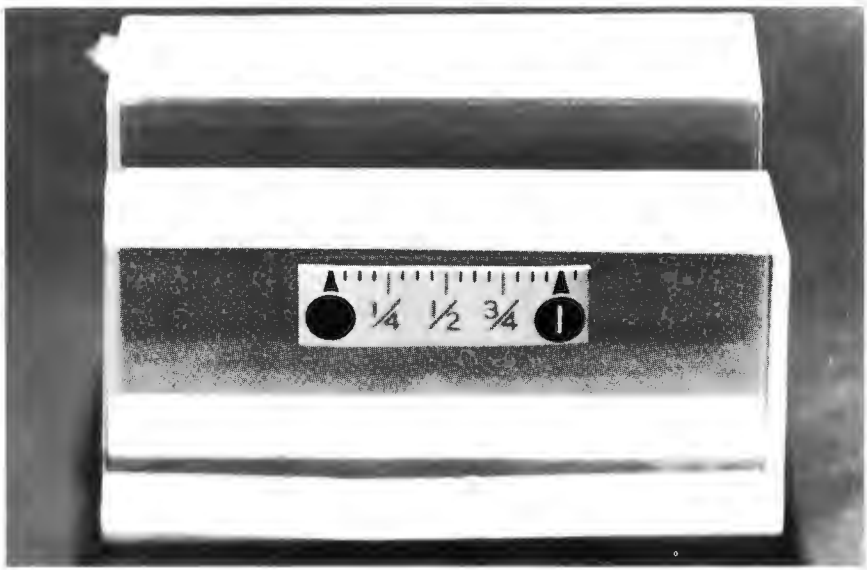

Figure 15
A ¾" thickness of lucite cut with the focussed output of a CO_2 laser.

wood, shown in Fig. 14. This is a ¾-in thickness of white pine cut at a rate of 7.5 inches per minute. Figure 15 shows a ¾-in. piece of lucite cut at a rate of 4.3 inches per minute. Since the laser beam is focussed onto only a small portion of the workpiece, the heating is quite localized and rapid, resulting in a smooth cut with little evidence of bead formation. Samples of rubber, cardboard and paper have also been cut using the CO_2 laser.

Figure 16
The CO_2 laser output beam focussed upon a 1 mm. wall sample of quartz tubing.

Glass and quartz have been cut using a CO_2 laser at power levels of ~70 watts. The focussed laser beam causes quartz samples to glow a dazzling white, due to the intense local heating, with material being vaporized and sputtered away. Because of its poor thermal conductivity, large thermal gradients exist in the quartz; nonetheless, quartz can be cut successfully without shattering. Figure 16 illustrates a 18-mm. i.d., 1-mm. wall quartz tube being rotated through the focussed output of a 70 watt CO_2 laser. The quartz tube is being rotated at 1½ rpm, with one complete revolution (*i.e.*: 40 seconds) being required to cut the tubing in two. The resulting cut, shown in Fig. 17, is very smooth and shows little evidence of a lip formation. Slower cuts produce even smoother surfaces. A 1-mm. thickness of glass plate is shown in Fig. 18 being cut at a rate of 30 in. per minute; the glasses tested so far have tended to shatter, however, due to thermal gradients.

Figure 17
← A 1 mm. wall quartz tube cut by the focussed output of a CO_2 laser.

Figure 18
The focussed output of a CO_2 laser cutting a 1 mm. thickness of glass.
↓

CONCLUSIONS

The state of the art in laser technology today is such that reliable commercial units are now finding military and industrial uses particularly suited to the unique properties of high power laser devices. Increasing numbers of applications are being uncovered as power levels, pulse lengths and component reliability are steadily improved. With the expanding use of laser systems, more human operators are coming into contact with them, desiring to know their capabilities, limitations and method of operation. Since for many applications laser beams can be dangerous to eyes and skin, education and understanding are prime requisites for safe and intelligent application. And as lasers continue to find new and exciting uses, it is only natural that workers in all branches of technology should seek to understand their operation and ask how these devices might possibly be applied to the solution of pressing problems in their own area.

This paper has attempted to fulfill these needs by outlining the gross features of several laser systems, introducing the fundamentals of laser generation, and concentrating specifically upon the most recent developments and potential applications in high power carbon dioxide lasers. Certain experiments, such as the cutting of quartz and glass, show sufficient promise that further investigation is warranted. Further experimentation with other types of glasses are also under way. For the glassblower, the possibility exists that the CO_2 laser might prove to be superior to conventional methods in the cutting, fusing and working of certain glasses. It seems entirely possible that the CO_2 laser might one day find itself an indispensable addition to the glassblower's bag of tricks. The pace of laser development still continues at a rapid rate, and as these devices emerge from the laboratory, it appears likely that an entirely new technological capability will evolve.

REFERENCES

1. A. L. Schawlow and C. H. Townes, *Phys. Rev.* **112**, 1940 (1958).
2. T. H. Maiman, *Nature* **187**, 493 (1960).
3. A. Javan, W. R. Bennett, Jr., and D. R. Herriott, *Phys. Rev. Letters* **6**, 106 (1961).
4. R. N. Hall, G. E. Fenner, J. D. Kingsley, T. J. Soltys, and R. O. Carlson, *Phys. Rev. Letters* **9**, 366 (1962).
5. A. Lempicki and H. Samelson, *Phys. Letters* **4**, 133 (1963).
6. E. I. Gordon, E. F. Labuda, and W. B. Bridges, *Appl. Phys. Letters* **4**, 178 (1964).
7. H. Steffen, P. Schwaller, J.-F. Moser and F. K. Kneubühl, *Phys. Letters* **23**, 313 (1966).
8. C. K. N. Patel, *Phys. Rev. Letters* **12**, 588 (1964).
9. J. J. Ehrlich, G. J. Hutcheson, W. L. Hales and T. G. Roberts, paper presented at the 1967 IEEE Conference on Laser Engineering and Applications, Washington, D. C., June 6-8, 1967.
10. E. N. Leith and J. Upatnieks, *J. Opt. Soc. Am.* **52**, 1123 (1962).
11. D. E. T. F. Ashby and D. F. Jephcott, *Appl. Phys. Letters* **3**, 13 (1963).
12. C. K. N. Patel, *Phys. Rev. Letters* **13**, 617 (1964).
13. G. Moeller and J. D. Rigden, *Appl. Phys. Letters* **7**, 274 (1965).

SEALING OF GASES UNDER POSITIVE PRESSURE

EDWARD C. BROSIOUS
Yale University, Physics Department
New Haven, Connecticut

In one of the experiments performed by a Ph.D. candidate at Yale it was necessary to attain an accurately measured positive pressure and to close it with a non-magnetic and non-contaminating seal.

The gas used was argon of high purity stored in one-litre flasks. The evacuation was performed by a three-stage mercury-diffusion pump. A suitable oven was provided for subsequent bake outs. Special 5-mm. diameter capsules were prepared with a fragile break seal and filled with refined rubidium metal.

After evacuating and baking two one-litre flasks which were to be used as optical pumping cells, we carefully broke the capsule closures. Our next steps were the maneuvering of the broken capsules through the seal-off constructions and the removing of the flasks from the vacuum system.

The cells were immersed in a water bath which provided a constant measurable temperature and were reattached to the vacuum system.

GENERAL ELECTRIC CODES: G-1, G-3, G-4 AND QUARTZ
CORNING CODES: 7052, 3320, 7740

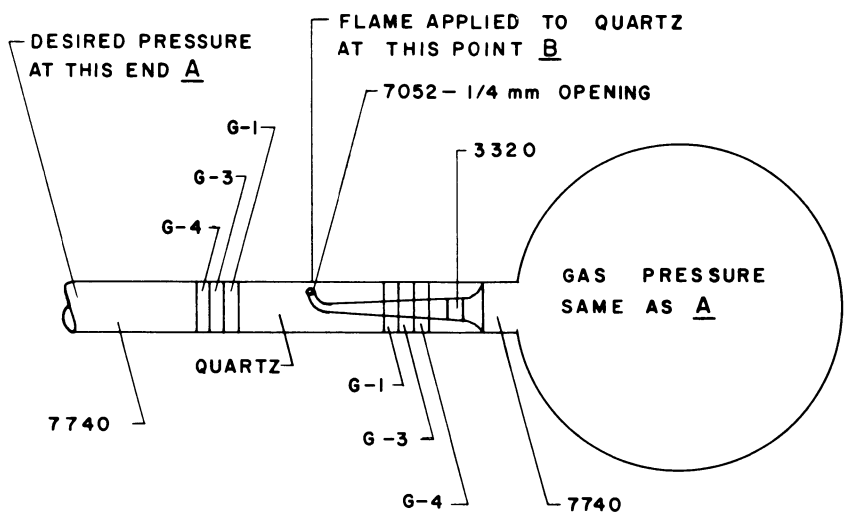

Figure 1

The tubulation connecting the flasks with the gas-filling manifold required a unique positive pressure seal which I devised to solve the problem of sealing a gas under positive pressure. This is a seal which can be sealed off inside the system when the pressure attained has been equalized on both sides of the seal. A description of the construction of the seal will follow later.

The next problem was to get the argon at a positive pressure and this was accomplished by a series of standard procedures. Four one-litre argon flasks were attached to a manifold containing barium gettering wire. After pumping and baking this manifold, it was sealed off. The getter was fired by an induction heater and the argon bottles were opened by use of enclosed glass slugs against the break seals. Next the manifold was incorporated in a common system with the optical pumping cells isolated only by a break seal.

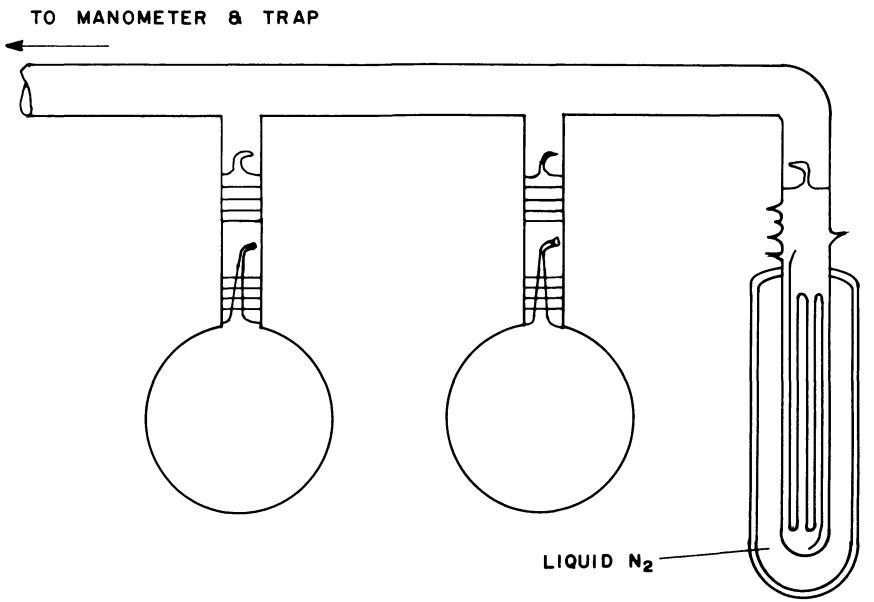

Figure 2

Subsequent evacuation techniques prepared the manifold to receive the argon gas. It is to be noted that the mercury manometer trap was cooled by dry-ice and acetone during this phase, avoiding the liquefying of the argon when it was introduced into the system.

The argon gas was concentrated by cooling the gettering appendage in liquid nitrogen thus as the gas was removed from the flasks they were sealed and removed.

Next we isolated the vacuum manifold at a prepared construction and broke the seal separating the argon manifold from the rest of the

system. The cells were then included in the common manifold also by breaking seals provided for this function.

The liquid argon was permitted to expand and return to a gas by removing the liquid nitrogen flask and the pressure increased as was previously calculated. The manometer was read with the telescope on the cathometer. After equilibrium was reached the positive pressure seals which I had devised were employed.The following is a description of the fabrication of these seals.

The construction starts with a piece of 12-mm. diameter pyrex glass tubing which is connected to a one-inch length of quartz tubing by means of General Electric's sealing glass, G_4, G_3 and G_1. On the end of the quartz the grading is reversed and the tubulation returns to pyrex. Then a trumpet-shaped piece of glass is formed, starting with pyrex of 12-mm. diameter, tapering down with 3320 glass and converging with an end piece of 7052 glass with an opening at its tip of $\frac{1}{4}$ mm. which has an angle bend.

When this trumpet-shaped piece of glass is inserted in the original pyrex tubulation it is positioned so that the wide-mouthed part is joined to the 7740 inside diameter of the outside glass tube. The other end of the trumpet-shaped piece with its angle bend comes very close to the inside wall of the quartz tubing. At this point a bushy gas-oxygen flame is applied to the quartz which when heated radiates enough heat to effect a closing of the 7052 tube inside at its $\frac{1}{4}$-mm. opening without affecting the rigidity of the outside tubing. Since the softening temperature of 7052 glass is 710°C. and the quartz is 1580°C. an adequate margin is afforded the glassblower when completing the seal.

As a result of the controls exercised on temperature and the internal pressure, we achieved a cell with a known amount of atoms per cubic centimeter of gas enclosed.

I would like to conclude with these comments. The pressure involved here was 20 p.s.i. We have tested the seal for 40 p.s.i. but we haven't really explored the limits. Theoretically higher pressures should not affect a differential preventing sealing. Thus the bursting pressure of the glass should be the only limiting factor.

This positive pressure seal has also been used under vacuum. It has been reopened when pressure inside the sphere was greater than that outside, by merely heating the spot opposite the 7052 closure. Thus is could be considered for use as an all-glass, non-metallic and contamination-free bakeable valve.

Some of our cells used in optical pumping ranged in size from a few cubic centimeters (about as big as a pea) to 72 litres (about twice the diameter of a volleyball).

I would like to thank Dr. Earl Ensberg and Phil Crane for their assistance in the preparation and review of this paper.

REFERENCES

Corning Glass
General Electric Company

OUTGASSING FROM GLASS BY BOMBARDMENT WITH ELECTRONS

P. H. DAWSON
General Electric Research and Development Center
Schenectady, New York

INTRODUCTION

The widespread use of glass as an envelope in electronic devices has required knowledge of any effect that the glass itself might have on the device. In cases where bombardment of the glass by electrons can occur, release of gas may shorten the life of an electron tube, or even a lamp, because of deterioration of the vacuum, or contamination of the gases present. Certain gases, and particularly oxygen, which, as we will see, is the most usual product of glass bombardment, may have very harmful effects on any sensitive components (such as hot cathodes) which are in the device.

For these reasons J. L. Lineweaver[1] and his colleagues at Corning Glass Works and we at General Electric Research and Development Center[2] have been interested in making controlled studies in the laboratory to measure the nature and amount of outgassing for various glasses. The studies complement each other since Lineweaver looked at energies of 10-30 thousand volts and we were interested in the 100-1000 volt energy range. The differences in energy led us to use slightly different methods but common to both was the use of a mass spectrometer to identify the gases released and to measure the amount. Oxygen was, in fact, the only gas detected.

High energy electrons penetrate long distances into the glass and Lineweaver found that when the electron beam was turned off, oxygen evolution continued for some time due to the gas slowly diffusing out from below the surface, so he measured the total amount of gas evolved owing to a particular time of bombardment, including that released after the bombardment ceased. Low energy electrons do not penetrate so deeply and in their case, the oxygen seemed to be released into the vacuum system very quickly and the rate of release could be measured directly and its variation with time examined.

HIGH ENERGY BOMBARDMENT

Unless special precautions are taken, when an insulator such as glass is bombarded by electrons its surface will charge up and after a while any more electrons will tend to be repelled and the bombardment will decrease. Lineweaver avoided this problem by coating the glass with a thin film of aluminum and using this to control the surface potential. The high energy electrons can pass through the aluminum without losing much energy. He used a 150μA electron beam and a 3″ x ¾″ raster in a cathode-ray type of sample tube.

For most of the glasses, the data can be expressed by

$$Q = Q_\infty(1 - e^{-t/K})$$

where: t is the bombardment time in hours, Q is the total amount of gas released from t hours of bombardment, Q_∞ is the total amount of gas that

it is possible to release with a very long bombardment. K is a characteristic of the glass which measures how quickly the oxygen can be released.

Table I lists some of Lineweaver's values for Q_∞ and K for various glasses bombarded with 20,000 volt electrons.

TABLE I

Corning Glass Code No.	Q_∞ *(micron-liters/cm.²)*	K *(hours)*
0081	17	23
0120	5	7.7
7740	4	5.5

The other variables, besides the time of release, which are important are the electron energy and the current density (that is, the number of electrons/cm²). It turns out that Q_∞ is proportional to the square of the electron energy. This simply arises because the depth of penetration of the electrons, and therefore the amount of glass really being affected depends on the square of the energy (V_p^2). The characteristic K was also found to depend on the mass of glass affected but to be inversely proportional to the current density (J), that is,

$$K \propto V_p^2/J$$

So, as you would expect, the more electrons used the quicker the oxygen is released.

LOW ENERGY BOMBARDMENT

Low energy electrons would not penetrate an aluminum coating, so a different approach had to be used. The surface potential of the glass

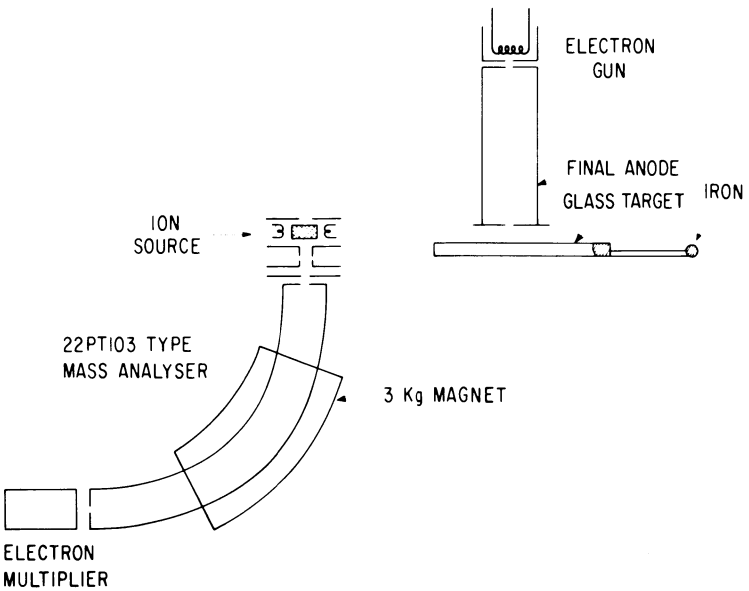

Figure I

was controlled by using an anode nearby to collect a chosen fraction of the secondary electrons emitted during bombardment of the samples. This method can be used between about 50 volts and 3000 volts energy. The tube is illustrated in Fig. 1.

The rate of oxygen release, R, at any given time of bombardment, t, was measured. There is a relationship between R and t, mathematically identical to that Lineweaver found between Q and t, except that at low energies two components are found. The relationship is

$$R = (R_o)_1 e^{-t/K_1} + (R_o)_2 e^{-t/K_2}$$

and

$$(R_o)_1 = (Q_\infty)_1/K_1 \qquad (R_o)_2 = (Q_\infty)_2/K_2$$

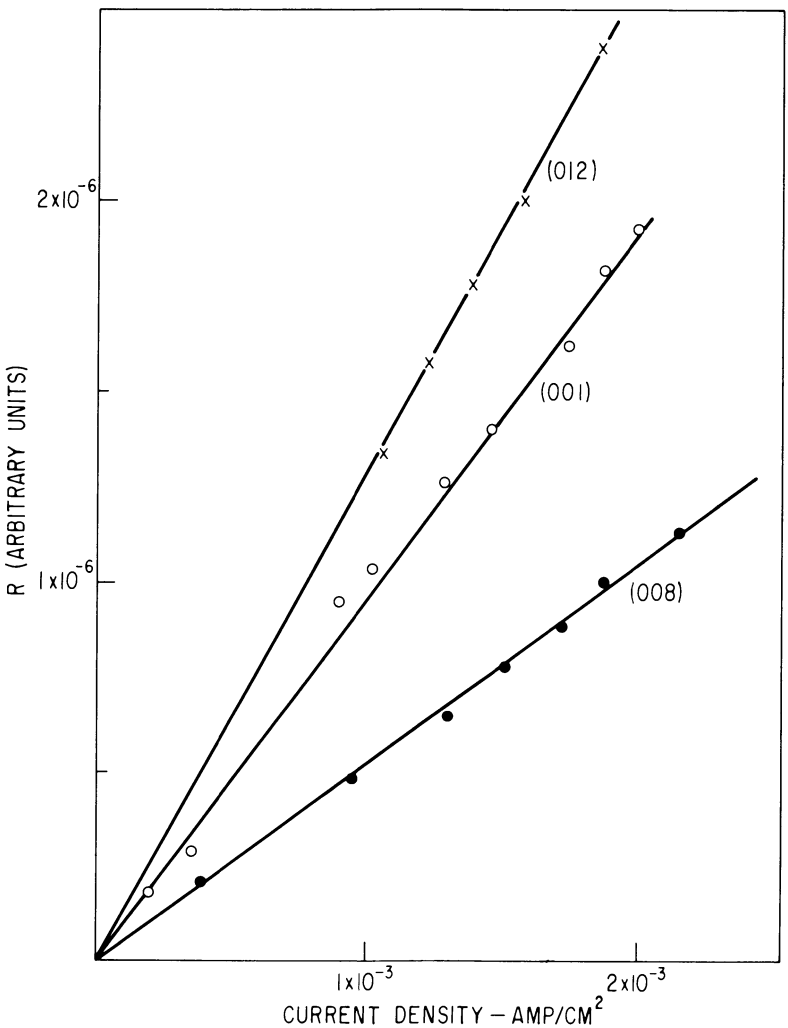

Figure 2

Note that if the high energy results also apply at low energies one would expect R_o to be proportional to the current density J but independent of the electron energy V_p. Figure 2 gives the experimental data for R_v. J for three glasses, confirming Lineweaver's findings. Figure 3 shows the relationship between R and V_p. The independence of primary energy does occur but only above about 800 volts. Table II lists the outgassing characteristics at low energies.

Extrapolating Lineweaver's results to low energies one would expect a Q_∞ of only a few hundredths of a micron-liter/cm^2 at 1000-volt energies, so the component 2 can perhaps be identified with that seen at high energies.

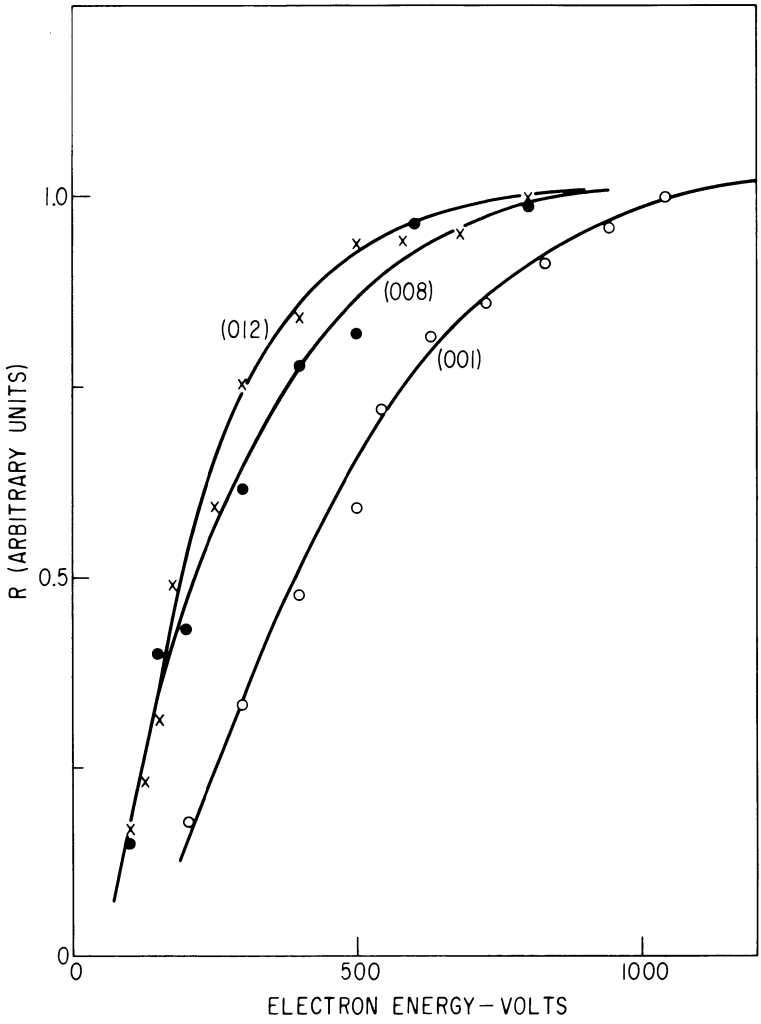

Figure 3

TABLE II

Glass-Code No.	V_p *(Volts)*	J *(Amp/cm²)*	K *(Hours)*	Q_∞ *(μ liters/cm²)*
008	800	2.2×10^{-3}	(1) 84	8
			(2) No measurement	
001	1000	2.2×10^{-3}	(1) 108	5.3
			(2) 2.2	4×10^{-2}
012	1000	2.2×10^{-3}	(1) 50	2.7
			(2) 0.6	8×10^{-2}

MECHANISM OF RELEASE OF OXYGEN

The oxygen atoms in a soft glass can be in either of two positions. In one the oxygen is bound to two silicon atoms as part of the silica network. In the other position, there is bonding to only one silicon atom, the oxygen is negatively charged, and there is a sodium or lead atom nearby to balance the charge. It is the latter oxygens which are easily removed by electron bombardment since only one bond has to be broken. After the bond is broken the electric fields set up in the glass by bombardment draw the oxygen to the surface where it escapes into the vacuum. At the same time the sodium or lead atoms move down deeper into the glass and eventually form a layer which is visible. This is called electron browning. The oxygen evolved at high energies and the component 2 at low energies correspond to these non-bridging oxygen atoms. Since low energy electrons are more likely to act at the surface of the glass than high energy electrons, it is possible that the component (1), which evolves so slowly but is very large, is the result of release of the doubly-bonded bridging oxygens which has to occur at the surface to be effective.

CONCLUSION

A simplified outline has been given of some of the factors involved in the release of oxygen from glasses by electron bombardment. This oxygen release can have important effects on device performance in many cases. Knowledge of the characteristics can help in finding ways to minimize the problems in critical applications by correct choice of glass or by appropriate pretreatment.

REFERENCES

1. J. L. Lineweaver, *J. Appl. Phys.* 34, 1786 (1963); J. L. Lineweaver, Proc. VIII Symposium on the Art of Glassblowing, American Scientific Glassblowers Society, 1963.
2. P. H. Dawson, *Supplemento al Nuovo Cimento*, 1967.

PROPERTIES OF MOLTEN GLASS AT HIGH TEMPERATURES: EXPANSION COEFFICIENTS

By

E. F. Riebling

Research and Development Laboratories
Corning Glass Works
Corning, New York

May 10, 1967

ABSTRACT

The nature of expansion coefficient changes that occur when a glass is heated through the strain point ($\eta \sim 10^{14.5}$ poise) to annealing point ($\eta \sim 10^{13}$ poise) region are discussed. Iso-expansion coefficient contours are compared for glasses and melts in several ternary oxide systems. The results suggest a relatively high sensitivity of melt expansion coefficient contours to structural changes that accompany composition changes. These findings are therefore in agreement with proposed glass and melt structure changes that have been based on recent extensive density, viscosity, and electrical conductance surveys.

I GLASSES

The relatively small thermal expansion coefficient of a given annealed glass [0-150 x 10^{-7} below $\eta \sim 10^{14.5}$ poise (Tg)] is most likely due to cation vibrational effects (ε_i) with a relatively small contribution from rotational effects caused by the presence of nondirectional bonds associated with modifying cations (ε_o). The latter would amount to thermally induced changes in the relative orientation of SiO_4 tetrahedra which, while small for pure SiO_2 glass and compositions close to it, can become significant as the O/Si ratio increases. An expression for the total expansion per gm. atom of oxygen (E) has been developed:[1]

$$E = \varepsilon_o + \Sigma\, \varepsilon_i\, n_i = \frac{3\alpha}{\delta N_o} \qquad (1)$$

where

ε_i = $z\, Ne_i$
z = valence of cation
N = Avogadro's number
e_i = expansion per O-Na or O-Si
3α = volume expansion per cc. of glass
δ = density of glass

Figure 1 shows a plot of density vs. temperature for several annealed borate glasses and their respective melts. The extrapolated intersection points of δ_{glass} and δ_{melt} vs. temperature occur quite close to or within the strain point to annealing point region. This particular region is of the

order of 35 to 50°C. for the glasses represented. The change of expansion coefficient can thus be thought of in a relative sense as representing a break, rather than a continuous change, in the δ vs. T curve.

The relatively sudden expansion coefficient increase in the strain point to annealing point region (Fig. 1) is definitely coincident with the onset of reasonable relaxation times for various transport phenomena.

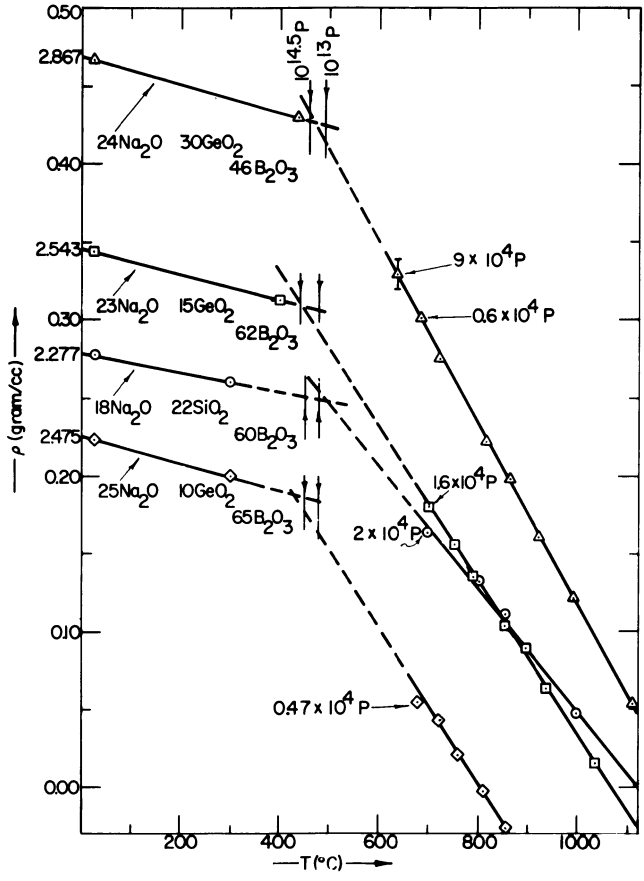

Figure 1

Density vs. temperature data for a series of borate glasses and melts.

This can be seen in Fig. 2 which depicts the log K vs. $1/T$ (°K.) curve (K = specific conductance) from 200 to 1000°C. for a $Na_2O{\cdot}SiO_2{\cdot}B_2O_3$ glass. There is a pronounced change of slope, with an increased cation mobility per °C., as the temperature rises through the Tg region.

The expansion coefficient change thus occurs after the glass has expanded several percent from 0°K., at least for the glasses in Fig. 1. One

could almost say that there is "critical" value of $V_T/V_{0°K}$ of about 1.03, beyond which any additional volume increase is concurrent with a significant decrease of relaxation times for transport processes.

II GLASS TRANSITION REGION

The *Tg* region is therefore one where positional disordering, usually associated with melting, can play a significant role in determining physical properties. It appears that expansion beyond V_{critical} may occur via an additional mechanism, namely, extensive positional randomization in an already expanded structure (the glass instead of a crystalline matrix). The stage appears to have been set, as it were, for the rigid but open structure (glass) to gradually collapse into an even more open, more flexible structure (liquid). Part of the reason for small values of V_{critical} is that a typical silicate glass at 0°K can be about 5 to 10% more voluminous than its stable crystalline modifications[2,3]. This volume difference can be thought of as representing most of the expected ΔV_{fusion} for a given composition. The volume difference between a glass and its crystalline form (ΔV_{g-c}) may thus represent most of the positional randomization that usually occurs at T_{fusion}. However, unlike ΔV_{fusion}, ΔV_{g-c} is irreversible and slightly dependent on cooling rate through the *Tg* region. Thus, the relatively large expansion coefficient change that occurs in the *Tg* to T_{fusion} region for most silicate, germanate, and borate glasses may also be related to the gradual onset of the small remaining portion of ΔV_{fusion}.

The change of $\Delta\delta/\Delta T$ close to the *Tg* region suggests a second-order phase change. It is, therefore, coincident with another apparent second-order change, namely the change of heat capacity (ΔC_p) that has been described by Gibbs, *et al.*[4] However, Temperley has suggested[5] that these changes should not be construed as indicative of a true second-order phase change when one is discussing a glass. Instead, the change of $\Delta\delta/\Delta T$ and the ΔC_p associated with *Tg* are supposedly associated with a "thawing out" of a particular degree of freedom. In essence, the time constant associated with this degree of freedom is merely changing from a large to a small value. The increase of $\Delta\delta/\Delta T$ with temperature, and the subsequent but gradual appearance of the remaining portion of ΔV_{fusion}, both occurring in the *Tg* region, may be merely symptomatic of the onset of a shorter relaxation time that is associated with structurally sensitive atomic displacements. The magnitude of $(\Delta\delta/\Delta T)_{\text{melt}}$ compared to $(\Delta\delta/\Delta T)_{\text{glass}}$ suggests that the former may be related to thermal displacements that involve more than just two atoms, that is, polyhedra and clusters of polyhedra.

One could therefore write the following equation for the expansion coefficient above *Tg*:

$$E_{\text{melt}} = E_{\text{vibrational}} + E_{\text{rotational}} + E_{\text{positional}} \quad (2)$$

where $E_{\text{positional}}$, which we shall relate to the structurally sensitive interpolymeric species displacement, suddenly becomes the dominant term by a factor of about ten times. The added volume introduced above *Tg* (above that expected from an extrapolation of the glass-state data) allows for a gradually increasing degree of positional disordering between T_g and T_{fusion}.

III MELT EXPANSION CONTOURS

Modifying cations, which are present in most typical glasses, appear to be responsible for most of the expansion changes that have been observed. These cations alter the continuous three-dimensional O-Ge-O, O-Si-O, and O-B-O bonding that tends to restrain the lattice expansion

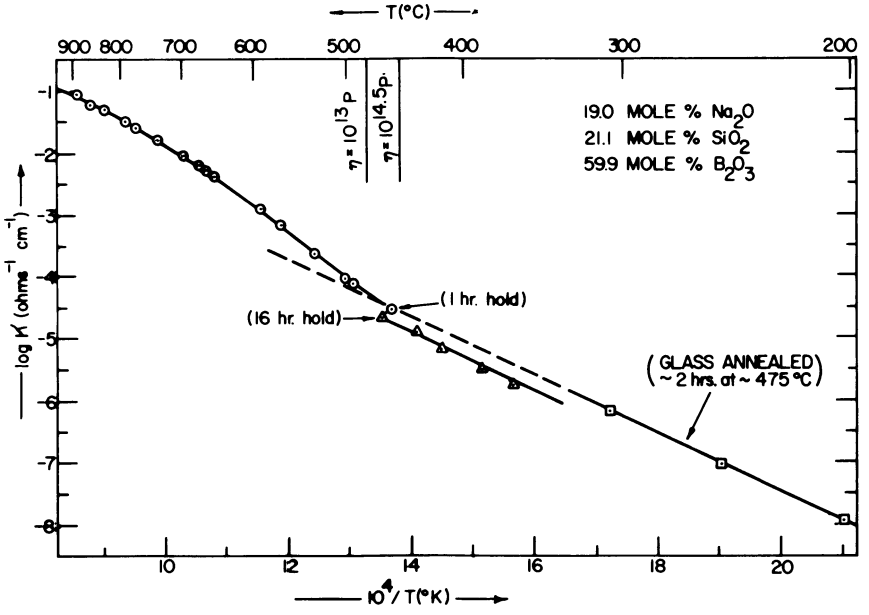

Figure 2

Specific conductance vs. 1/T(°K) of an alkali silicoborate composition.

of pure network-forming oxides. For example, the highly directional and, hence, restrictive O-Si-O bonds tend to be confined within anionic aggregates in most multicomponent melts and glasses. The more voluminous packing of oxygens around the interstitial cations, that occurs when there is a coordination increase for the network former, can also lead to sizable expansion increases.

It is possible that the "thawing out" of a particular degree of freedom[5] or the onset of a measurable configuration entropy[4] which occurs close to and above *Tg* (the liquid state), may be associated with a greater degree of cooperative movement within just such anionic aggregates. If so, then one would expect to see a relationship between melt expansion coefficient (determined primarily by $E_{positional}$ in equation 2) and the character and/or absence of a given polyanionic aggregate.

An example of the apparent structural sensitivity of E_{melt} is shown in Figures 3 and 4 which depict E_{melt} and E_{glass} contours for compositions in the $Na_2O{\cdot}GeO_2{\cdot}B_2O_3$ system. This is one of the few systems for which we possess extensive $\Delta\delta/\Delta T$ data for *both* the liquid and glass states.

Figure 3

Iso-expansion coefficient contours for melts in the $Na_2O \cdot GeO_2 \cdot B_2O_3$ system.

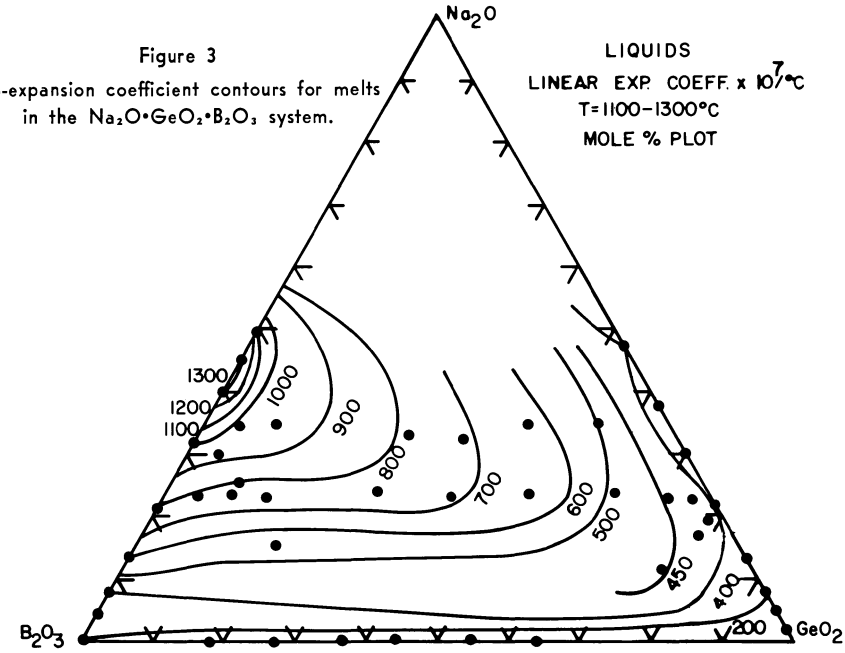

Figure 4

Iso-expansion coefficient contours for glasses in the $Na_2O \cdot GeO_2 \cdot B_2O_3$ system.

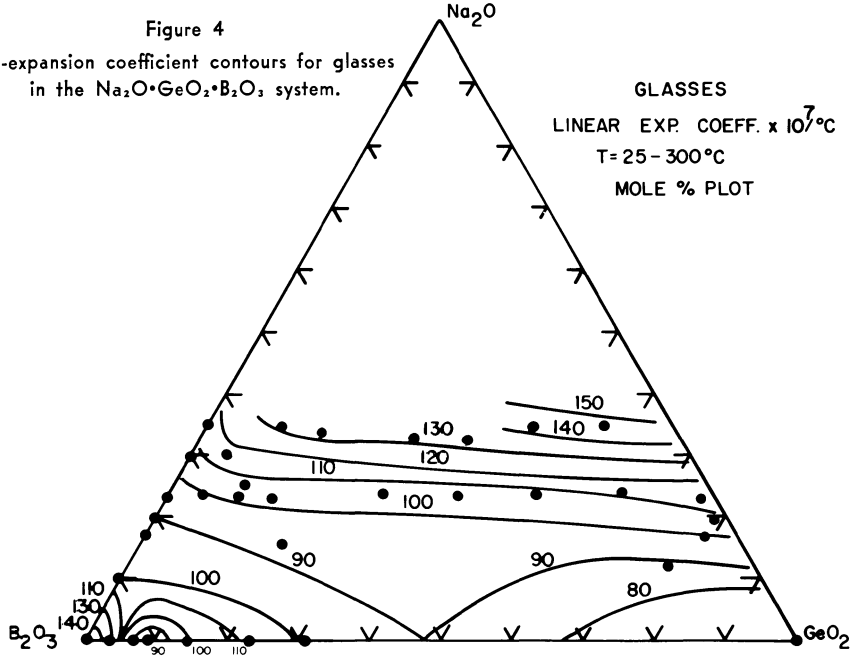

The $\Delta\delta/\Delta T$ contour maximum in Figure 3 is definitely associated with the presence of BO_4 tetrahedra in the molten state.(6) The maximum associated with the $Na_2O{\cdot}B_2O_3$ binary persists almost across the ternary to the $Na_2O{\cdot}GeO_2$ binary. This is exactly the same pattern that was deduced from the volume data for the presence of BO_4 tetrahedra.(6). There is no $(\Delta\delta/\Delta T)_{melt}$ maximum associated with the GeO_6 octahedra in the ternary because the $(\Delta\delta/\Delta T)_{melt}$ maximum in the $Na_2O{\cdot}GeO_2$ binary is only of the order of about 400 x 10^{-7}. The persistence of a reasonable concentration of BO_4 tetrahedra (2B/Ge on a mole % oxide basis) and their relatively large $\Delta\delta/\Delta T$ contours (»400 x 10^{-7}) tend to obliterate any evidence of a $\Delta\delta/\Delta T$ maximum associated with GeO_6 octahedra. The glass $\Delta\delta/\Delta T$ contours (Fig. 4) experience no maxima and reveal no significant correlation with the melt contours. This agrees with the above postulates concerning the significance of the additional term that enters into E_{melt}.

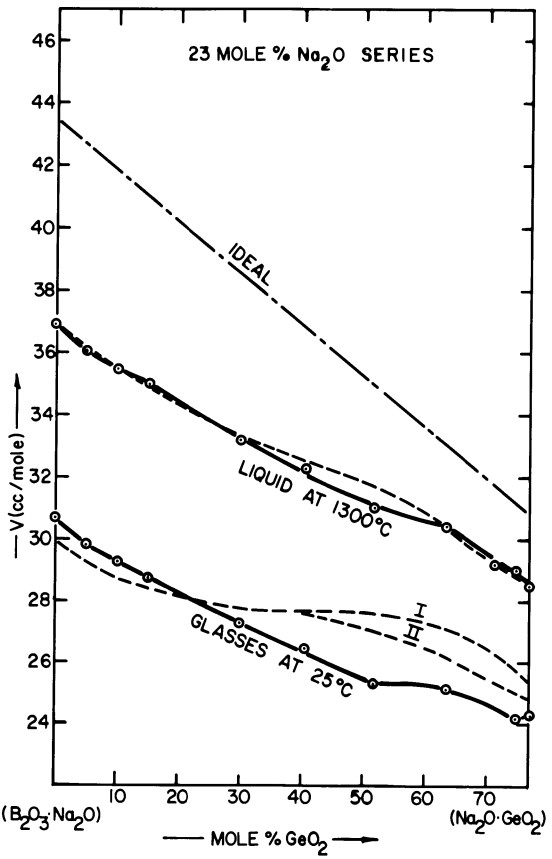

Figure 5

Volume isotherms for 23 mole % Na_2O borogermanate glasses and melts.

Figure 5 shows molar volume data and models for a series of melts and glasses in the $Na_2O{\cdot}GeO_2{\cdot}B_2O_3$ system. It had been previously found that high-temperature melt models can be used to obtain glass models.[7] However, this high-temperature ($\sim$1300°C.) melt model, which involved

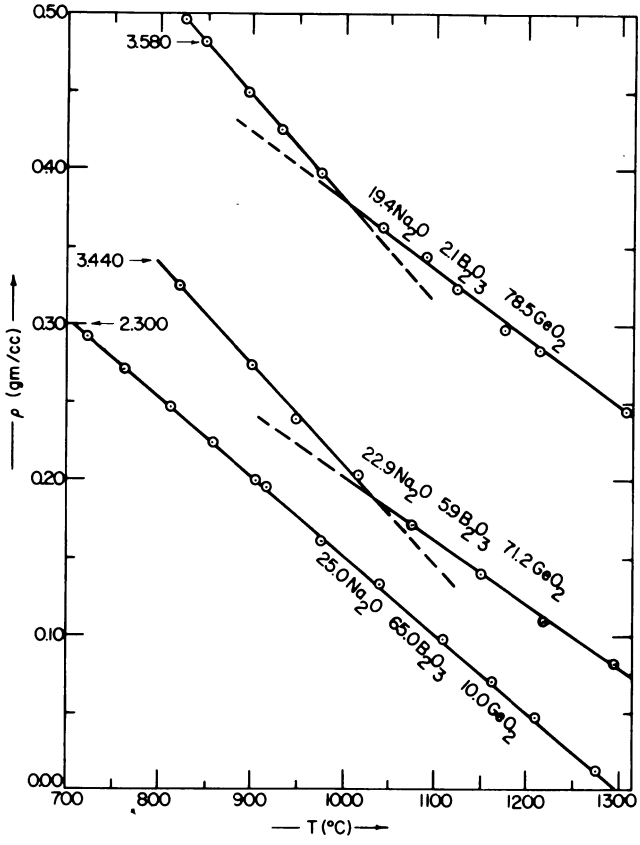

Figure 6

Density vs. temperature data for several GeO_2-rich and B_2O_3-rich melts in the $Na_2O{\cdot}GeO_2{\cdot}B_2O_3$ system.

GeO_6 octahedra for GeO_2-rich melts, had to be modified to give a glass model that more closely agreed with experiment for the GeO_2-rich glasses. This modification involved a greater concentration of GeO_6 for the glass state than postulated for melts at 1300°C. The reason for this discrepancy is quite apparent in Fig. 6, which shows breaks for the density vs. temperature lines of two of these GeO_2-rich compositions at about 1000°C, as opposed to the more normal linear behavior exhibited by a B_2O_3-rich composition.

The above $(\Delta\delta/\Delta T)_{melt}$ increases below $\sim$ 1000°C. can definitely

be associated with a shift to the left in the $GeO_6 \rightleftarrows GeO_4$ equilibrium at lower temperatures (a more efficient oxygen packing is associated with octahedra) for these still rather fluid melts ($\eta < 10$ poise)[6]. Figure 7 depicts the GeO_6 octahedra stability region suggested by the high-temperature ($<1000°C.$) viscosity and density data. Only the compositions within this region possessed $(\Delta\delta/\Delta T)_{melt}$ breaks at $\sim 1000°C$. Figure 8 shows the $(\Delta\delta/\Delta T)_{melt}$ contours as they exist below 1000°C. Note that, although there is not a $(\Delta\delta/\Delta T)_{melt}$ contour maximum in the GeO_2-rich region, the effect of the $(\Delta\delta/\Delta T)_{melt}$ increases in this region is to produce a subtle flattening out of the contours. In other words, the steep decrease of the $(\Delta\delta/\Delta T)_{melt}$ contours has been eliminated. This finding is significant, because it reinforces the idea that a glass possesses the general structure of the liquid state *just above Tg*. In some cases, this equilibrium polyhedral distribution can remain to quite high temperatures.

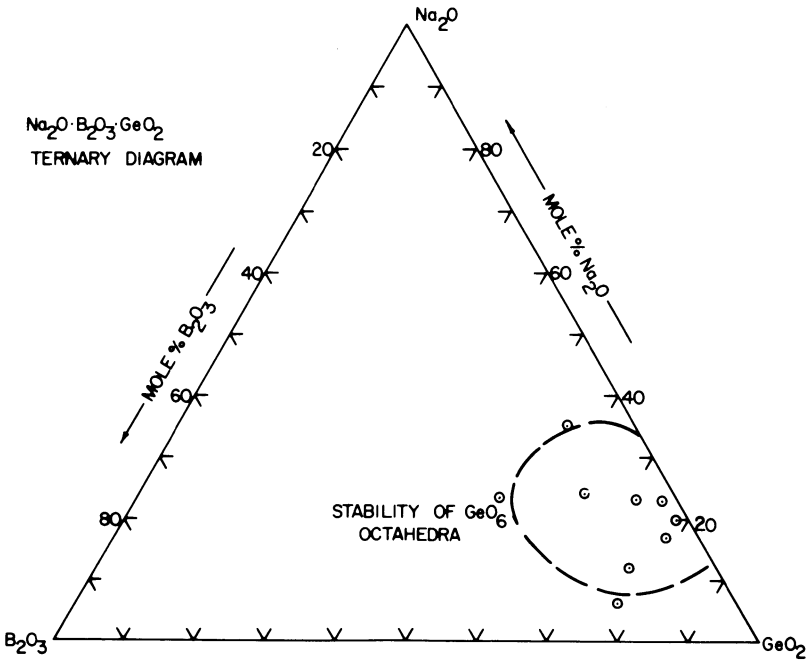

Figure 7

Stability region for GeO_4 octahedra in Na_2O·GeO_2·B_2O_3 melts.

Another system for which sufficient data are available for both states is the Na_2O·SiO_2·B_2O_3 ternary.[8] Again, the melt data show a pronounced $\Delta\delta/\Delta T$ contour maximum of about 1300 x 10^{-7} that is associated with BO_4 tetrahedra (Fig. 9). However, the expansion coefficient contours of

binary sodium borate glasses are ~160 x 10^{-7}, while there is a steady decrease for the binary silicoborate glasses to about 70 x 10^{-7} at the 50 wt. % SiO_2 point. Most of the intermediate B_2O_3-rich ternary glasses possess expansion coefficient between 75 and 95 x 10^{-7}. Thus, the glass $\Delta\delta/\Delta T$ contours again do not match those reported for the melts.

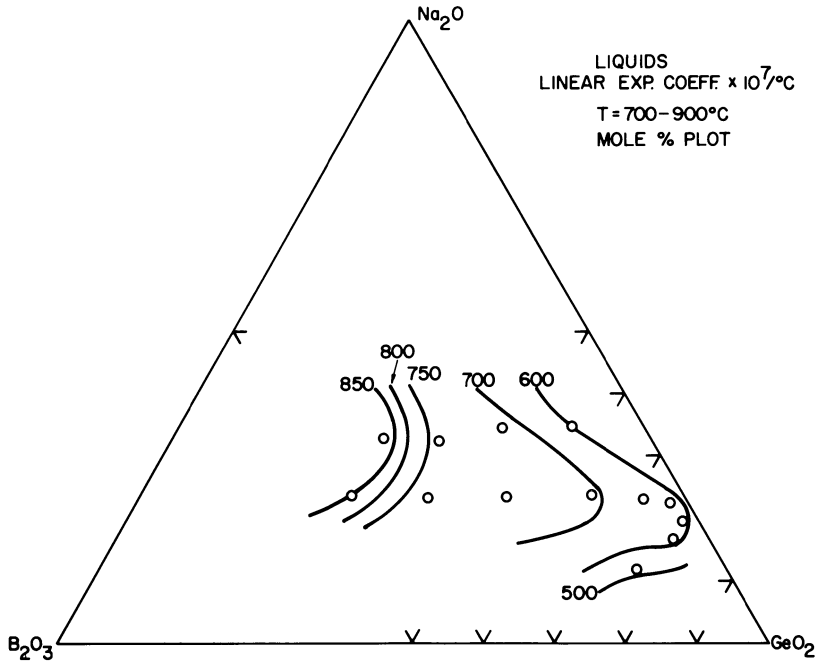

Figure 8

Iso-expansion coefficient contours for Na_2O•GeO_2•B_2O_3 melts between Tg and 1000°C.

Other systems for which $(\Delta\delta/\Delta T)$ melt contour maxima have been observed for the molten state are the Na_2O•SiO_2•GeO_2 and Na_2O•Al_2O_3•GeO_2 ternaries.[7] Again, contour maxima can be associated with coordination phenomena for the major melt constituent.

Finally, two systems have been studied in which the major melt constituent or network former did not appear to change coordination number. No $(\delta\Delta/\Delta T)_{melt}$ contour maxima were observed in the MgO•Al_2O_3•SiO_2 and the Na_2O•Al_2O_3•SiO_2 system (shown in Fig. 10).[7] The expansion coefficient trough in Fig. 10 tends to confirm the three-dimensional nature (SiO_4 and AlO_4 tetrahedra) of the Al/Na = 1.0 compositions. These last findings therefore also tend to support the proposed qualitative relationship between melt expansion coefficient contour and the structure and/or absence of polyanionic aggregates in ternary molten oxides and their glasses.

Figure 9

Iso-expansion coefficient contours for $Na_2O \cdot SiO_2 \cdot B_2O_3$ melts.

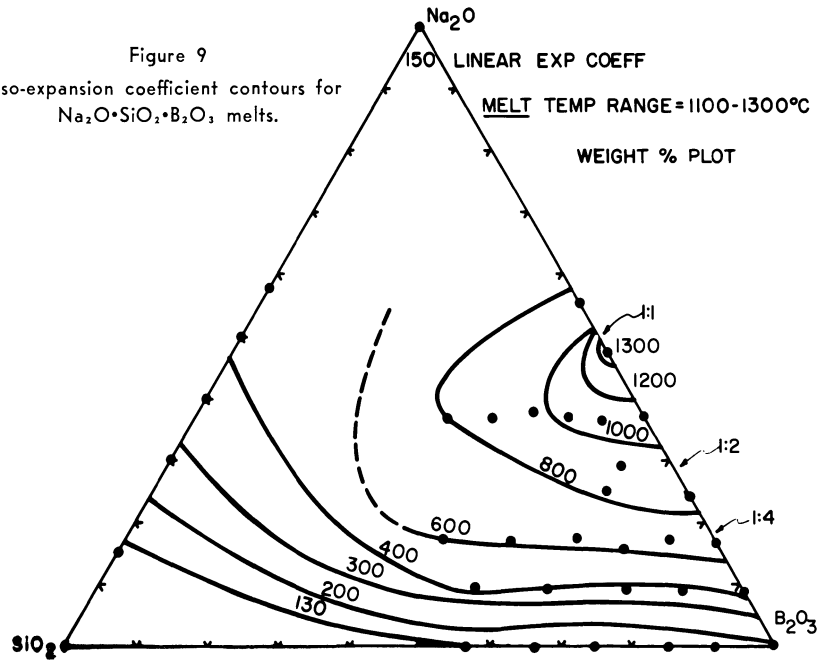

Figure 10

Iso-expansion coefficient contours for $Na_2O \cdot Al_2O_3 \cdot SiO_2$ melts.

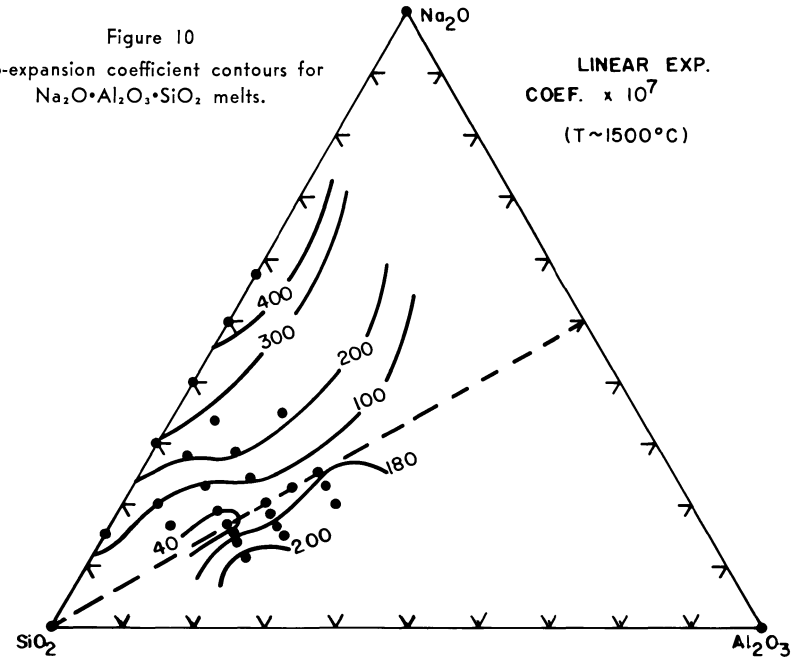

CONCLUSIONS

The expansion coefficient of a glass above its annealing temperature is a more sensitive indicator of structure than is the more familiar expansion coefficient in the zero to 300°C. temperature range. This relationship of α_{melt} to structure can be exploited to deduce and confirm structural changes that accompany change of composition. This is particularly true for ternary oxide systems that exhibit glass formation.

REFERENCES

1. S. Kumar, *Glastech. Ber.* **32K** [V], 26-35 (1959).
2. F. Birch, J. F. Schairer, and H. C. Spicer, "Handbook of Physical Constants" (Geological Society of America, Special Paper No. 36, New York, (1950), pp. 15, 184.
3. A. Winter, *Verres et Refr.* **20** [6], 448-49 (1966).
4. G. Adams, and J. H. Gibbs, *J. Chem. Phys.* **43** [1], 139-146 (1965).
5. H. N. V. Temperley, "Changes of State; a Mathematical-Physical Assessment," Cleaver-Hume Press Ltd., London, 1956.
6. E. F. Riebling, P. E. Blaszyk and D. W. Smith, submitted to *J. American Ceramic Society.*
7. E. F. Riebling, *Rev. Hautes Temp. Refr.* **4** [1], 1-12 (1967).
8. E. F. Riebling, *J. Am Ceram. Soc.* **50** [1], 46-53 (1967).

SUPERCONDUCTING GLASS-TO-METAL SEALS

JOHN LEES
Dept. of Physics, University of British Columbia

The phenomenon of superconductivity exhibited by certain metals at very low temperatures is currently the subject of a vast amount of research. During one phase of such work at the University of British Columbia a need arose for glass-to-metal vacuum seals which would allow leads of a superconducting alloy to pass through glass or metal. This paper describes the development of these seals and gives details of the critical currents which were attained during their use in liquid helium at 4°K.

Perhaps it would be of advantage to first give a short account of superconductivity. This phenomenon was discovered by Kammerlingh Onnes in 1911, when he reported the complete absence of measurable electrical resistance in Mercury at very low temperatures. He first used the term "Superconductivity" in 1913 when reporting the fact that lead and tin also became superconductors at liquid helium temperatures. At first, it was thought that only pure soft metals possessed this property but then a new series of superconductors, hard metals like tantalum, niobium, and titanium, were discovered by Meissner. As lower and lower temperatures were reached experimentally, the list of superconductors grew. Attempts to construct a small high field magnet of superconducting lead wire failed when it was found that the wire returned to normal at field strengths of only a few hundred oersted. Soon, however, it was discovered that certain alloys also became superconductors at temperatures ranging downwards from 20°K. Some of these alloys also had the additional advantage of retaining their superconducting properties at much higher field strengths than pure metals. Lead-Bismuth, for example, was found to have a magnetic threshold of 20,000 oersted. Eventually, after much practical and theoretical research, a superconducting solenoid, producing a field of 100,000 oersted, was constructed of Niobium-Tin alloy in 1963. Other alloys have been found to be equally suitable, NiObium-Zirconium, and Niobium-Titanium being most used in Current work. A further discovery of some importance in the making of glass-to-metal seals is that an alloy wire in a strained condition will exhibit a higher magnetic threshold (or critical current), than an annealed sample of the same wire. Also, the discovery of certain peculiarities in the penetration of magnetic flux into superconductors made it evident that thin wires would be most suitable for use in high field coils. The standard wire now in use for this purpose is therefore a specially prepared, copper coated alloy of Niobium-Zirconium, or Niobium-Titanium, of about .010″ in diameter.

Wire of this type is used in our Low Temperature Laboratory in the construction of a device known as a "Heat Switch". This makes use of the fact that when a wire becomes electrically superconducting, its heat conduction drops to almost zero. When again becomes electrically conducting, then heat will once more flow through the wire. This device is used to control heat flow into a metal chamber. Electrical leads through the walls of the chamber were originally conventional Kovar seals, which are not superconducting. In order to thermally isolate the chamber, it was

necessary to use superconducting leads. A small coil around the wire will then make it possible to control the state of the wire—allow it to be superconducting or not, thus also allowing control of the heat flow. In the literature, there is a mention of seals soldered through platinum, or sealed with epoxy cement.[1] We have found that it is possible to seal superconducting alloys directly through glass. The construction of these seals is shown in Fig. 1.

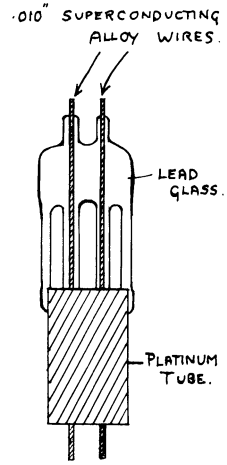

Figure 1
Two wire superconducting glass-to-metal vacuum seal.

The criteria for our seals were that (1. They should be vacuum tight from room temperature to 4°K. (2. They should be able to stand sudden and repeated immersion in liquid helium. (3. They should be superconductive at 4°K. and have a critical current of approximately 15 amps. (The critical current is that current at which the wire loses its superconducting qualities and "goes normal".) The alloys used were uncoated Niobium-Zirconium, and copper-clad Niobium-Titanium. We were unable to obtain any accurate information regarding the respective expansion coefficients of the alloys, and so proceeded in what is often termed the empirical manner.

The first seals were made with Niobium-Zirconium wire, and we rapidly established the fact that standard lead glass was a good expansion match. In attempts to seal the wire through Pyrex brand borosilicate glass, we used Housekeeper's technique, flattening the wire (and incidentally putting a beautiful groove in the nice hard steel rollers of our metallurgy department). This technique produced seals which were satisfactory in everything except that they had very low critical currents. We therefore concentrated on lead glass seals, using a platinum tube to connect the glass to the metal chamber. One difficulty found during sealing was the tendency of the wire to exhibit a strong exothermic oxidation at temperatures just above the sealing temperature. To overcome this, and

to encourage better adhesion between the glass and the wire, we plated the wire with copper, and used a longer bead than is usual, so as to protect the wire from flame "splash". Eventually, we flashed the wire with nickel, before copper plating, to give better adhesion between alloy and copper. We also tried a vacuum bake of the plated wire before sealing. This reduced the number of bubbles in the seal, but we had 100% success with or without baking. The final technique then was to plate the wire first with nickel, then with copper, then to bead the wire with lead glass and finally seal it through a lead glass tube which had previously been joined to a platinum tube. The seals were either single wire, or pressed into a multiple pinch type. They were very similar in appearance to the well known Dumet type. We used a helium mass spectrometer leak detector for vacuum testing, and repeatedly immersed the seals in liquid helium during this process. At 4°K. the critical currents varied in individual seals from 20 to 50 amps. We assumed that variations in working while sealing caused sufficient differences in the state of the wire to account for the variations in critical current.

We used the same techniques to produce seals of Niobium-Titanium wire. This was copper clad, but it was necessary to remove most of the copper coating in order to avoid cracking due to mismatched expansion. Successful seals were produced by reducing the copper thickness to about 20 microns, but this was difficult to estimate. We found it to be little more trouble to remove the copper completely, and replate as with Niobium-Zirconium wire. The results of tests on these seals were a little disappointing. They were vacum tight and unaffected by dunking in liquid helium, but the critical currents were only about 15 amps. There was, however, a relatively slow rise to normal, and there was very little variation from one seal to another. Within these limits they are more reproducible than Niobium-Zirconium seals.

I would like to refer once again to the odd fact that we proceeded with this project with virtually no knowledge of the physical properties of the materials involved. The old adage says that "Where ignorance is bliss, 'tis folly to be wise." A sufficient number of anomalies, as yet unexplained, have been produced during this work to make us feel that there is great merit in feeling as blissful as possible when working with glass.

In conclusion, I would like to thank my colleagues, Dr. P. W. Matthews, and Dr. P. R. Critchlow for much help, fun, and encouragement during this project.

REFERENCES

1. I. M. Templeton, *Solid State Electr.* **1**, 258 (1960).

THE PHYSICS OF GLASS

GEORGE W. MCLELLAN
Corning Glass Works
Corning, N. Y. 14830

Anyone who works with glass comes sooner or later (usually sooner) face to face with some of the strange things that glass does when it is heated or cooled. Sooner or later (usually later) it is plain that glass can be heated or cooled only with skill, care and consideration for the nature of the material. It is this nature of glass that this paper will explore with the hope of providing some helpful ideas that will prevent those disappointing times when you find two pieces of glass where one used to be.

In most lamp working operations glass is heated unevenly and it is uneven heating that causes stress within glass. When this stress is too great the glass breaks. Even when glass is heated or cooled in an oven or furnace, it does not heat or cool uniformly and may develop stress. In an oven, breakage is much more likely during cooling than heating.

Thermal stress that results from non-uniform heating or cooling is directly proportional to the thermal expansion rate (or coefficient) of the glass and the temperature difference between the hot and cold parts of the glass. Consider the case of a piece of glass heated on one side. (Fig. 1)
The stress can be calculated from this equation:

$$S = K \times a \times (T_h - T_c)$$

S = Stress
K = A constant for each glass composition
a = Thermal expansion coefficient
T_h = Temperature of hot side
T_c = Temperature of cold side

Values of K for some compositions:

Corning No.	*K (pounds per square inch or psi)*
7740	1.138×10^7
0080	1.316
1720	1.694
0010	1.127
0120	1.103
7900	1.235
7940	1.250

For other compositions K can be computed from this equation:

$$K = \frac{E}{1 - n}$$

E = Elastic Modulus
n = Poisson's Ratio

For example, if a piece of Corning No. 7740 glass is heated so that one side is 300°C. hotter than the other side, the stress will be:

$S = 1.138 \times 10^7$ psi. $\times$ 33 $\times$ 10^{-7} in/in/°C. $\times$ 300°C.
$= 11{,}250$ psi.

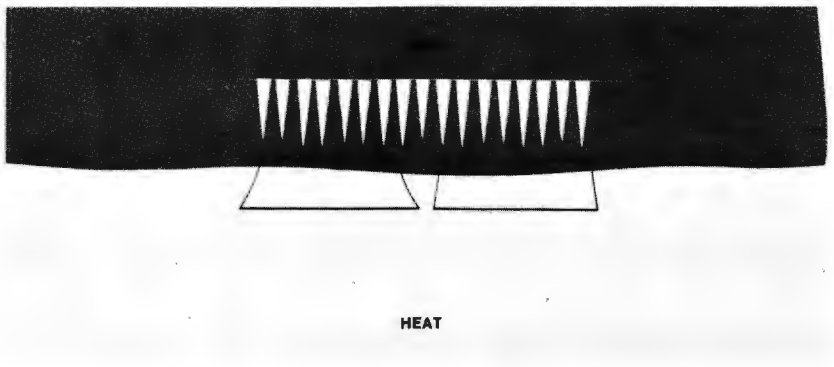

Figure 1
When a piece of glass is heated on one side, the hot side expands while the cool side retains its size. High-expansion glass on the left distorts more than the low-expansion glass on the right.

This amount of stress can break glass or it can be harmless, depending on the type of stress and the condition of the glass. There are three basic types of stress—tension, compression and shear. Tension pulls the glass

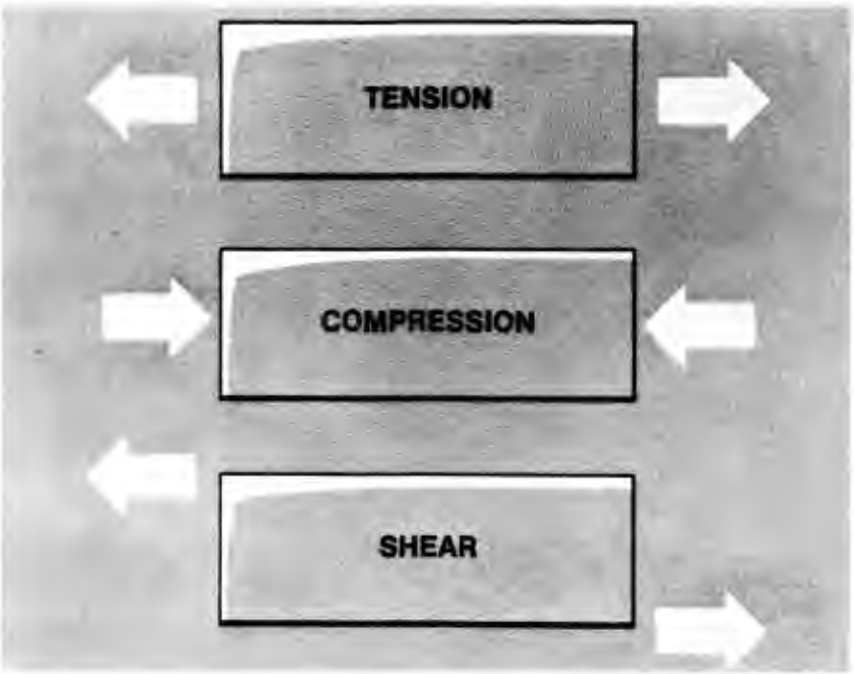

Figure 2
Tension stretches glass, compression squeezes it and shear pulls two opposite sides of a piece of glass in opposite directions.

and will pull it apart if the tension is great enough. Compression squeezes the glass and shear acts as if one side of the glass were pulled in one direction while the opposite side is pulled in the opposite direction (Fig. 2). In the case of a piece of glass heated on one side, the cold side is in tension and the hot side in compression.

Tension is the most important type of stress to a glassworker or glass designer since glass always breaks from tension. Even though glass does not break from compression, compression is sometimes important because the presence of compression means there is an equal amount of tension to balance this compression somewhere else in the glass. Shear can be disregarded except in cases where local tension results from a shear stress.

The amount of tension required to break glass depends on the method by which the glass is formed, the condition of the glass surface and the length of time the tension is applied. Glass is decidedly stronger in fiber form than glass in more massive form and glass freshly formed is much stronger than glass that has been scratched or bruised (Fig. 3). Glass that has been ground or severely abraded with silicon carbide or a diamond is the weakest of all.

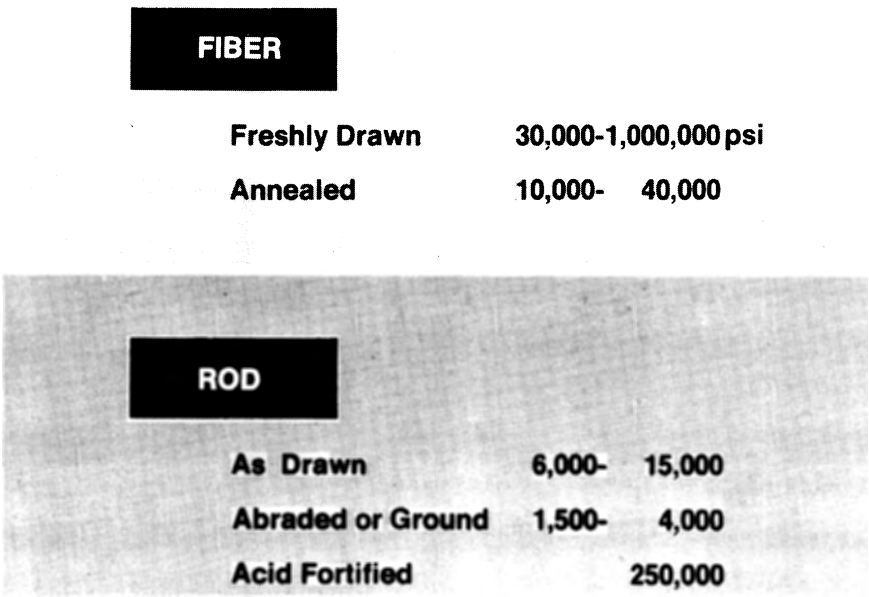

Figure 3
Strength of glass is influenced by condition of the glass surface. Fibers are much stronger than glass in bulkier forms.

Stress and strain are two terms that are frequently used interchangeably as if they mean the same thing. Since stress and strain exist together and one cannot exist without the other, it is natural that they should get confused with one another at times. Stress is measured in units of force per unit area (pounds per square inch or kilograms per square milli-

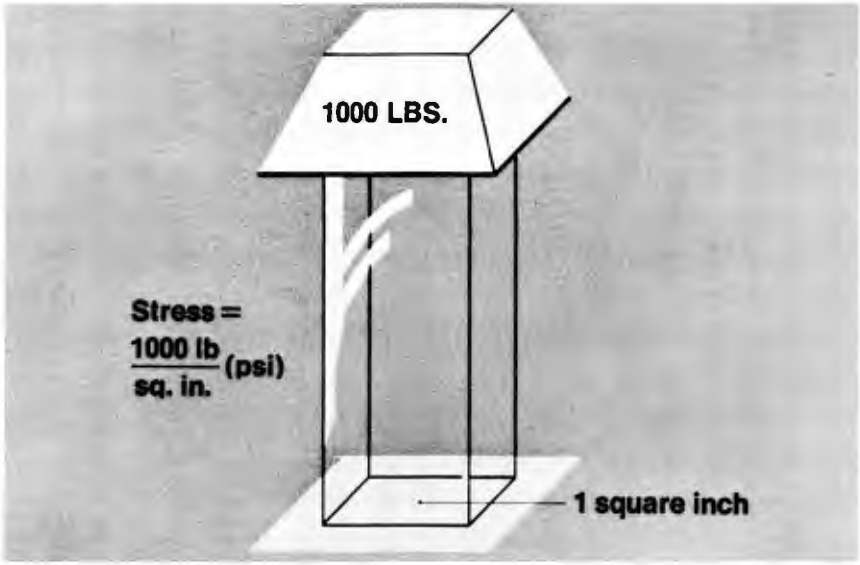

Figure 4
Stress is a measure of force per units of area. Units may be pounds per square inch or kilograms per square millimeter.

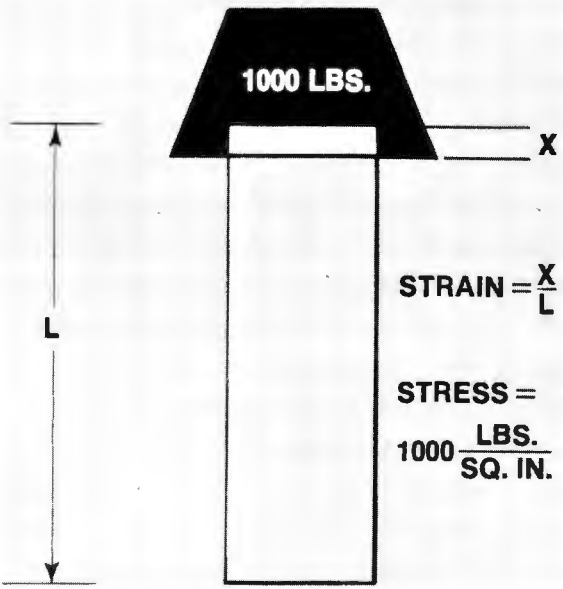

Figure 5
Strain is the change in length of this bar (X) produced by applying a force of 1000 pounds to the bar. Strain is a pure number, not expressed in any units.

meter). (Fig. 4) Strain is the proportional change in length or width produced by the application of stress (Fig. 5). Strain is a pure number and is not expressed in units of any sort.

Glass weakens when held under stress for periods up to 1000 hours but after 1000 hours does not weaken further. This effect, known as the time-load effect, must be taken into account when designing a glass product for long time use under load (Fig. 6). Sometimes a glass item will

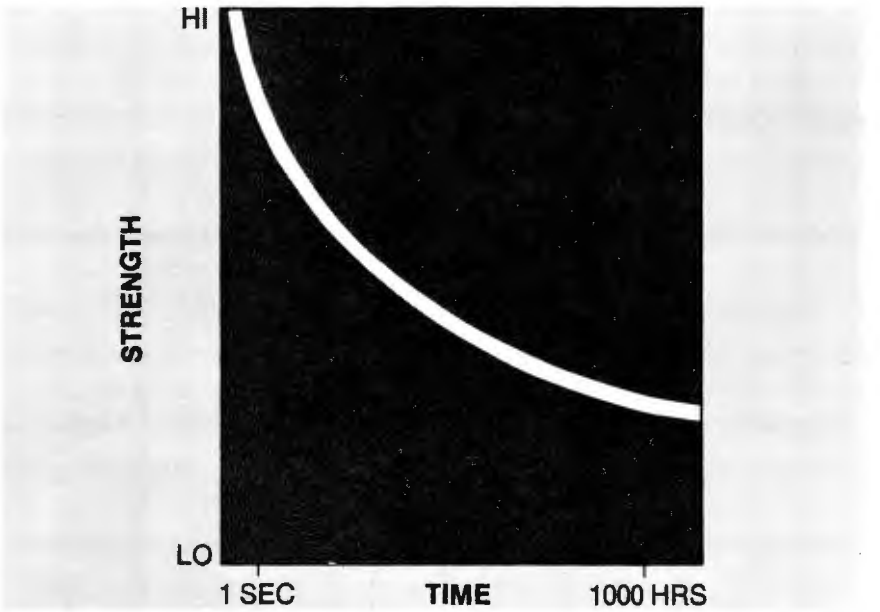

Figure 6

When glass is loaded for 1000 hours, its strength is approximately one-third its strength when loaded for one second. Beyond 1000 hours strength remains constant.

break when being used under conditions that seem perfectly normal and that the glass has withstood previously. The answer may be in such cases that the time-load effect weakened the glass until it no longer could support the load that it had supported a number of times previously. This load may be in the form of a temperature difference, an internal pressure or a mechanical force.

One reason why non-uniform heating of glass is frequently a problem is the low thermal conductivity of glass. Heat one side of a piece of metal and the opposite side will heat up also because the metal conducts heat readily. Heat one side of a piece of glass and the opposite side remains relatively cool for a longer time than in the case of the metal (Fig. 7). While glass compositions vary somewhat in thermal conductivity, no glass conducts heat as well as a metal, any metal.

However, heat is transferred by radiation as well as conduction and glass radiates much more rapidly than it conducts. If you heat a metal rod

in a flame, the cool end of the rod soon gets hot by conducting heat through the rod from the hot end. Now heat this rod until the hot end is red hot and hold your hand a few inches from it. Your hand is now being warmed by radiation.

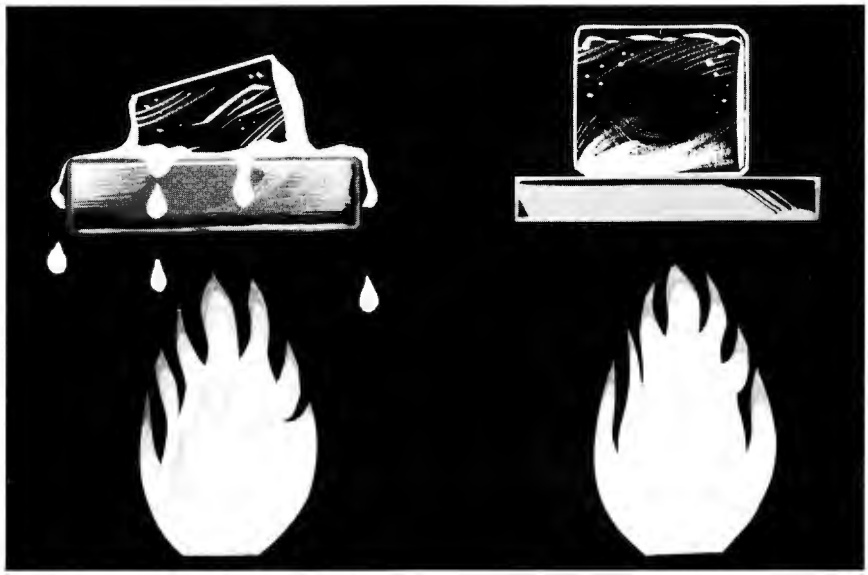

Figure 7

Metal plate on left conducts heat rapidly from flame to ice cube. Glass plate on right conducts heat much less readily.

This difference between the ability to conduct heat and the ability to radiate heat is one of the principal reasons why it is necessary to anneal glass after most hot operations. When glass is left to cool at its own rate, heat flows from the surface of the glass more rapidly than heat flows from the interior of the glass to the surface. (Fig. 8). Therefore, the surfaces cool and shrink more rapidly than the interior. This means that the interior of the glass, because it cannot shrink as rapidly as the surfaces, pulls on the surfaces with the result that the surfaces are then in tension. If the glass goes below the strain point in this condition, the surfaces are frozen in tension and the glass is thus weakened.

The purpose of annealing, whether in an oven or a flame, is simply to slow the cooling of the surfaces to let the interior of the glass catch up. Usually the glass is heated to a temperature somewhat above the annealing point, then cooled slowly to the strain point. (Fig. 9) Below the strain point, permanent stress cannot be introduced so the glass can be cooled in this region as rapidly as necessary providing it doesn't break before it gets to room temperature.

There is no fixed rule for determining an annealing schedule that will work in all cases. If the glass is heated initially to the annealing point, the holding time at that temperature will be rather long. If a quicker

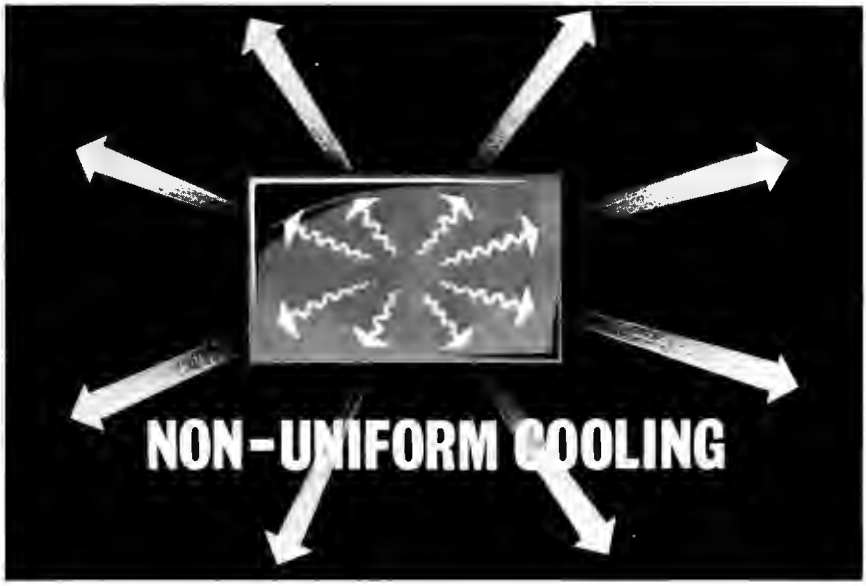

Figure 8
Heat flow by radiation from the surface of glass is much more rapid than heat flow by conduction from the interior of glass to the surface.

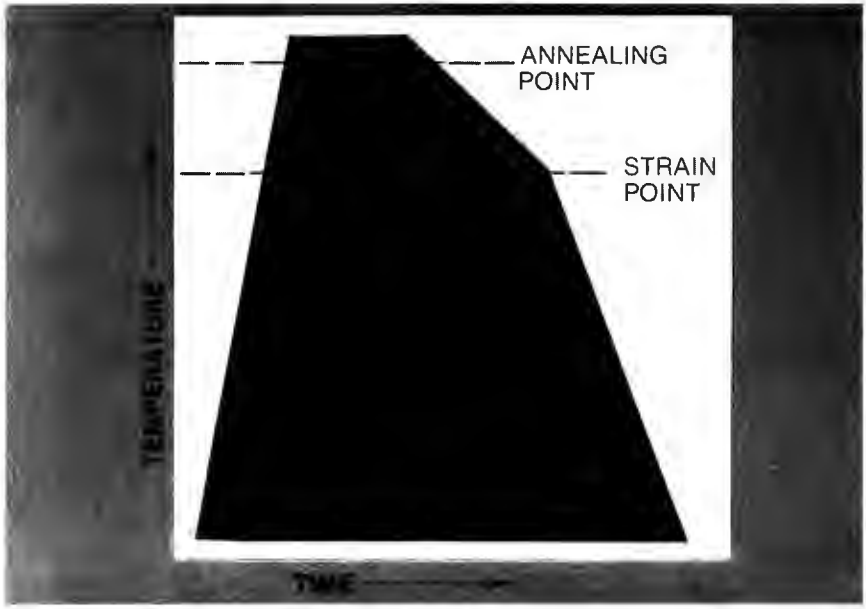

Figure 9
Typical annealing schedule heats glass to slightly above the annealing point, cools gradually to the strain point then cools more rapidly from the strain point to room temperature.

schedule is necessary, then the glass must be heated above the annealing point. How far above the annealing point it is safe to go depends on the thickness and shape of the glass item being annealed as well as how much distortion can be tolerated. The higher the initial temperature, the greater the risk that the glass will sag out of shape. A look at a curve of viscosity plotted against temperature shows how rapidly glass softens above the annealing point. (Fig. 10)

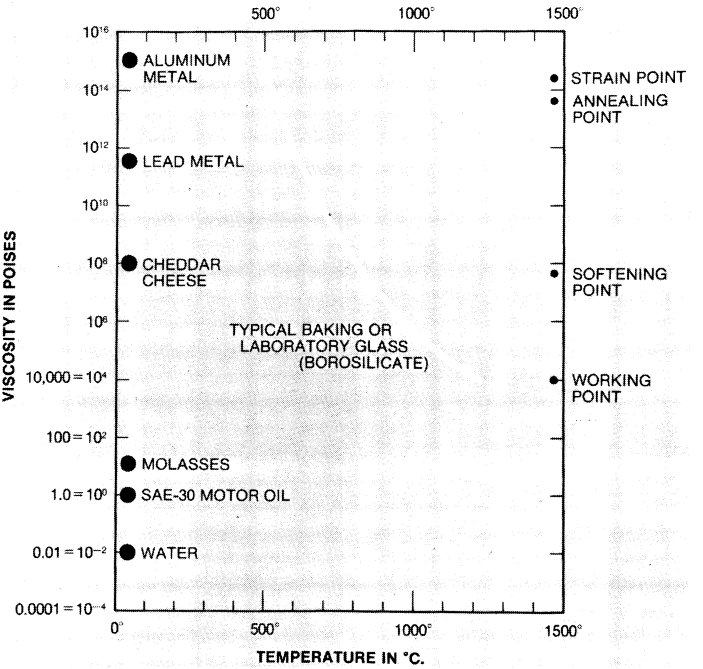

Figure 10
Viscosity of glass decreases sharply above the annealing point.

Tempering is the opposite of annealing. Instead of cooling the glass slowly and uniformly, glass is first heated to a temperature between the annealing and softening points, then suddenly quenched. First the surfaces shrink while the interior is still soft, then the interior shrinks and compresses the surfaces. (Fig. 11) It might seem that the glass should break under such sudden cooling and it would if the whole cycle were carried out to a lower temperature where the glass hardens and is unable to adjust to the differential shrinkage between the interior and the surfaces.

Tempered glass is stronger than annealed glass because of the compression built into the surfaces. Any load applied to tempered glass must first overcome this compression before the surfaces can be put in tension.

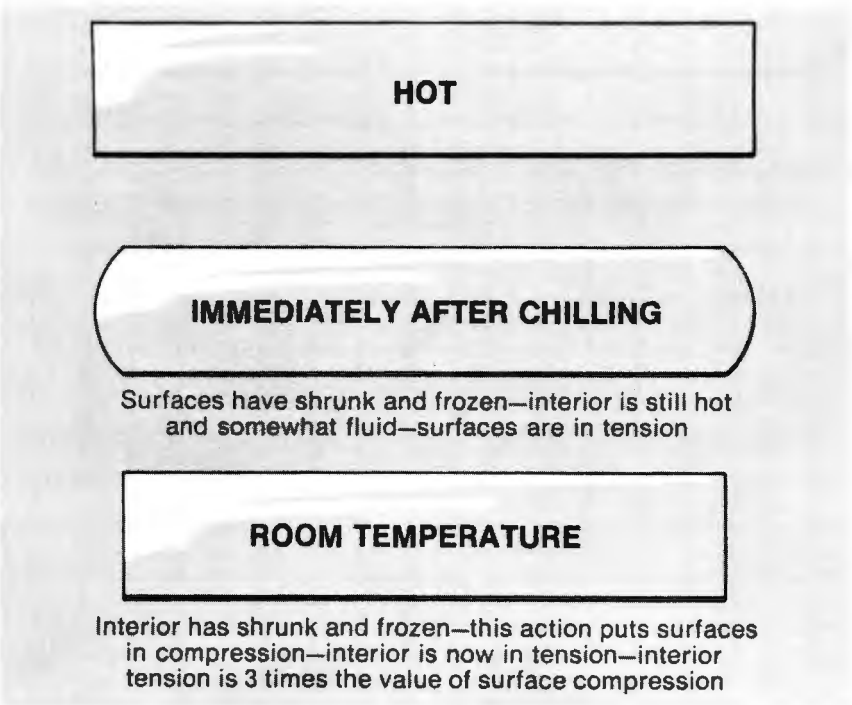

Figure 11
In tempering, glass is heated to above the annealing point then suddenly chilled.

Probably the most useful point to remember from this brief discussion of the physical behavior of glass is that the most sensitive period in the life of a piece of glass is when it is cooling just after a forming or hot-working operation. Remove a piece of glass from the flame, put it down on a bench top where it will pick up a scratch from a scrap of glass and the result may be a break immediately. Or if not an immediate break, the time-load effect may produce a break in several minutes or several hours when apparently nothing was happening to the glass.

SUITABILITY OF IRON-NICKEL-COBALT ALLOY TO GLASS SEALS FOR CRYOGENIC USE

CARL J. HUDECEK *and* JOHN B. FINN
Owens-Illinois Technical Center
Toledo, Ohio 43601

ABSTRACT

When tubular graded glass-to-metal seals (borosilicate to iron-nickel-cobalt) were immersed in liquid nitrogen and then brought into room temperature air, catastrophic fractures were observed in some samples while other samples showed no adverse effect. An investigation was made to determine the cause of breakage. The problem was examined using low temperature dynamic stress measurements and thermal shock tests as tools.

A conclusion was reached that the cause of breakage was due to a low temperature "phase transformation" in the iron-nickel-cobalt alloy. In other words, the crystal structure of the metal changed (from the metastable gamma phase to the alpha phase). This change caused a sudden dimensional expansion of the alloy, which in turn fractured the glass.

Herein we present a method by which the glassblower can determine the suitability of his alloy for cryogenic use.

INTRODUCTION

When tubular graded glass-to-metal seals, *i.e.* iron-nickel-cobalt alloy to borosilicate glass, were immersed in liquid nitrogen and then brought into room temperature air, some samples fractured catastrophically while other samples showed no adverse effect. Figure 1 shows three typical graded seals after the liquid nitrogen immersion.

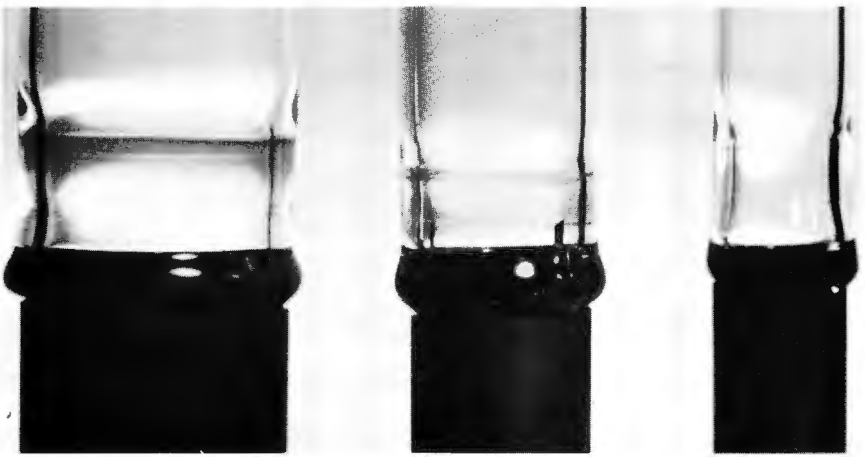

Figure 1

Two of these seals show no adverse effect after the thermal shock. The center one, however, illustrates the breakage which occurred as a result of immersion in liquid nitrogen. The axial fracture penetrates from the outer to the inner glass wall.

We investigated this problem with the following objectives:

1. To determine the cause of the catastrophic failure.
2. To develop a test which would predict suitability of metal for cryogenic (liquid nitrogen) seals.

TEST RESULTS

1. *Graded Tubular Seals.*
   Five different sizes (¼", ⅜", ½", ¾" and 1") of tubular graded seals were immersed in liquid nitrogen (six seals of each size). The ½-inch, ¾-inch and 1-inch diameters survived the immersion. The ¼-inch and ⅜-inch sizes fractured.
2. In order to simplify the investigation of the cause of breakage, laboratory "Butt Seals" as shown in Figure 2 were prepared. The butt seals have the advantage of simple, planar geometry and allow easy measurement of stress patterns with a polarimeter.

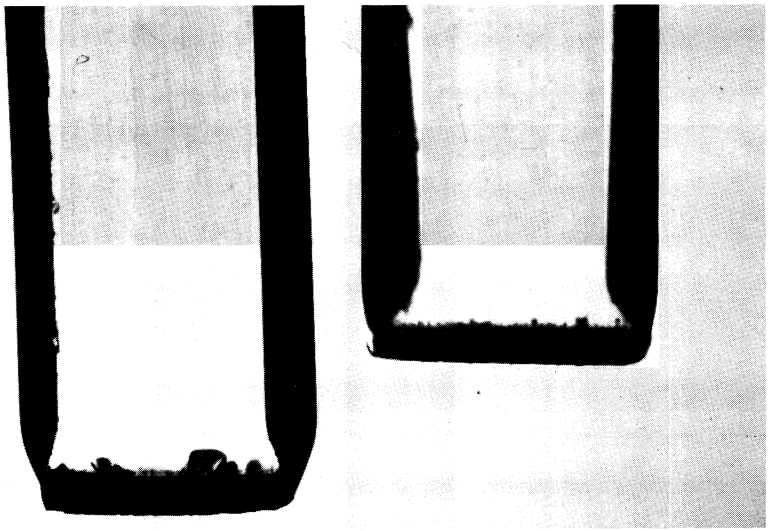

Figure 2

The butt seals were prepared from $\frac{5}{16}$-inch squares of sealing alloy obtained by flattening out the metal from its originally tubular form. Pieces of ¼-inch diameter EN-1 borosilicate glass cane were butt sealed to the metal squares, using R.F. heat.

The seals were annealed in a lab furnace at 972°F. for 15 minutes and cooled at 10°F. per minute. The resulting stresses are shown in Table I.

TABLE I

Tubing Size	*Stress in Butt Seals (psi)*
1/4"	790 compression
3/8"	1150 compression
1/2"	770 compression
3/4"	770 compression
1"	800 compression

These data show that metal from the 3/8-inch tubing produced a noticeable stress difference. However, *butt* seals made with metal from *both* the 1/4-inch and 3/8-inch sizes exhibited catastrophic failure when immersed in liquid nitrogen. This corresponded to the results obtained when *tubular* graded seals were immersion tested. We concluded that a measurement of residual stress at room temperatures alone could not reliably indicate which metal samples would catastrophically fail.

3. *Low Temperature, Stress-Temperature Results*

Since room temperature stress measurement was not a suitable indicator, we decided to measure stress in the seal at intervals down to liquid nitrogen temperature. We call this test the "low temperature stress-temperature" test. We chose as samples the 1/4-inch

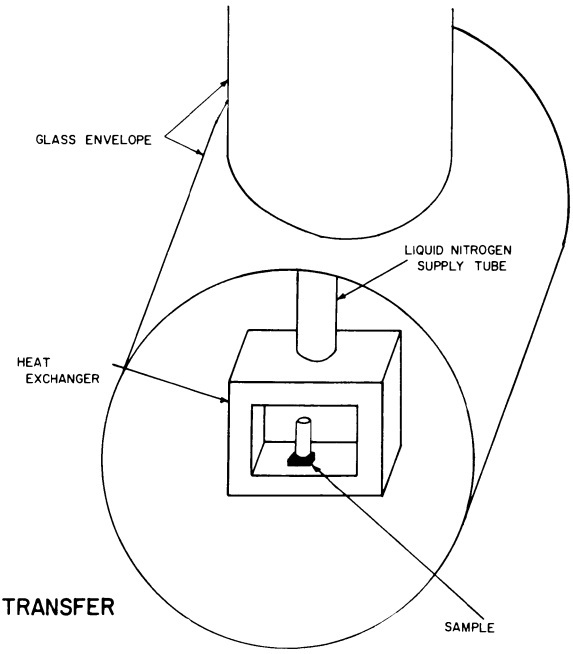

LOW TEMPERATURE HEAT TRANSFER APPARATUS

Figure 3

diameter and the ¾-inch diameter metal. The basic apparatus is shown in Figure 3. The test seals were prepared in the same form as the butt seals used in the butt seal immersion experiments, Figure 2. Figure 4 graphically shows the test results. Both samples had approximately the same stress level at 25°C. They continued to exhibit the same stress level down to about –50°C. Below –50°C. the rate of stress increase in the ¼-inch sample was less. From –100°C. down to –165°C., its stress moved 500 psi. toward neutral. As it was heated back from liquid nitrogen temperature, fracture occurred at the seal interface at approximately –100°C. The stress continued to move in the direction of increased tension even though the sample was fractured, until at 25°C. it was nearly 3000 psi. tension.

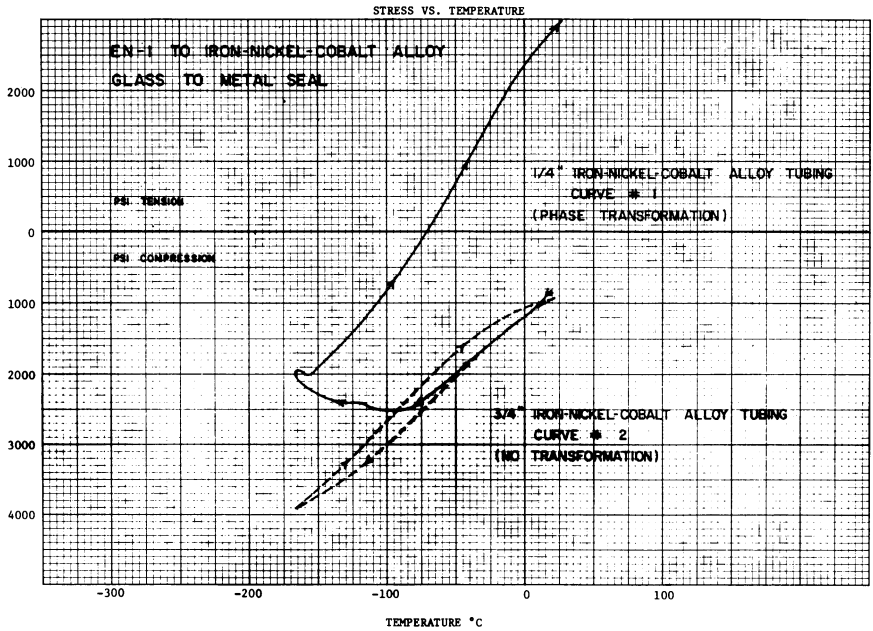

Figure 4

The behavior of the ¾-inch sample differed appreciably. After cooling and subsequent reheating, it underwent a "stress hysteresis" loop and returned to its original stress at 25°C. It did not fracture.

4. *Metallographic Analysis*

The above experiments all indicated that certain metal samples changed appreciably when immersed in liquid nitrogen, while others were not affected.

To determine the basic differences, metallographic analysis was made on ¼-inch and ¾-inch specimens, both before and after

immersion in liquid nitrogen. This analysis indicated that areas of the ¼-inch material had undergone a basic structural transformation. The chemical nature of the change was from gamma phase (face-centered cubic) to alpha phase (body-centered cubic). The body-centered structure has a greater volume, and thus causes an increase in tensile stress in the glass.

We later learned that iron-nickel-cobalt alloy is basically metastable and will transform when cooled below a certain point. The transformation temperature depends on composition control during manufacturing.

CONCLUSIONS

Fracture will occur when iron-nickel-cobalt to glass seals are immersed in liquid nitrogen, if the metal undergoes a phase change from gamma to alpha phase. This phase transformation causes the alloy to change in dimension, thermal expansion coefficient, and resistivity.

The immediate increase in dimension of the alloy tends to fracture glass seals to it. If the seal does not fracture at the instant the phase transformation occurs, fracture occurs during subsequent reheating, because of the severe increase in the thermal expansion coefficient of the alloy.

COMMERCIAL APPLICATION OF TEST RESULTS

In order to apply to advantage the results obtained, we established contact with the laboratory of one of the primary suppliers of iron-nickel-cobalt alloy. In our discussions we learned that the chemical constitution of the alloy, including the balance between the major constituents, and the amount and type of trace constituents are the primary factors which determine whether or not the alloy will undergo phase transformation. The carbon content is very influential on where the phase transformation occurs. An increase in carbon from 0 percent to 0.05 percent will lower the phase transformation point from about –50°C. down to about –200°C. The gamma to alpha phase transformation will always occur in this type of alloy, but the temperature at which it occurs is governed by the metal composition.

The metal supplier felt that he could furnish metal which *would* withstand a liquid nitrogen temperature immersion (–196°C.) without undergoing phase change. Presently, the ASTM has a specification on this alloy which requires that the phase transformation point is at –80°C. or lower. This limit is usually used by the metal suppliers. However, in view of the increasing commercial need for cryogenic vacuum equipment, the vendor felt that on request, allowances could be made during batching and melting of the alloy which would depress its transformation point the additional required 120°C.

By specifying "metal to withstand –196°C. immersion" on our purchase orders, the vendor now delivers an alloy melt which is suitable for cryogenic seals.

TEST METHOD

A glassblower can employ the following test method to determine whether or not his metal supply is adequate for liquid nitrogen use. All pieces of metal not known to be from the same lot or melt should be tested since it is possible, even probable, that metal from several different melts was used in preparing a given shipment of material.

1. The metal should be cut into $\frac{5}{16}$-inch squares, with thickness between .008 and .250 inch.
2. All burrs and sharp edgs should be removed by filing, sanding or grinding with a wet belt or aluminum oxide wheel. Silicon carbide wheels, belts or papers should not be used because they induce contamination.
3. The test samples should be degreased in acetone or trichloroethylene and air dried, followed by degassing in a wet hydrogen or cracked ammonia atmosphere.
4. After degassing, the samples should be sealed to the end of $\frac{1}{4}$-inch diameter glass cane, preferably Kimble K-650 or EN-1 glass. The seal can be made by R.F. heat, or with a flame.
5. The test seals should be annealed at 15°C. above the annealing point of the glass for 15 minutes, employing a heating rate of between 3 and 10°C. per minute and a cooling rate of 3 to 7°C. per minute down to 250°C., after which the samples may be removed from the furnace. Next the seals are dropped into a small Dewar flask of liquid nitrogen, with sufficient liquid nitrogen in the flask to allow the seals to be totally immersed. After 30 seconds the seals are removed using tongs or forceps and placed on several sheets of soft tissue paper to allow them to reheat to a point near room temperature. Care should be taken not to touch the seal interface during handling. A frost will form on the seals from condensation and freezing of water vapor from the ambient air, but the frost will disappear as the seal temperature moves back toward ambient.
6. The seals are now examined for fracture using jeweler's glass or 10 power microscope. If a fracture is detected, it is probably due to a phase transformation. If the seal is not fractured, the glassblower can be fairly certain that the metal has not undergone phase change and is suitable for use at liquid nitrogen temperatures.

SUPERCONDUCTING MATERIALS— PRINCIPLES AND APPLICATIONS

PETER R. SAHM
RCA Laboratories
Princeton, New Jersey

ABSTRACT

Superconductivity, truly a "space-age effect", awaits numerous applications in the future. While high field magnets for the control of nuclear fusion, particle acceleration in high energy physics, or in electron microscope lenses with higher resolution power, and while improved computer memories or switching elements constitute areas of serious research and development, other devices such as friction and lossless electric motors, energy storage circuits for space flight, heat valves at low temperatures, etc. are feasible but not yet reduced to practice. The practicality and the extent to which all of these concepts will be verified depends on superconducting materials' research. The greatest challenge to the materials' scientist is to overcome the low temperature limit of superconductivity, as the underlying principles do not suggest that a theoretical limit exists. The tremendous diversification of superconductors in recent years, from bulk to the form of thin films, from single phase to multiphase structures, from crystalline to amorphous structures, and from metallic to organic materials promises the discovery of improved superconductors in the future.

INTRODUCTION

Not long ago a friction-and loss-less running electric motor would have seemed a ridiculous thought—but the phenomenon of superconductivity has made it feasible today. When Kammerlingh Onnes, in 1911, discovered mercury with no detectable electrical resistance, he may have had a vague premonition that he just had opened one of the doors into the age that would fulfill many an engineer's dream. The obstacles that separated him from seeing any such realization were materials and the associated technology. However, since 1945 materials' science has become a broad and vigorous field of research and we are, indeed, approaching the realization of such dreams.

Superconductivity is peculiarly bound to the properties of materials as few other effects are and thus presents a special challenge to the materials' scientist. The interplay of thermodynamics, quantum mechanics, experimental physics, and metallurgy, all in view of extraordinary potential applications, make superconductors "space age stuff" that permit a realistic glimpse into future developments. In the following a simplified introduction into some of the basic phenomena, pertinent to the later discussion of applications and materials, will be given. Due to space limitations it cannot be all-inclusive. Nevertheless, it is hoped to develop a perspective of the direction into which materials' research in superconductivity is heading.

PHENOMENON OF SUPERCONDUCTIVITY IN THE LIGHT OF CURRENT THEORY[1-7]

Although a variety of phenomena occur in the superconducting state, the two that stand out (Fig. 1), also historically seen, are zero electrical

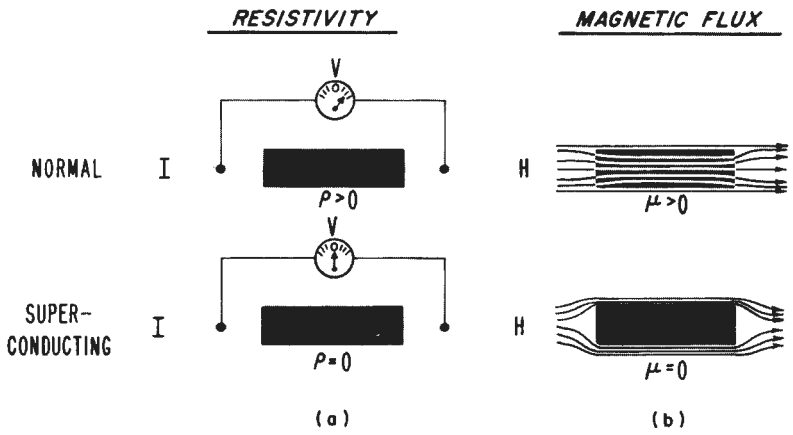

Figure 1

Two basic effects in superconductors: zero electrical resistance, f, and zero magnetic permeability, μ (magnetic flux expulsion).

resistance (Onnes, 1911) and expulsion of magnetic flux (Meissner-Ochsenfeld, 1933).

The Normal Metal Lattice

For reasons of comparison, first a normal metal lattice is sketched in Fig. 2b. It shows atoms arranged in a regular fashion with conducting electrons traveling randomly in between (Drude, 1900). Although in very pure specimens at low temperatures these electrons are transmitted through the lattice with mean free paths, l, up to 10^9 atomic spacings, they nevertheless encounter finite resistance during their flow through the metal (Fig. 1a) on account of collisions with the vibrating lattice cores, foreign atoms, irregularities in the structure, and, much less frequently, collisions among themselves. This gives rise to the electrical resistance. Heat is transferred both by the lattice vibrations (=phonons) and the electrons. Magnetic fields normally are attracted (Fig. 1b), either weakly (=paramegnetism) or strongly (= ferromagnetism). No metal is known that completely expels magnetic flux in the normal state (= perfect diamagnetism).

Zero Electrical Resistance

The interactions of electrons and atoms in a normal metal can be described as basically random. In contrast, superconductors can be understood as materials where a well ordered interaction between lattice cores and electrons takes place below a transition temperature, T_c, (Fig. 2a),

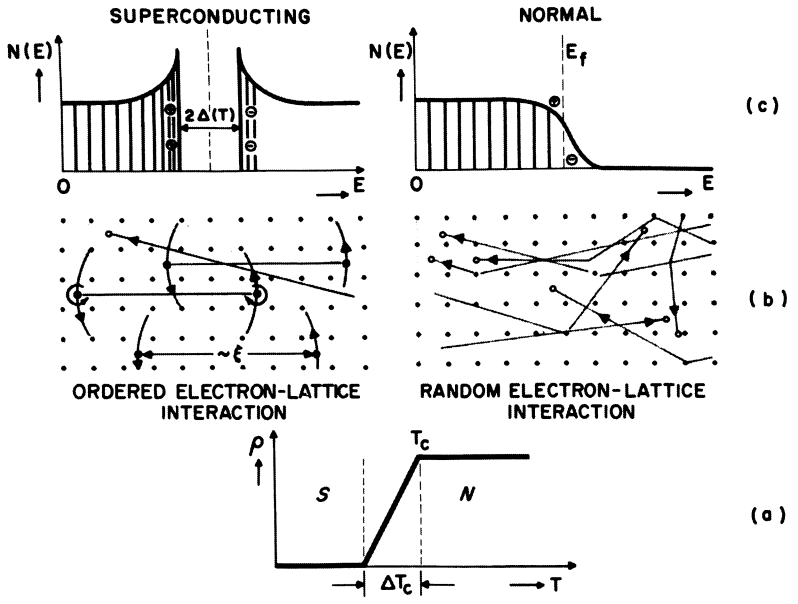

Figure 2

Schematic representation of the normal metal and superconductor behavior. (a) shows transition from normal to superconducting state in terms of vanishing resistivity, f. (b) compares electron movement in n. and s. lattice (each point represents approx. 100 real lattice points). (c) shows the energy gap $2\triangle(T)$ that exists between n. and s. states.

This can be envisioned by a conduction electron moving through the lattice creating a lattice wave ("virtual phonon") that attracts, in turn, another electron, thus forming electron pairs (Cooper, 1956). These coupled electrons are of opposite spin and, in the non current carrying case, of opposite but equal momentum (in Fig. 2b visualized as circular movement of 2 electrons around a common center). The average size of Cooper pairs can be identified with Pippard's range of coherence, ζ (1950), and varies between 50 and 10,000 Å for different superconductors. Not all of the electrons become superconducting below T_c; above 0°K. there is always a certain supply of normal electrons. Thus, the "two-fluid model" (Gorter and Casimir, 1934) considers a superconductor as a state with both normal and superelectrons. Only very few Cooper pairs are required to induce superconductivity. To break up the pairs again, an energy of the order of $2\triangle$ (=superconducting energy gap) must be supplied (Bardeen, Cooper, and Schrieffer, 1957). This is demonstrated in Fig. 2c by a plot of the density of electron state $N(E)$ against energy, E. While in the normal metal a continuous excitation is possible around the Fermi energy, E_f, in the superconductor a gap must be overcome to give excited states (=normal electron fluid).

Due to the well correlated interaction between electrons and atom cores no energy is lost and electric current is transferred without resist-

ance from one end of the crystal to the other. It has been shown that the resistivity of such materials, if at all present, is less than 10^{-29} Ω cm., which, if applied to a 1 cm. diameter ring with a selfinductance of $1\mu H$, would allow a "persistent current" to flow for longer than the age of our universe (according to present knowledge). Alternating currents are also freely transmitted up to frequencies which enter the range of the energy gap, $2\triangle$, where-upon the crystals transform into the normal state. Another feature of superconductors directly related to the ordered electron-lattice interaction is that heat conduction is drastically cut because normal lattice vibrations and normal electrons cannot couple into the superconducting lattice or the "super-electron fluid", and thus prevent any heat transfer.

The electron pair concept has been an extremely fruitful one. It has, for example, helped to predict the Josephson effects. Due to the dual nature of the electron, the correlated motion of Cooper pairs can also be understood as a completely correlated or "in-phase" wave motion through the entire lattice. In order to disturb this in-phase motion in a controlled manner, one separates two sections of a superconductor by a thin, insulating oxide layer (Fig. 3a), just enough to allow the tunneling of electrons through this layer. Two conditions are then found to exist in the I-V characteristic (Fig. 3b). In one, Cooper pairs tunnel through the oxide barrier such that a voltageless current persists up to a critical value (d.c. Josephson effect). In the other, Cooper pairs can only maintain their tunneling through the oxide by oscillation at infrared to microwave frequencies accompanied by the generation of electromagnetic radiation (Fig. 3a). Also, a small voltage, v_j, between 0 and $2\triangle$ (= the superconducting band gap) is then measured.

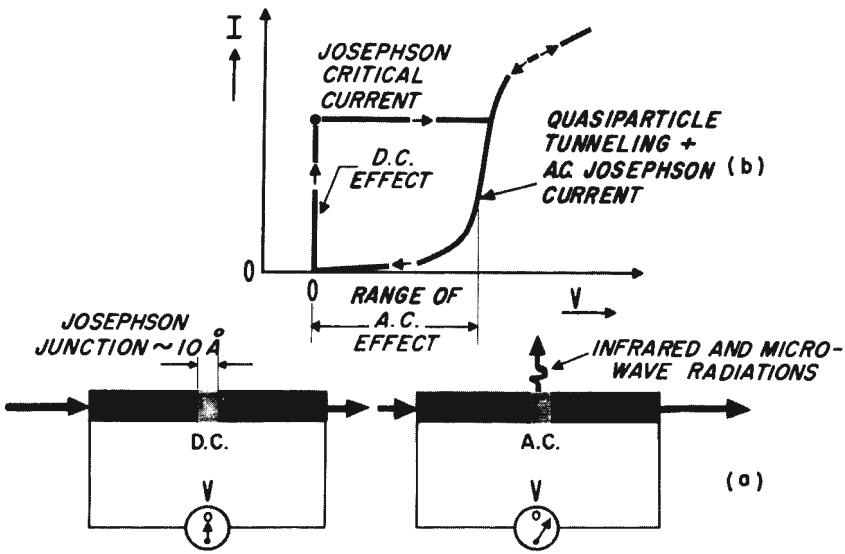

Figure 3
The d.c. and a.c. Josephson effects.

The Expulsion of Magnetic Flux

As indicated above, superconductors, besides being perfect conductors, may also be considered perfect diamagnets because they expel all magnetic flux. It is a rule of thumb, therefore, that ferromagnetism and superconductivity are not normally compatible (although in certain cases overlapping behavior has been reported). This rule can be qualitatively understood, if one remembers that ferromagnetism is due to spin alignment in a preferred direction whereas superconductivity requires a cancelling of spins (Fig. 2b). The interaction with magnetic fields has been widely studied and has led to the distinction of types I, II, and surface superconductivity.

Basically, all superconductors turn normal upon the application of a supercritical magnetic field, $H > H_{cx}$. To distinguish between the different types of superconductivity, we follow the GL theory (Ginsburg and Landau, 1950) which is based on 2 parameters: the coherence distance, ζ, which is the distance required for an appreciable change in the number of superelectrons, and the penetration depth, λ, which signifies the depth beneath a superconductor's surface where the magnetic field has decayed to a negligible value (London 1935). Using these, GL defined a dimensionless parameter

$$K(T) = \lambda(T)/\zeta(T) = 2\pi\sqrt{2}H_c\lambda^2/\varphi_0 = 8.87\ H_c\lambda^2/\varphi_0 \qquad (1)$$

which allows a conventional distinction between types I, II, and surface superconductivity (Fig. 4).

Superconductors for which $\lambda < \zeta$ (or more precisely $k < 0.707$) are said to exhibit type I superconductivity. As a rule, type I materials will not tolerate magnetic fields of more than a few hundred gauss. Larger fields than the "thermodynamical critical field", H_c, induce an abrupt transition into the normal state (Fig. 5). Type I materials are mostly elemental and highly pure metals with long mean free paths.

Type II superconductivity, found mostly in alloys, compounds, and impure materials with short mean free paths, is characterized by $\lambda > \zeta$ or $k > 0.707$ (Fig. 4). Here the thermodynamical critical field is replaced by two critical values: H_{c1} below which no magnetic flux is allowed into the specimen and H_{c2} ($>H_{c1}$) above which the specimen becomes normal (Fig. 5). While H_{c1} values are of the same order of magnitude as H_c in type I superconductors, H_{c2}-values may extend well into the 100,000 gauss region. This is made possible by the formation of essentially normal cores containing magnetic flux (for $H_{c1} < H_c < H_{c2}$, Fig. 5) which is maintained through the flow of vortex currents around each such core (Fig. 6b). In this "mixed state" normal cores and a superconducting matrix coexist due to negative interface energies between these two phases. The packing arrangement of these vortices follows geometric laws known from crystallography, and the packing density is a function of the external magnetic fields. Each flux line represents a magnetic quantum of the amount

$$\varphi_0 = hc/2e = 2 \times 10^{-7} \text{ gauss cm.}^2$$

where h = Planck's constant (6.625×10^{-27} erg sec.), c = speed of light (2.998×10^{10} cm/sec) and e = elementary charge (4.803×10^{-10} cgs.).

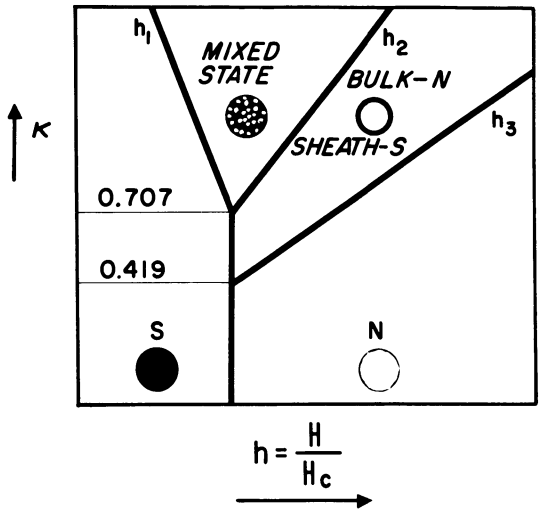

Figure 4
Relationship between reduced magnetic field, h, and Landau parameter, k.

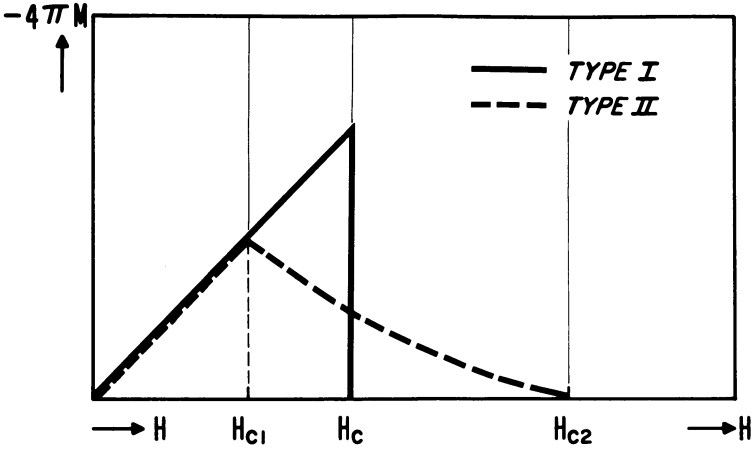

Figure 5
Behavior of magnetization, $4\pi M$, in type I and type II superconductors.

Finally, for $k > 0.419$, there can be surface superconductivity which exists only on surfaces that are parallel to magnetic fields, thus constituting a predominantly geometric effect. The critical fields, denoted by H_{c3}, are the largest possible of all. Surface superconductivity can be induced in type I of sufficiently large k (Fig. 4) and in type II superconductors and can also be found in the bulk of materials along inclusions which are parallel to the applied fields.

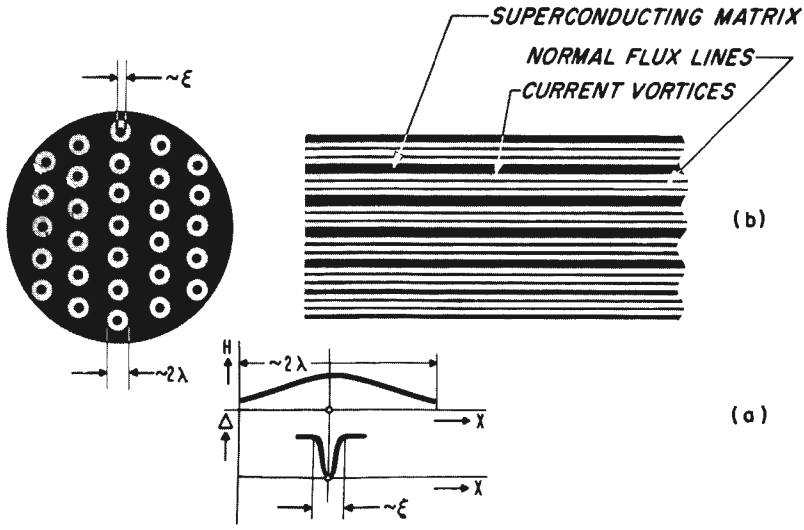

Figure 6

Magnetic flux quanta in type II superconductor (mixed state). (a) shows the conditions for type II behavior: $\lambda > \zeta$, and (b) envisions the arrangement of flux lines.

APPLICATIONS[3,8]

Although, at present, superconductors find several applications, much more potential use is indicated. In general, superconductivity does not open completely new fields of application, but rather improves old ones permitting higher efficiencies. Given the right materials, any of the following disciplines could be deeply affected: general electrical equipment, energy conversion, computer technology, communication, power transmission, transportation including space travel, as well as basic and applied research in numerous areas.

In Table I are compiled and correlated to the particular field of interest the basic superconductive phenomena. As apparent from the table, the most widely employable phenomena are zero electrical resistance, expulsion of magnetic flux, and the Josephson effects.

Zero power losses in superconductors are the most general reason for their use as perfect conductors. Efficiencies can thus be increased in the transmission of currents or permit, for example, printed or vapor deposited rather than heavily wrapped wires or coils for numerous devices, such as power lines,[9] transformers, motors, dynamos, electromagnets, etc. The fact that supercurrents do not decay makes also possible energy storage and computer memories.

Besides the Joule heat, another loss factor in present day machinery, namely loss by mechanical friction, can also be minimized by superconductive devices on account of magnetic flux expulsion or the principle of the superconductive bearing. Frictionless running gyroscopes, rotors,

and, possibly, friction reduced surface transport systems have been visualized.[10]. Other applications are in flux pumps used to concentrate magnetic fields through a "superconductive pumping action".

TABLE I

EXAMPLES OF SUPERCONDUCTIVE APPLICATIONS

Superconductive Phenomena		Existing and/or Potential Applications
1. zero electrical resistance	1.1 lossless current transmission	communication power lines coils (in transformers, motors, magnets, dynamos, rotors)
	1.2 persistent currents	power storage computer memory
2. magnetic flux expulsion (Meissner effect)		superconducting bearing superconducting gyroscope flux pump magnetic shield electric motor dynamo
3. Josephson effect	3.1 d.c. effect	computer switching element
	3.2 a.c. effect	microwave and infrared radiation -generator -detector -amplifier
4. normal to superconducting transition		switching element (cryotron)
5. steep or gradual resistance change in transition region		bolometer thermometer
6. zero electronic thermal conductance		heat valve
7. heat of transition		cooling device

Both the d.c. and a.c. Josephson effects (Fig. 3) promise important applications. The d.c. effect, in conjunction with normal superconductive tunnelling, promises use as a fast switching computer element[11] replacing its slower precursor, the cryotron (Fig. 7). The a.c. Josephson effect which has been compared to an "electromagnetic organ pipe"[7] effect, yields itself to the generation of coherent microwave and infrared radiation and also to their amplification and detection.

Other intriguing possibilities of use lie in the drastic change of resistivity within the transition region (Fig. 2). While broad transitions (impure materials with distorted microstructure) could be useful as low temperature thermometers, narrow transitions (very pure materials with equilibated microstructure) have rendered extremely sensitive radiation detectors, known as bolometers. Finally, the disappearance of the electronic contribution to the thermal conductivity in superconductors suggests the construction of heat valves at low temperatures. Cooling devices have been proposed utilizing heats of transition involved.

Both type I and II superconductors find use in the applications outlined above. The presently most active areas of research and development are computer elements and superconductive magnets, utilizing type I and type II materials, respectively. A quick look at each is taken in the following.

In computer switching elements and memory cores, tin and lead films have been most widely investigated. Their type I behavior, *i.e.* their

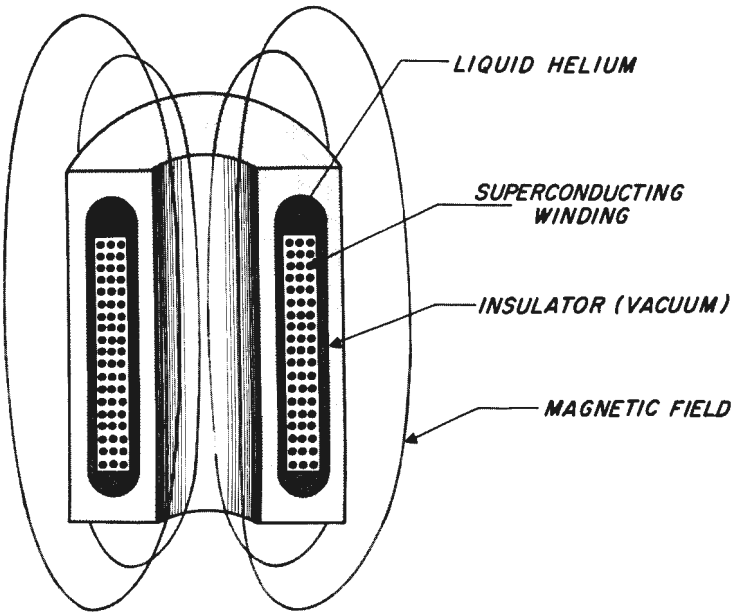

Figure 7

Principle of superconducting magnet for room temperature operation. Coil is cooled by liquid He to operating temperature.

toleration of only small currents and magnetic fields, makes them ideal for the low power requirements in computer switching. Referring to Fig. 7, lead would be used as the high and tin as the low T_c-and H_c-material. The film rather than the wire wound versions (Fig. 7) are employed exclusively. Their smaller dimensions, and thus resistance and inductances, assure much faster switching. The advantage of cryotrons above ferrite and/or transistor elements are their negligible energy consumption, because no power is dissipated, thus allowing very compact construction.

The large power requirements of high field magnets[12,13] utilize type II superconductors such as niobium stannide, niobium alloys with zirconium or titanium, and others. Nb_3Sn, in particular, finds use today both in small and large laboratory magnets after much developmental work to wind coils from the extremely brittle material.[13]

The great drawback of conventional high field magnets is their extremely high power consumption. A 100,000 gauss magnet with a 3 cm. bore, for example, requires a power of approximately 150 kw. and a cooling capacity of about 4,000 ltr/min of water.[3] This same magnetic field could be generated by a persistent current of 20A in a superconductive coil with no power loss involved[3]. Such devices (Fig. [8]) are only limited by the critical fields attainable. Large magnetic fields are needed, for example, in high energy physics for particle acceleration, particle tracking in spark or bubble chambers, in electron microscopes for the magnetic lenses (which would enable one to see individual atoms), and in energy conversion devices utilizing magneto-hydrodynamics or nuclear fusion. Last no least, space travel could benefit from magnetic shielding holding back dangerous cosmic radiation or in controlling the plasma in plasma propulsion systems.

The greatest difficulty with all mentioned applications is the "cryogenic barrier", *i.e.* the requirement of liquid helium temperatures (boiling point of liquid He is 4.2°K.) for their operation. Recently a superconductor has been synthesized[14] that may permit the practical use of liquid hydrogen (boiling point 20.4°K.). Although superconductors at room temperature, or higher, are the "ultimate dream", superconductivity at liquid nitrogen temperature (77°K.) would already signify a major advance in this field. In the following discussion, therefore, the emphasis will be placed on transition temperatures of materials.

THE SUPERCONDUCTING TRANSITION TEMPERATURE[1,2,6]

Transition temperatures are not yet quantitatively predictible. Nevertheless, the BCS theory (Bardeen, Cooper, and Schrieffer, 1950) has provided several criteria by

$$T_c = 1.14\ (h\nu)_{av} exp[-1/N(0)V] \qquad (2)$$

where $(h\nu_{av}) \simeq$ Debye temperature in °K, $N(0)$ the density of states at the Fermi surface in $1/eV\text{cm}^3$, and V = interaction energy between electrons and phonons in eV cm^3.

The Debye temperature can be approximated by[15]

$$\theta = (4385\sqrt{z/M})/d^{1.23} \qquad (3)$$

where z = number of outermost shell electrons, M = molecular weight in

g/mol, and d = average/distance between lattice sites in cm. Eq. (3) leads to the "isotope effect" (Maxwell and Reynolds *et al.*, 1950)

$$T_c \sim 1/M^{1/2} \tag{4}$$

for an individual material (where d_m and z are approximately constant). Eq. (4) has been verified in several cases and emphasizes the importance of lattice waves (and their dependence on the mass of lattice cores)—electron interactions. However, Eq. (4) does not hold in certain transition metals compounds, and the recent discovery of a "positive isotope effect"[51] in U^{235} (T_c = 2.10°K.) and U^{238} (T_c = 2.19°K.) suggests that other superconducting mechanisms than BCS must be valid for certain materials. Direct proportionality between specific heat, c_v, and θ have stimulated c_v measurements in superconductors. Furthermore, θ is directly related to the atomic volume by the Grüneisen constant. Thus, also a pressure dependence of T_c can be expected (and has been shown), mostly where dT_c/dp values are negative.[16]

The density of states, $N(0)$, should be large for large T_c. Thus, materials with an even number of valence electrons per atom, e/a, are less likely to be superconductors than such with an odd number because in the

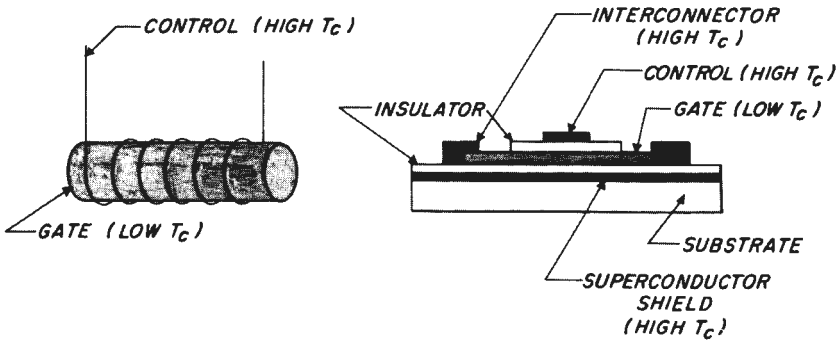

Figure 8

Wire wound and thin film cryotron. If, in (a), sufficient current is sent through the control coil of high Tc and Hc material, a field greater than the critical field of the gate is generated, switching the gate to normal. (b) shows the thin film version of the cryotron.

first case the filling of a Brioullin zone is favored and thus $N(0)$ will be small. This expectation has been substantiated for the transition metals by an empirical rule (Matthias, 1957) which shows that the highest T_c's do, indeed, occur at approximately uneven e/a ratios, 5 and 7, whereas in non-transition metals a smooth rise of T_c with e/a is found (Fig. 9). $N(0)$ is related to the Sommerfeld specific heat constant by

$$\gamma = (2/3)\pi^2 k^2 N(0) \tag{5}$$

where k = Boltzmann's constant (1.38×10^{-16} erg/deg).

The constant and the electronic contribution to the specific heat, C_{es}, relate numerically to the transition temperature:

$$T_c = C_{es}\ (T)/2.43\gamma \tag{6}$$

The interaction energy, V, can only be estimated from the electrical conductivity or mean free path, l. It is seemingly paradoxical that low normal conductivity metals will more likely become superconductors than normally high conductivity metals. In the former the interaction between lattice and electrons is greater and thus V can be expected to be higher than in the latter. To outline qualitatively how T_c depends on the conductivity or the mean free path, l, we look for a relationship of T_c with the coherence distance ζ. With the help of the BCS relation

$$T_c = 2\triangle(0)/3.52k \qquad (7)$$

where $\triangle(0)$ is the energy gap at 0°K., the following formula can be derived:

$$T_c = 0.18\ hv_o/k\zeta \qquad (8)$$

where v_o is the Fermi velocity at 0°K. Eq. (8) holds true only for pure type I superconductors where $l \gg \zeta$, a modified coherence length, ζ', must be introduced where $\zeta' \cong l$ as l tends to zero.

Thermodynamically, the transition temperature also allows certain conclusions to be drawn with respect to critical fields:

$$H_c = 0.413\ T_c\sqrt{\gamma}(oe),$$

in other words, larger critical fields can be expected in higher T_c materials.

Principally, no upper limit for T_c can be set. According to Eq. (2) the highest possible limit has not been reached yet. Numerous attempts have been proposed to increase T_c by artificially affecting some of the constants, for example by widening the energy gap[17] $\triangle(0)$ in Eq. (7) or by creating special surface conditions through monolayers of foreign atoms,[18] the application of electric or magnetic fields,[19] etc.

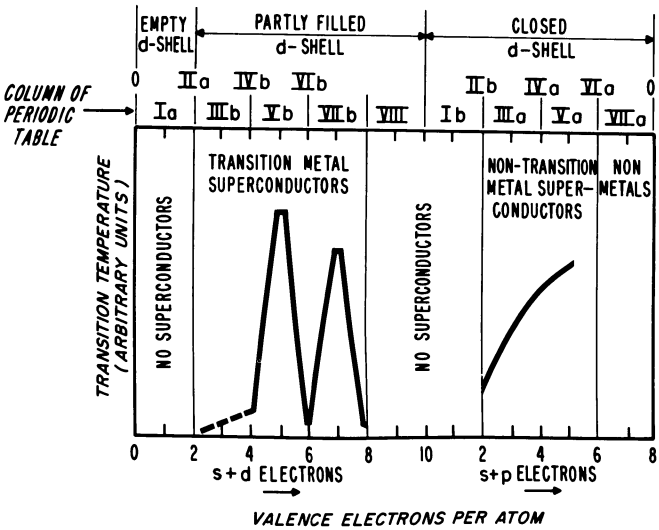

Figure 9

Transition temperature of elements, compounds, and alloys as a function of the average electron to atom ratio with nomenclature from the periodic system of elements (see also Fig. 11).

SUPERCONDUCTING MATERIALS

The immense diversity of materials makes it difficult to choose a frame of reference which encompasses all types of materials known. To simplify the procedure for our purpose we adopt, with minor modifications, a schematic proposed by Seitz[20] in Fig. 10. Referring to this, super-

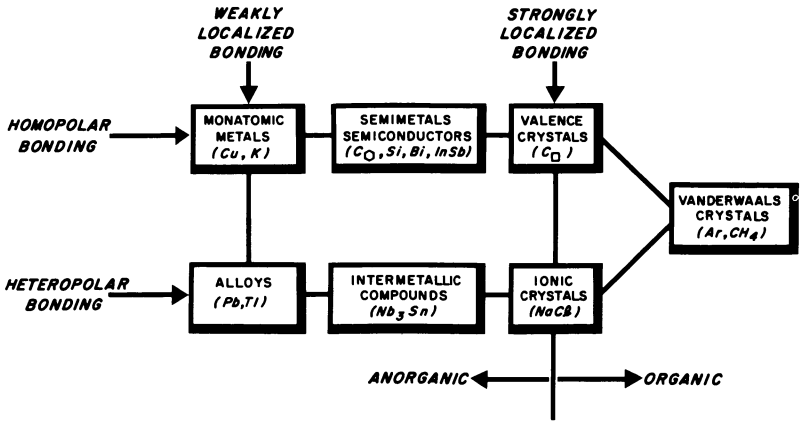

Figure 10
Bonding relationship between solids.

conductivity is most pronounced in intermetallic compounds, in elementary metals and alloys, and in semiconductors, in the order of decreasing T_c. There has been very little indication of superconductivity in valence and ionic crystals so far,[21] although considerable interest exists, for example, in organic superconductors.

The Elements

In Fig. 11 all reported superconducting elements are listed. In terms of Fig. 10 we are dealing here with "monatomic metals". Elements which are normally non-metallic must be converted into the metallic state (Si, Ge, Bi, Se Te) before they become superconductors, for example by the use of elevated pressures. Thus, the numbers given in Fig. 11 do not represent the only possible T_c-values, as many of the "normal" superconductors change their transition temperatures when subjected to special treatment such as noted above or other metallurgical variables, for example straining by cold work, addition of soluble or insoluble impurities, evaporation in thin films, etc. From Fig. 11 the following general criteria (Fig. 9) have been derived for the occurrence of superconductivity.[22]

Superconductors are metallic substances with e/a ratios between 2 and 8 where maxima are found at values of 5 and 7 in many cases. Certain crystal structures (A1, A2, and A3 in the elements), high atomic volumes, and small atomic masses are favorable for their occurrence.

Intermetallic Compounds and Intermediate Phases

This is the realm of type II superconductors with the highest T_c's and H_c's so far known. Their type II behavior is linked with low elec-

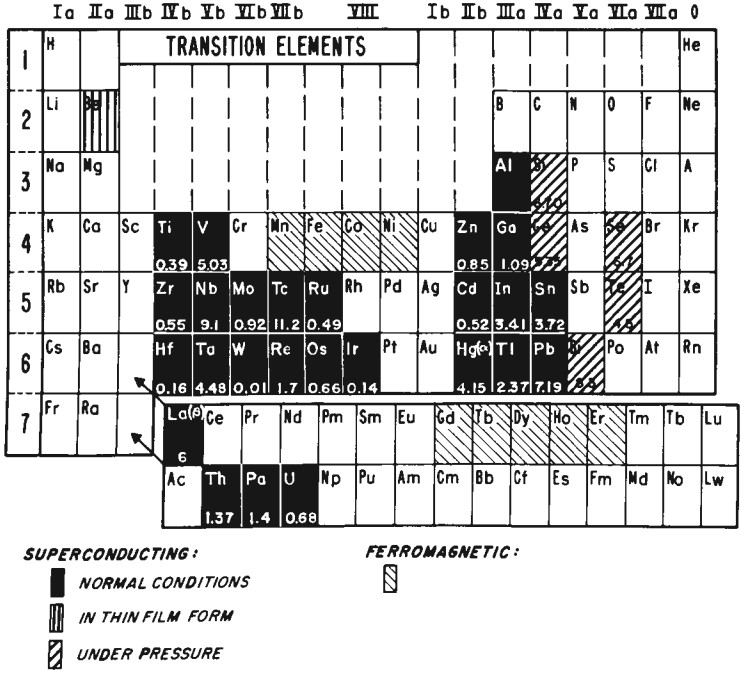

Figure 11

Superconductivity in the periodic system of elements. Transition temperature values are for bulk material. Only for Be a thin film value is given as no bulk transition has been yet reported.

trical conductivity and thus small mean free paths and coherence lengths. Important applications are in superconductive magnets, for which the material utilized mostly is Nb_3Sn.

The transition temperatures of intermetallic compounds appear to be strongly linked to crystal structures as shown in Table II. This is particularly obvious in Nb_3Au[23] where a change in structure, not in stoichiometry or in the e/a ratio, results in remarkable T_c changes. It is conjectured, for example, that the feature conducive to supecronductivity in the A-15 structure are the three straight chains of transition metal atoms extending through the lattice with interatomic separations smaller than in elementary or otherwise alloyed form. Stoichiometry (Table II, Nb_3Ge) and mean atomic volume [24] have proved to be important as well. While in the most favorable, the A 15 types structure (Table II), the mean atomic volumes vary between 14 and 22Å^3, most other structures show maximal T_c-values at 16 Å^3. In connection with the atomic volume dependence, it may also be mentioned that n-n (nearest neighbor) separations between the host lattice atoms of particular compound classes such as La- or Bi-compounds[25] were shown to have optimal values (3.5 in Bi- and 3.6Å in La-compounds) for the highest T_c's. The table further demonstrates that for each structure class certain e/a ratios are preferred.

Order, *i.e.* the nonrandom, symmetrical arrangement of atoms in the lattice ("superstructures") is another term often believed to favor high T_c values. In general, the high T_c compound superconductors deviate from BCS-behavior more than other bulk superconductors. For example, deviations from the isotope effect have led Matthias to suggest that electron pairing by magnetic polarization could be involved[26] rather than the normal BCS behavior.

Alloying of two high T_c-superconductors, in some cases, raises T_c. It appears that in many of these pseudo-binary systems slight maxima are observed on the higher T_c-compound rich sides. The most pronounced such case has recently been announced in the Nb_3Al-Nb_3Ge system with the highest T_c so far known[14] (Table II).

TABLE II

EXAMPLES OF HIGH T_c SUPERCONDUCTORS

Compound	*Transition Temperature* (°K.)	*Crystal Structure*	*Electron to Atom Ratio*	*Remarks*
NbT_{c3}	10.5	cubic(A12)	6.5	
Nb_3Au	11.0	cubic(A15)	4.0	
Nb_3Au	1.2	cubic(A2)	4.0	
Nb_3Ge	~17	cubic(A15)	4.75	metastable stoichiometric
Nb_3Ge	6.9	cubic(A15)	4.75	stable, nonstoichiometric
Nb_3Al	18.3	cubic(A15)	4.5	
Nb_3Sn	18.4	cubic(A15)	4.75	
Nb_3Ga	14.5	cubic(A15)	4.5	
V_3Sn	16.5	cubic(A15)	4.75	
V_3Si	17.1	cubic(A15)	4.75	
$Nb_3Al_{0.8}Ge_{0.2}$	20.1	cubic(A15)	4.55	
NbN	16.0	cubic(B1)	5	
$NbC_{0.977}$	11.1	cubic(B1)	4.75	
$NbN_{0.65}C_{0.35}$	16.7	cubic(B1)	4.83	
La_3In	10.4	cubic($L1_2$)	3	

Metal Alloys (Solid Solutions)

In alloying all of the factors in Eq. (2) are affected such that θ (and thus the specific heat and atomic volume), $N(0)$, and V changes must be considered. In addition to these factors the "anisotropy effect" (Fig. 12) is observed in dilute solutions responsible for an initial drop of T_c in numerous cases. [6] This drop depends on the normal reciprocal electron mean free path, $1/l$, which causes a washing out of the energy gap anisotropy present in the pure metal. Only after sufficient alloying, when $l < \zeta$, a "charge effect" and an "isotropic mean free path effect" become predominant. These are summarized both under the term "valence effect".[27] In the valence effect region normally a proportionality is found between T_c and the electron concentration (see also Fig. 9) and $1/l$, affecting $N(0)$ and V of Eq. (2), respectively.

When considering the behavior of metal alloys one should distinguish between transition and non-transition metals[26] (Figs. 9 and 11). While for the latter, as well as for a combination of both, the statements made above, typically apply, transition metal alloys show deviations. Maxima are observed due to improved e/a ratios in terms of Fig. 9. However, also ordering phenomena can cause maxima in the T_c behavior as in the case of the isoelectronic system Ti-Zr[28] (Fig. 12), where a superstructure[29] is observed in the center of the system.

A further parameter to be considered in alloying is ferromagnetism, which, as pointed out earlier, is not usually compatible with superconductivity. A particularly interesting case of interaction has been reported for

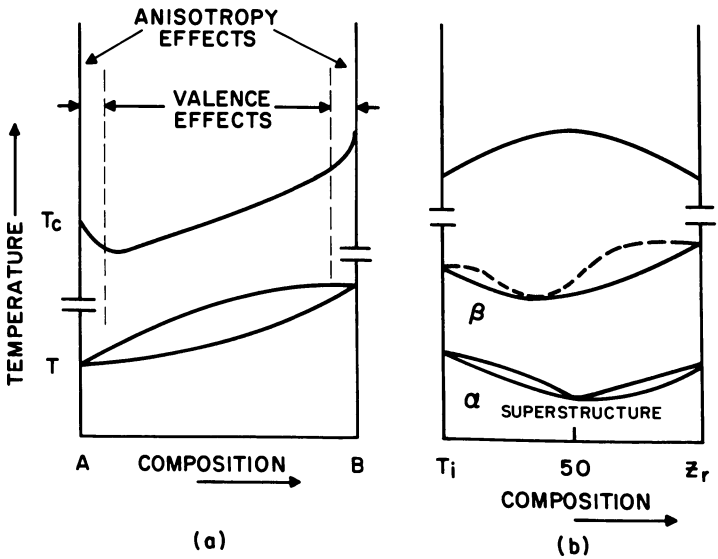

Figure 12

Schematic representation of the superconducting behavior of metal alloys with complete mutual solubility. (a) demonstrates expected behavior of nontransition meals, (b) the effect of order.

lanthanum alloys containing 1 at .% of rare earth elements. From Fig. 13 it is seen that gadolinium, being the strongest ferromagnetic metal in this series, causes the largest T_c depression. [26] In other alloys, however, as in the case of Ti-Fe solid solutions, increases of T_c have been reported despite the addition of a ferromagnetic substance.[30] Under certain circumstances even the coexistence of ferromagnetism and superconductivity has been suggested.[30,31]

Superconducting Semiconductors

Superconducting semiconductors require a minimum amount of 10^{19} cm.$^{-3}$ positive carriers (hole conduction or positive Hall coefficients) and a polar, multivalleyed band structure.[32] Due to these limitations not many have become known so far. From Table III is seen that their transition temperatures are all below 1°K.

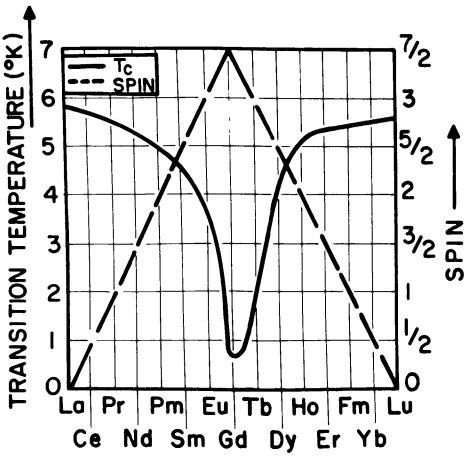

Figure 13
Superconductivity of La-solid solutions with 1 at .% rare earth metals of systematically changing spin.

TABLE III

TRANSITION TEMPERATURES OF SEMICONDUCTING SUPERCONDUCTORS[33,34,50]

Material	*Transition Temperature* °K.	*Carrier Concentration* cm.$^{-3}$
$SrTiO_3$	0.25 0.28	2.5×10^{20} 3.3×10^{19}
GeTe	0.08 to 0.30	8.5×10^{20} to 15×10^{20}
SnTe	0.10 to 0.21	

Other semiconductors,[35] such as Si and Ge, GaSb, InSb, or AlSb,[36] and the semimetals Bi, Se, and Te can also be superconducting, but only after transformation into a metallic phase attained under high pressures (Fig. 11). It may be of interest to note that $SrTiO_3$ besides being a semiconductor is also a ferroelectric material. It has been suggested that under extremely high magnetic fields of several 100,000 gauss materials such as those in Table III may become high temperature superconductors.[19]

Organic Superconductors

An almost entirely untapped field of materials lies in carbon chemistry. Although little practical success has so far been achieved, theoretical expectations run high in that room and higher temperature superconductors might be produced.[37] The interesting aspect in organic substances is that engineering a superconductor from first principles, *i.e.* the "elementary bricks of nature" appears feasible. The basic thought, as put forth by A. W. Little,[10,37] is to synthesize a central chain molecule (Fig. 14) that will have highly polarizable side arms attached to it, in such a way as will allow an interaction between electrons and lattice vibrations (=phonons) and thus produce "one-dimensional superconductivity". In practice, recently a vanadium-organic composite has shown first promising results.[38]

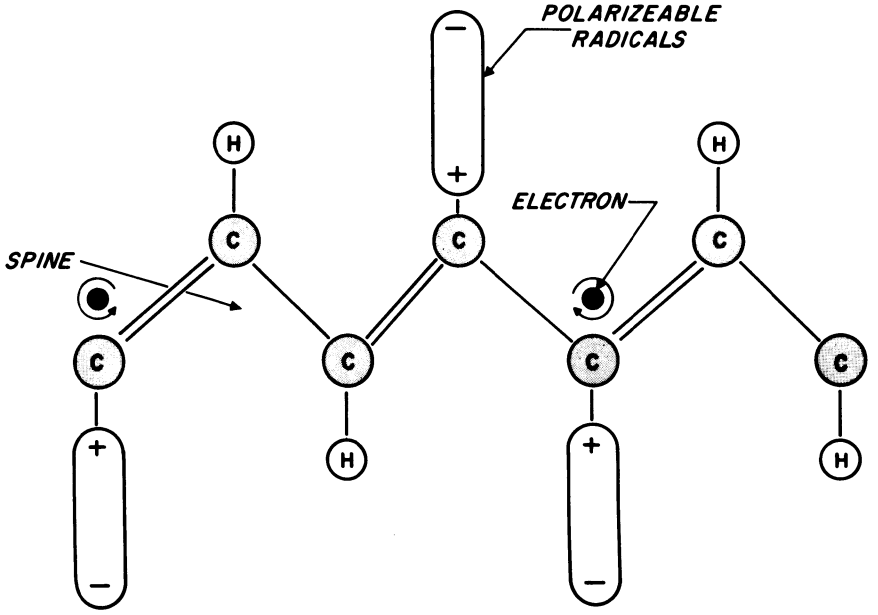

Figure 14
Hypothetical organic superconductor after W. A. Little. An electron carrying "spine" (chain of C-atoms) is lined by polarizeable side molecules which induce the phonon-electron interaction required by the BCS-theory.

Limited success has also been reported in "two dimensional" C_8M (M = K, Rb, or Cs) graphite lamellar compounds,[39] although their two-dimensionality has not been established beyond doubt.

Multiphase Structures (= Composites)

The engineering on the elementary particle level, such as sketched in the previous paragraph, has not yet yielded practical results; however, metallurgical efforts on a somewhat more macroscopic basis, in the field of immiscible systems or multiphase structures, has already provided several interesting materials and concepts.

By introducing one or more additional phases into a material, another degree of freedom is gained in the control of its physical properties. To fully characterize a composite material, primarily geometric factors must be considered besides chemical composition as shown in Table IV,[40] head row. Geometric dimensions also affect very strongly the superconducting behavior of multiphase structures.

Historically, the first composite to show a remarkable change, namely from its normal type I to type II superconductivity, was mercury metal that had been squeezed into a matrix of Vycor glass such that its dimen-

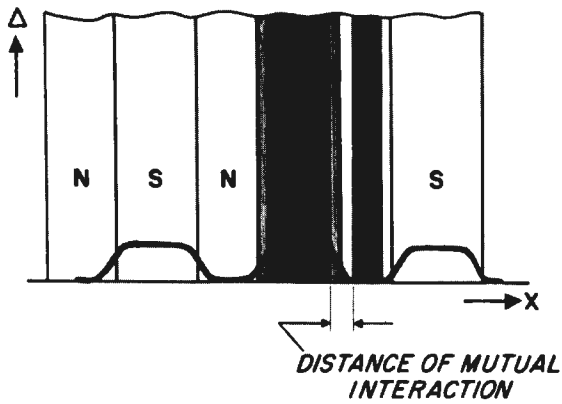

Figure 15

The proximity effect in a two-phase structure. The energy gap, $\triangle$, is affected over approximately the coherence distance at the phase boundaries.

sions were smaller than the penetration depth, λ.[41] The transition temperature, however, was not much affected. Other "artificial eutectics" produced by complex processes (Table IV), using superconductor-normal metal combinations (niobium wires imbedded in a copper matrix) have shown T_c degradations due to the proximity effect[42] (Fig. 15). This effect predicted not only that normal metals can become superconducting when in close proximity to a superconductor but also that T_c decreases for superconductors in proximity to normal metals.

An active area of composite structures for superconductivity has been in eutectics (Table IV).[43,44] Cline *et al.*[49] could, for example, show that a Nb-Th eutectic withstood critical fields 40 times higher than either

TABLE IV

CHARACTERIZATION OF COMPOSITE MATERIALS (Head Row from (1) to (4))

EVALUATION OF PREPARATIVE METHODS ((0)-Column)

SEVERAL SUPERCONDUCTOR EXAMPLES ((00)-Column)

0. *Method of Preparation*	*Scope of Possible Phase Combinations with Respect to*									00. *Examples of Superconductive Composites*
	1. *Chemical Composition*	2. *Spatial Arrangement*					3. *Phase Boundary Condition*	4. *Lattice Continuity*		
		2.1 *Relative Quantities*	2.2 *Relative Distribution*	2.3 *Geometrical Dimension*		2.4 *Orientation*		*Orientation*	*Density*	
				Size	*Shape*					
1. Vapor Deposition	$\frac{+}{-}$	+	$\frac{-}{+}$	$\frac{+}{-}$	$\frac{-}{+}$	$\frac{-}{+}$	−	+	+	Thin Films: Switching devices Josephson junctions Granular supercon.[47]
2. Melt Growth	−	−	−	−	−	$\frac{-}{+}$	−	+	+	Nb-Th[49] Controlled[45] Eutectics
3. Powder Metallurgy: Sintering	$\frac{+}{-}$	+	$\frac{-}{+}$	+	+	−	$\frac{-}{+}$	−	$\frac{-}{+}$	
Sintering with Liquid Infiltration	$\frac{+}{-}$	+	$\frac{-}{+}$	$\frac{-}{+}$	$\frac{-}{+}$	−	$\frac{-}{+}$	−	$\frac{+}{-}$	
Hot Pressing	+	+	$\frac{-}{+}$	+	+	−	$\frac{-}{+}$	−	+	Nb_3Sn-Al_2O_3[40] Nb_3Sn-ferrite[40]
4. Complex Processes	+	+	+	+	+	+	+	+	+	Hg-Vycor glass[41] Nb-Cu[42]

+ no limitation; − limited; $\underline{+}$ few limitations; $\overline{+}$ many limitations

Nb or Th alone. The advent of "controlled eutectics"[45] promises more interesting such materials in the future, in particular with respect to the proximity effect, type II, and surface superconductivity as well as other geometrical considerations. "Thin films" is the most active area in composite materials. For superconducting applications films normally are used in multiphase form, be it in cryotrons (Fig. 7), Josephson junctions (Fig. 3) or as granular superconductors,[46] *i.e.* extremely fine grained polycrystalline films. In particular the latter have been intensely pursued recently with respect to their transition temperatures. For example, in Al-films with average grain size diameters of 40Å and Al_2O_3-enriched grain boundaries, a sixfold increase in T_c has been reported.[47] Similar observations have been made with tin, gallium,[47] and tungsten[48] where stabilization of such small grain sizes was apparently achieved through recrystallization inhibiting agents in the grain boundaries. Explanation for this T_c increase is, although no unambiguously so, considered due to a grain size effect where superconductivity is enhanced by a large grain boundary surface area. If T_c-increases of the magnitude shown above could be verified with high T_c superconductors such as Pb, Nb, Nb_3Sn, or the like, then the jump into "warm superconductivity" would be accomplished.

OUTLOOK

While extensive research has been carried out in superconductivity, much more is required to understand all observed phenomena. In the light of the anomalous behavior of numerous superconducting materials it can be expected that the known mechanisms of superconductivity will be supplemented by modifications or even new concepts. Better understanding augmented by several recently approached fields of materials preparation promise the discovery of new as well as improved superconductors. In particular, high pressure technology, rapid quenching methods, and the synthesis of multiphase structures both in macroscopic eutectics, thin films) and in microscopic dimensions (organic materials) appear significant. Also, "artificial superconductivity," induced by external condition such as electric or magnetic fields, surface layers, etc. seems possible.

ACKNOWLEDGMENTS

It is a pleasure to acknowledge several inspiring discussions with J. I. Gittleman, F. Kolondra, and R. M. Williams.

REFERENCES

1. E. A. Lynton, *Superconductivity,* 2nd ed., J. Wiley and Sons Inc., New York 1964.
2. C. Kittel, *Introduction to Solid State Physics,* 3rd ed., J. Wiley and Sons Inc., New York 1967.
3. V. L. Newhouse, *Applied Superconductivity,* J. Wiley and Sons Inc., New York 1964.
4. W. Finkelnburg, *Einführung in die Atomphysik,* Springer Verlag, Berlin 1962.
5. W. Schallreuther, *Grimsehl Lehrbuch der Physik,* vol. 4, 13th ed., B. G. Teubner, Verlagsgesellschaft, Leipzig 1959.
6. J. D. Livingston and H. W. Schadler, *Progress in Materials Science,* vol. 12, ed. B. Chambers, p. 183 (1963).
7. D. N. Langenberg, D. J. Scalapino, and B. N. Taylor, *Sc. Amer.* **214,** May 1966, p. 30.
8. T. A. Buchhold, *Sc. Amer.* **203**, March 1960, p. 74.
9. R. L. Garwin and J. Matisoo, *Proc. IEEE* **55,** 538 (1967).

10. W. A. Little, *Sc. Amer.* **212,** Febr. 1965, p. 21.
11. J. Matisoo, *Proc. IEEE* **55,** 172 (1967).
12. J. E. Kunzler and M. Tanenbaum, *Sc. Amer.* **206,** June 1962, p. 60.
13. Several articles in *RCA Engineer* **12,** pp. 7-29 (1967).
14. B. T. Matthias *et al., Science* **156,** 645 (1967).
15. F. Halla, *Kristallchemie und Kristallphysik metallischer Werkstoffe,* Johann Ambrosius Barth Verlag, Leipzig 1957.
16. J. L. Olsen *et al., Rev. Mod. Phys.* **36,** 168 (1964).
17. R. H. Parmenter, *Phys. Rev.* **140,** A1951 (1965).
18. V. L. Ginsburg, *Phys. Letters* **13,** 101 (1964).
19. J. A. Hulbert, *Proc. Phys. Soc.* **90,** 237 (1967).
20. F. Seitz, quoted in: W. Schallreuther, *Grimsehl Lehrbuch der Physik,* Vol. 4, 13th ed., B. G. Teubner Verlagsgesellschaft, Leipzig 1959.
21. K. Andres, N. A. Kuehler, and M. B. Robin, *J. Phys. Chem. Solids* **27,** 1747 (1966).
22. B. T. Matthias, *Progress in Low Temperature Physics,* Vol. 2, p. ed. C. J. Gorter, *Interscience Publ.,* New York 1957.
23. E. Bucher *et al., Phys. Letts.* **8,** 27 (1964).
24. B. W. Roberts, *Intermetallic Compounds,* ed. J. H. Westbrook, p. 581, John Wiley & Sons, New York 1967.
25. T. F. Smith and H. L. Luo, *J. Phys. Chem. Solids* **28,** 569 (1967).
26. B. T. Matthias, T. H. Geballe, and V. B. Compton, *Rev. Mod. Phys.* **35,** 1 (1963).
27. J. S. Shier, University of Illinois, Ph.D. Thesis, 1966.
28. E. Bucher *et al., Rev. Mod. Phys.* **36,** 146 (1964).
29. M. Hansen, *Constitution of Binary Alloys,* 2nd ed., McGraw-Hill Book Co. Inc., New York 1958.
30. B. T. Matthias, *IBM J.* **6,** 250 (1962).
31. J. E. Crow, R. P. Guertin, and R. D. Parks, *Chemical and Engineering News,* May 1, 1967.
32. M. L. Cohen, *Phys. Rev.* **134,** A511 (1964).
33. J. F. Schooley and W. R. Thurber, *J. Phys. Soc. Japan,* Suppl. **21,** 639 (1966).
34. R. A. Hein, J. W. Gibson, and R. L. Falge, *J. Phys. Soc. Japan,* Suppl. **21,** 643 (1966).
35. J. Wittig, *Z. Phys.* **195,** 215 (1966).
36. J. Wittig, *Science* **155,** 685 (1967).
37. W. A. Little, *Phys. Rev.* **134,** A1416 (1964).
38. H. McConnell, F. R. Gamble, and B. M. Hoffman, *Proc. Natl. Acad. Sci.* **57,** 1131 (1967).
39. F. J. Salzano and M. Strongin, *Phys. Rev.* **153,** 533 (1967).
40. P. R. Sahm, Synthesis and Characterization of Electronically Active Materials, p. 77, Contract No. SD-182, ARPA Order 466, RCA Labs., Princeton, N. J., 1966.
41. C. P. Bean, M. V. Doyle, and A. G. Pincus, *Phys. Rev. Letts.* **9,** 93 (1962).
42. H. E. Cline *et al., J. Appl. Phys.* **37,** 5 (1966)
43. S. A. Levy, Y. B. Kim, and R. W. Kraft, *J. Appl. Phys.* **37,** 3659 (1966).
44. O. S. Lutes and D. A. Clayton, *Phys. Rev.* **145,** 218 (1966).
45. R. W. Kraft, *J. Metals* **18,** 192 (1966).
46. R. H. Parmenter, *Phys. Rev.* **154,** 353 (1967).
47. B. Abeles, R. W. Cohen, and G. W. Cullen, *Phys. Rev. Letts.* **17,** Q562 (1966).
48. W. Buckel and R. Hilsch, *Z. Phys.* **138,** 109 (1954).
49. H. E. Cline, R. M. Rose, and J. Wulff, *J. Appl. Phys.* **34,** 1771 (1963).
50. L. Finegold, R. Mazelsky, B. B. Triplett, Y. K. Huln, and N. E. Phillips, *Proc. 1966 Low Temperature Calorimetry Conf.,* ed. O. V. Lounasmaa, Ann. Acad. Sci. Fennicae A VII, No. 210 (1966), p. 129.
51. R. Fowler, J. Lindsay, and R. White, H. H. Hill, and B. T. Matthias, *Phys. Rev. Letts.* **91,** 892 (1967).

A SIMPLE COMPARATOR FOR COMPARING SEALING GLASSES

J. L. A. FRENCH
Department of Chemistry
University of Toronto
Toronto 5, Canada

The principle of comparing sealing compatability of pairs of glasses by attaching them together along their longitudinal axis and drawing them out as a double fibre so that distortions caused by unequal coefficients of linear expansions become visible as a curve is well established. This paper is devoted to a qualitative examination of this principle in order to determine the feasibility of applying it as a guide to the selection of suitable glasses for the construction of seals. At the same time the method may be applied to sorting glasses which have been inadvertently mixed together.

In recent years the design and construction of graded seals has received close attention. Their reliability has been improved and they are available in a more compact form than they used to be. When consideration is given to the amount of time and trouble involved in making grades in one's own shop, it may well be that a more logical solution lies in encouraging the purchase of these items. This is analogous to the modern practice of purchasing stopcocks and joints. Only an unfortunate few make such things themselves anymore.

Nevertheless, in spite of the desirability of utilizing commercially available materials, most of us know to our dire cost, that we must often resort to trial and error methods. The problem has been compounded in recent years by the introduction of glass instruments from countries outside of North America. Excellent though many of these products may be, the materials used in their construction do not always possess physical characteristics entirely compatible with those with which we are familiar. As a general rule equipment of this type is purchased without any consideration being given to the problems confronting the glassblower (a fact we are well aware of). Having laboured mightily to construct apparatus out of our own materials—we are set upon with demands that an object the like of which we have never seen before, be sealed forthwith to our systems. Enquiries as to its characteristics produce, at best, a blank stare—"Well it's glass is it not." We may well consider ourselves fortunate if indeed the material does prove to be glass at all.

Excluding the problems which arise due to composition differences, the fundamental factor which determines sealing compatability is the linear coefficient of expansion. For the sake of convenience this physical quantity is expressed as a scale of number multipled by 10^{-7} per degree centigrade. In this way we have at one end fused silica at 5×10^{-7}, 7740 or KG-33 at 32×10^{-7}. There are several coating glasses with higher expansion still but they are of no interest in our field of work.

Most of the glasses used in scientific glass shops are listed below:

	Coeff. of Expansion	*Coeff. of Contraction*
Fused Silica	5×10^{-7}	..
GS1	13	..
GS3	14.5	..
GS4	24.1	..
7740	32.5	35
KG33	32	38
7070	32	39
5420	36	41
3320	40	43
7750	40.5	..
7052	46	53
7050	46	51
EN-1	47	64
7510	50	..
7520	60	..
7530	71	..
7550	79	..
7560	86	..
KG-12	90	103
0080	92	103
0010	93	100
R-6	93	113

I would draw your attention to the definitions in the above list wherein I have included the coefficient of linear contraction for these glasses where this information is available. The difference between the two sets of figures for any given glass is significant. Indeed, it supplies the reason why on some occasions results are not what they should have been. All that goes up does not necessarily come down. Where possible seals should be designed on the basis of the coefficient of linear contraction, provided of course, that you have available to you a sufficiently comprehensive selection of glasses.

No glass shop that I have ever visited has possessed equipment for measuring expansion coefficients. This is understandable because accurate instruments for this type of measurement are expensive and complex, and furthermore the sample has to be in the form of a rod of several inches long. Only on very rare occasions are we fortunate enough to have our suspicious material in this form. However, should difficulties be encountered in sealing a strange glass we need to have some means of comparing sealing compatability with known glasses. The well known double fibre method is sufficient to indicate differences but interpretation of the resulting curve requires considerable experience. The reproducibility of these curves depends upon the amount of control applied when making them. Tests have indicated that there is sufficient similarity between one curve and another to form the basis for identification. The basis of comparison are the amounts of horizontal displacement which take place when double fibers are made up of a control glass and the unknown.

The amount of horizontal displacement is measured on a simple Comparator. (Fig. 1)

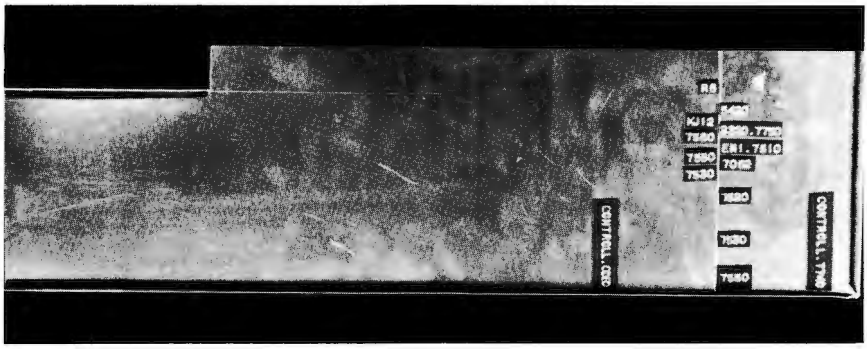

Figure 1

Before discussing that construction of the Comparator, I want to deal with the question of preparation of the sample. It is of the utmost importance that the procedure outlined herein be followed, failure to do so will result in gross errors being introduced into the measurements.

Two controls are used, namely, 7740 or KG-33 for low and intermediate expanding glasses, and 0080 for high expansion glasses. While this process was still in the thinking state I had intended to compare all the glasses against the borosilicate controls. Tests proved that errors magnified rapidly when expansion differences between control and sample exceeded 40×10^{-7}. These errors take two forms, firstly the amount of curvature increases until it becomes almost a portion of a circle—7740/0080 for example results in a quarter circle of about 5″ radius which is useless as a basis for measurement; secondly stresses set up in the cooling fibre cause twisting in some cases as much as 90°, so that again measurements are meaningless. For practical purposes an angular displacement of 20° has been found to be the maximum that may be tolerated, this corresponds roughly to a difference of 40×10^{-7}. Using two controls solves the problem satisfactorily.

The sample and the steps taken to make it are illustrated in Figs. 2 and 3.

The control rods are 4 mm. in diameter. This size is easy to handle, is readily available, and furthermore does not require much sample material. The length of the rod is not critical, but should not be less than 4″ when finished. A rod of the specimen is prepared approximately 4 mm. in diameter, small variations have no noticeable effect on the results. As shown in Fig. 3 it is melted along the edge on one extremity of the control rod to form a double layer about 1¼″ long, a handle is sealed onto the end of the twin rods to facilitate pulling. Care must be taken to lay the specimen along the longitudinal axis of the control. The attaching of the specimen glass is facilitated if it is preheated along its length, so that the control rod does not bend in the process. The foregoing has been found convenient where a 7740/KG-33 control is used. However, the assembly

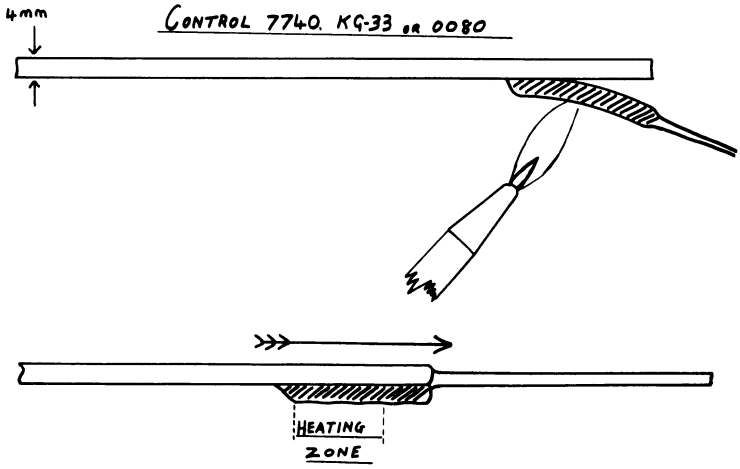

Figure 2

technique is reversed when using a 0080 control because in this case it is usually softer than the specimen. A handle is sealed to the short rod of specimen glass and about 1¼" of control rod is flowed onto it, taking the precautions already mentioned. Having reached this point the region starting at the end of the specimen and the material encompassed by about ¾" of its length is softened and drawn out into a double fibre some 15" in length. Tension is maintained until all the glass has hardened. It is important that twisting be avoided when heating and pulling. For best results heat should be applied preferentially to the harder glass.

Where a relatively large difference in expansion exists, distortion of the thicker regions where the specimen joins the control will be noticed. *Do not* attempt to straighten this out. All the comparisons are based on

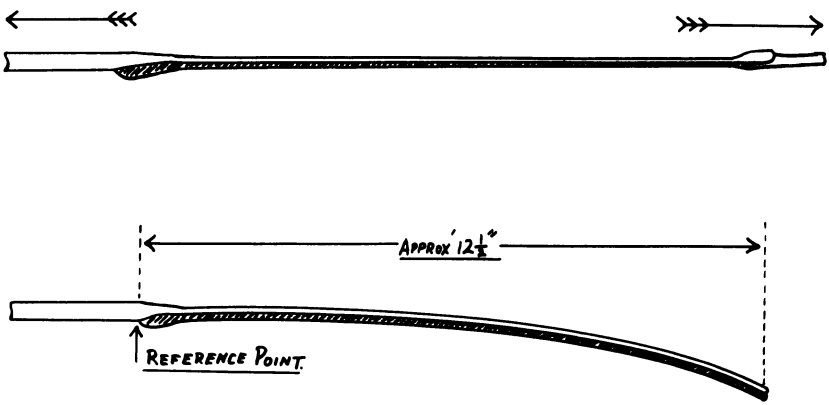

Figure 3

fibre which is pulled straight and allowed to cool under tension. It is for this reason that no attempt has been made to indicate coefficients of expansion on the instrument. Different glass combinations distort so that they lay on a certain portion of the horizontal line indicating that they will seal to the glass indicated thereon. Remember that the instrument is a Comparator—no more, no less.

The construction of the Comparator is simple. A sheet of 20 gauge Aluminum is marked out and folded to the dimensions given in Fig. 4.

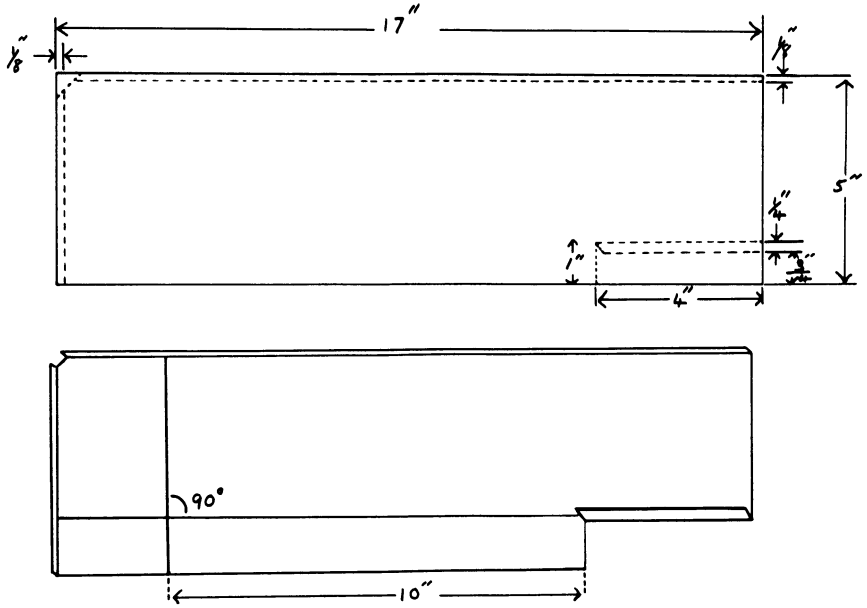

Figure 4

Folds along the right hand side and top serve to stiffen the plate, and consequently are not critical. The important part of the construction is the bending up of the 4" long edge; it should be parallel with the left hand edge of the plate and should itself be flat. This set in the plate is used to locate the control rod. Having completed the folding, the calibration of the Comparator is as follows: a line is scribed exactly 10" from the top of the control guide and parallel with the base. A piece of 4-mm. rod 14" long previously checked for straightness is located so that its end reaches the scribed line and its left side is held firmly against the guide piece, mark where the center of the rod corresponds to the scribed line. Make a second mark at the other end, scribe a line between these marks. This line corresponds to an identical fibre, deviations are marked out along the top line to the left and right. The positions of these marks for glasses measured against the two controls are given in Figs. 5 and 6.

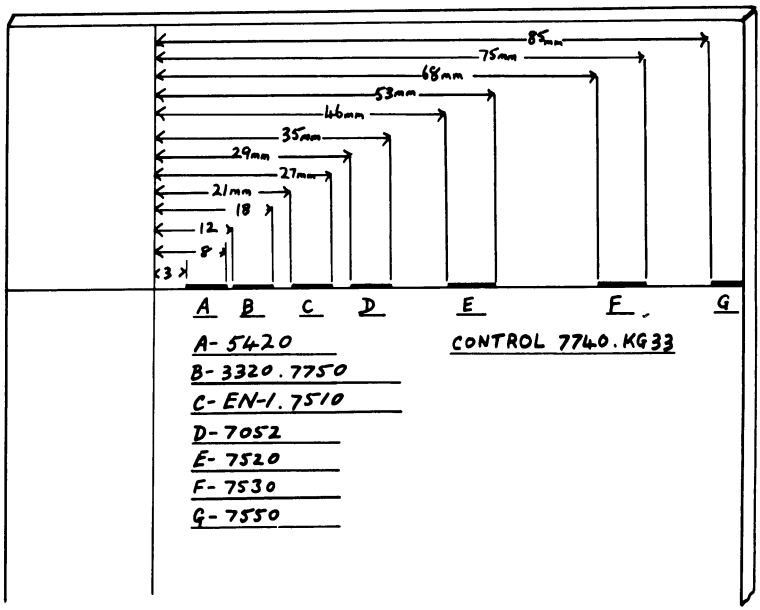

Figure 5

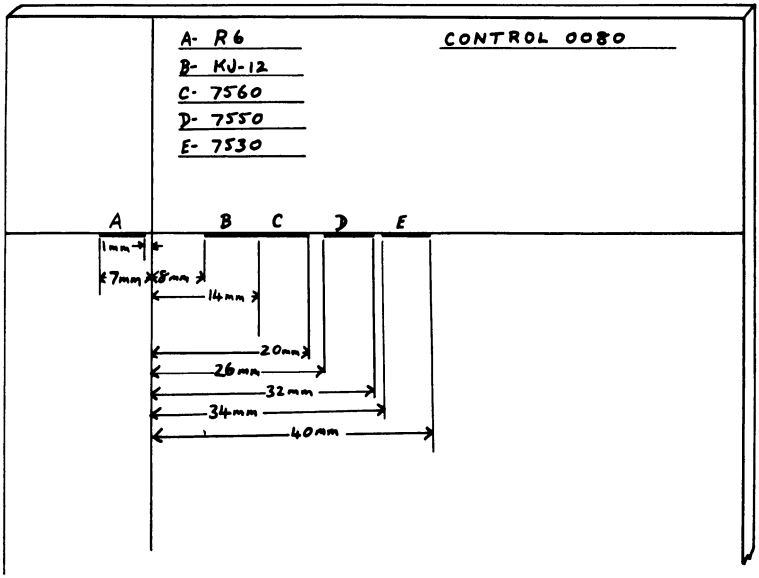

Figure 6

The different sections may be marked, and data relating to the corresponding glasses inserted using metal stamps. This problem has been conveniently solved in my own shops by putting the data on plastic self adhesive lettering tape, cut to the required width and attached.

Having completed the Comparator and prepared 2 or 3 samples, measurements are taken as follows: The sample is adjusted so that total fibre length is about 12½". When using a 7740/KG-33 control the sample fibre should be on the right hand side, and when using 0080 control it should be on the left. The reason for this situation is that in the case of a hard glass control the sample may be expected to have a higher expansion, while with a soft glass control the sample will expand less. The positioning of the sample is illustrated in Fig. 7. The point where the fibre crosses

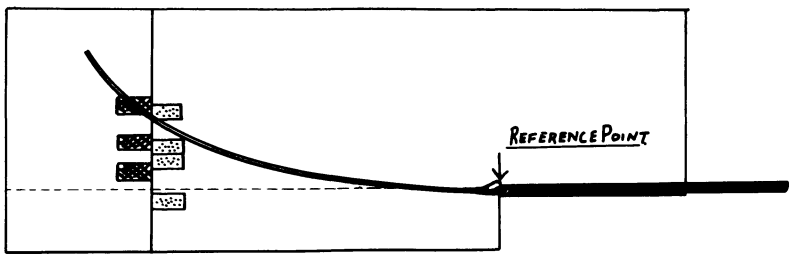

Figure 7

the reference line will correspond to a known glass. The remaining samples are tested and a selection is made on the law of averages. Having thus discovered a glass with similar expansion characteristics to the sample material, it becomes a simple matter to prepare a graded seal compatible to the material used in the system.

I would like to express my thanks to the Department of Chemistry and to Dr. R. G. Barradas for the encouragement to undertake this project, and thank the Corning Glass Co. and Owens Illinois of Canada Ltd. for supplying me with samples of their sealing glasses.

IN ATTENDANCE

The following are on record as having attended the Twelfth Symposium on the Art of Glassblowing held at the Dinkler Plaza Hotel, Atlanta, Georgia, June 28, 29, 30, 1967. As a fully registered participant, these persons are entitled to a copy of the "Proceedings".

REGISTRATION LIST — MEMBERS

Abel, Gustav B. ..... Laser, Inc., 320 Old Briarcliff Rd., Briarcliff Manor, N. Y. 10510

Adkins, M. Wayne ..... Oklahoma State University, Chemistry Dept., Stillwater, Okla. 74075

Airey, Andrew ..... Smith Kline & French, 1530 Spring Garden St., Philadelphia, Pa. 19130

Alexander, J. Allen ..... Alexander Glassblowing Service, Inc., #20 Merwood Dr., Upper Darby, Pa. 19082

Altman, Kenneth B. ..... Dow Chemical Co., Midland, Mich. 48630

Anderson, Robert ..... Crystalite & Glass Corp., 1 Pittsburgh Ave., Nashua, N. H.

Andrews, Frank ..... Wheaton Glass Co., Millville, N. J. 08344

Armstrong, Gilbert ..... The Rauland Corp., 2407 North Ave., Melrose Park, Ill.

Bacon, Dennis ..... Labglass, Inc., P. O. Box 5067, Kingsport, Tenn.

Barr, William E. ..... Gulf Research Center, P. O. Drawer 2038, Pittsburgh, Pa. 15230

Baum, Joseph ..... Sterling-Winthrop Res. Inst., Rensselaer, N. Y. 12144

Benbenek, Jules E. ..... RCA Labs., Princeton, N. J. 08540

Bennett, Charles A. ..... Frankford Arsenal, Philadelphia, Pa. 19137

Bergen, George ..... Goddard Space Flight Ctr. (NASA), Greenbelt, Md.

Bishop, Jim ..... Battelle Memorial Inst., 505 King Ave., Columbus, Ohio 43201

Bivins, John H. ..... Philip Morris Research Ctr., P. O. Box 3-D, Richmond, Va. 23206

Blessing, S. David ..... Univ. of Notre Dame, Notre Dame, Ind. 46635

Blomquist, Theodore V. ..... Harry Diamond Labs., Washington, D. C. 20438

Boehner, George R. ..... Dade Reagents Inc., 1851 Delaware Pkwy., Miami, Fla.

Bolan, T. W. ..... Philips Labs., 345 Scarborough Rd., Briarcliff Manor, N. Y.

Boussert, Christian ..... Purdue University, Chemistry Dept., West Lafayette, Ind.

Brandler, Frank ..... Hoffman-LaRoche Inc., Kingsland St., Nutley, N. J.

Brereton, Walter ..... University of New Brunswick, Fredericton, N. B., Canada

Brewin, Thomas A., Jr. ..... TAB Glass Co., P. O. Box 24, Burlington, Mass.

Buckley, Monroe L. ..... The Aerospace Corp., 2400 El Segundo Blvd., El Segundo, Calif.

Burke, Robert ..... Dade Reagents, Inc., 1851 Delaware Pkwy., Miami, Fla.

Burt, Stewart W. ..... Xerox Corp., 800 Phillips Rd., Webster, N. Y. 14580

Butler, Robert M. ..... Carler Products Corp., 119 Seeley Rd., Syracuse, N. Y. 13224

Buttino, Albert L. ..... Albo Associates, 13 Miles Standish Rd., Schenectady, N. Y. 12306

Byram, Theodore ..... Perkin-Elmer, MS83-Main Ave., Norwalk, Conn.

Cabaniss, Robert H. ..... McDonnell-Douglas Co., Dept. 220, Bldg. 33, Lambert Field, St. Louis, Mo. 63066

Campbell, Clair ..... Battelle Institute, 505 King Ave., Columbus, Ohio 43201

Campbell, Robert G. ..... Food & Drug Directorate, Dept. Nat'l Health & Welfare, Tunney's Pasture, Ottawa 4, Ont., Canada

Campbell, William A. ..... Warner Lambert Research Inst., 170 Tabor Rd., Morris Plains, N. J. 0795

Campbell, William W. ..... Naval Research Labs., Washington, D. C.

Capurso, Maurice ..... ITEK Corporation, 10 Maguire Rd., Lexington, Mass.

Carter, Frank B. ..... MIT Lincoln Lab., 244 Wood St., Lexington, Mass.

Caselli, Michael J. ..... Argonne National Lab., 9700 S. Cass Ave., Argonne, Ill.

Cassidy, C. J. ..... Westinghouse R&D Center, Beulah Rd., Pittsburgh, Pa. 15235

Castle, Francis J. ..... Northern Regional Res. Lab., 1815 N. University, Peoria, Ill.

Chipperfield, Ronald F. ..... Consolidated Vacuum Corp., 1775 Mt. Read Blvd., Rochester, N. Y. 14603

Christie, Henry L. ..... Carleton University, Chemistry Dept., Ottawa 1, Ontario, Canada

Cinalli, D. A. ..... Pan Aura Corp., Crescent Blvd., Pennsauken, N. J.

Clark, Wellman L. ..... Night Vision Labs., Fort Belvoir, Va. 22060
Coleman, David M. ..... Sprague Electric Co., Pembroke Rd., Concord, N. H. 03301
Darsey, James W. ..... Darsey Neon Co., 222 Margaret, Atlanta, Ga. 30315
Deardorff, Keith L. ..... Tektronix Inc., P. O. Box 500, Beaverton, Oreg. 97005
DeCesare, Frank G. ..... Edgewood Arsenal, Edgewood Arsenal, Md. 21010
DeCesare, J. V. ..... Shell Development Co., P. O. Box 481, Houston, Texas 77001
Deery, Edward D. ..... Heights Laboratory Glass Co., 965 Nepperhan Ave., Yonkers, N. Y. 10703
DeFelice, Alex ..... Owens-Illinois, 1700 N. Westwood, Toledo, Ohio
DeLeonibus, Enrico ..... National Bureau of Standards, Gaitherberg, Md. 20760
DeMaria, Vincent C. ..... Thermal American Fused Quartz Co., Montville, N. J. 07866
Deminet, Czeslaw ..... The Boeing Co., Boeing Scientific Res. Labs., P. O. Box 3981, Seattle, Wash. 98124
Dempsey, James ..... I.B.M. Research Lab., Kitchawan, N. Y.
deWilde, Gerrit ..... University of Oregon, Science Bldg., Rm. 40, Eugene, Ore.
DeWolff, W. N. ..... Upjohn Co., 301 Henrietta, Kalamazoo, Mich. 49001
Dixon, Rufus ..... Purdue University, Chemistry Dept., Lafayette, Ind.
Dolenga, Arthur ..... General Motors Research Labs., 12 Mile and Mound Rds., Warren, Mich. 48090
Dombi, Geza ..... National Center for Atmos. Res., P. O. Box 1470, Boulder, Colo. 80302
Domizio, Arthur ..... Geigy Chemical Corp., Saw Mill River Rd., Ardsley, N. Y.
Doody, Thomas J. ..... Argonne National Lab., 9600 Cass Ave., Argonne, Ill.
Dougherty, Richard ..... University of Arkansas, Fayetteville, Ark.
Dunlap, Morris ..... Louisiana State University, Baton Rouge, La.
Eberhart, W. R. ..... University of Windsor, Windsor, Canada
Elsholz, William E. ..... Lawrence Radiation Lab., P. O. Box 808, L 121, Livermore, Calif.
Epperson, Howard L. ..... University of Georgia, Athens, Ga. 30601
Falconer, Dennis G. ..... University of Pittsburgh, School of Medicine, Pittsburgh, Pa. 15213

Fink, Morton ..... U. S. Naval Res. Lab., Washington, D. C. 20390

Fisher, Charles ..... IBM Company, Box 218, Yorktown Heights, N. Y.

Fox, Joseph J. ..... National Institutes of Health, Bethesda, Md.

Fraebel, Godo ..... Georgia Tech., 225 North Ave., Atlanta, Ga. 30332

Frain, Chizuko ..... The Fredericks Co., Huntingdon Valley, Pa. 19006

Franer, William L. ..... Monsanto Res. Corp., Mound Ave., Miamisburg, Ohio

Franzyshen, Frank P., Jr. ... Dow Badische Co., Williamsburg, Va. 23185

French, J. L. A. ..... Dept. of Chem., University of Toronto, Toronto 5, Ont., Canada

Garner, T. H. ..... T. H. Garner Co., Inc., 177 S. Indian Hill, Claremont, Calif. 91711

Glover, John A. ..... Sinclair Res. Inc., Sibley Blvd., Harvey, Ill.

Goar, T. E. ..... Gould Natl. Batteries, Inc., 2630 University Ave., Minneapolis, Minn. 55414

Goldman, David ..... Polytechnic Inst. of Brooklyn, 333 Jay St., Brooklyn, N. Y.

Good, Gordon ..... University of Mass., Goessmann Lab., Amherst, Mass. 01003

Grant, Richard A. ..... University of Dayton, 300 College Park, Dayton, Ohio

Gray, Louis ..... Koppers Co., Inc., 440 College Park Dr., Monroeville, Pa. 15147

Green, Harry F. ..... Lawrence Radiation Lab., University of Calif., P. O. Box 808, Livermore, Calif. 94550

Greiner, Siegfried ..... The Rauland Corp., 2407 North Ave., Melrose Park, Ill. 60160

Grindrod, Richard ..... U.A.C. Research Lab., Silver Lane, E. Hartford, Conn.

Gunther, Adolf P. ..... Stauffer Chemical Co., Dobbs Ferry, N. Y.

Haak, W. H. ..... Purdue University, W. Lafayette, Ind.

Hagedorn, James A. ..... University of Illinois, Chicago Campus, Box 4348, Chicago, Ill. 60680

Henson, Tom ..... Duke University, Dept. Physics, Durham, N. C.

Hewitt, John M. ..... Field Emission Corp., P. O. Box 58, McMinnville, Oreg. 07128

Heyn, Hermann A. ..... Jet Propulsion Lab., 4800 Oak Groove Dr., Pasadena, Calif.

Heyn, Hilmar M. ..... Westinghouse Electric Co., P. O. Box 284, Elmira, N. Y. 14902

Hill, Norman ..... York University, Keele St., Downsview, Ont., Canada

Hines, Olin ..... ITT Industrial Labs., Fort Wayne, Ind.

Horn, Francis ..... Atlantic Richfield, 500 S. Ridgeway Ave., Glenolden, Pa.

Hoyt, Homer L. ..... National Bureau of Standards, Boulder, Colo.

Huth, Harry J. ..... Washington University, School of Medicine, 4550 Scott Ave., St. Louis, Mo. 63110

Hydro, George ..... Naval Ordnance Lab., Code 43, Corona, Calif. 91720

Hydro, John Jr. ..... National Bureau of Standards, Gaithersburg, Md.

Hyland, Edwin J. ..... Northern Illinois University, Dekalb, Ill. 60115

Johnson, W. L. ..... W. L. Johnson Co., 1401 W. Chestnut St., Louisville, Ky.

Johnson, Walter R. ..... Johnson Bros. Inc., N. 10th St., Millville, N. J. 08322

Jones, Charles H. ..... C. H. Jones & Co., 506 Carondelet St., New Orleans, La. 70130

Jonson, Jacob ..... University of Washington, Seattle, Wash. 98105

Jubera, Andrew M. ..... Mellon Institute, 4400 Fifth Ave., Pittsburg, Pa. 15213

Kalbin, Alexander ..... 16000 Jerald Court, Laurel, Md.

Kane, Thomas J. ..... Fisher Scientific Co., 633 Greenwich St., New York, N. Y.

Keene, Melvin E. ..... International Telep. & Teleg., 3301 Electronic Way, West Palm Beach, Fla.

Kelly, John J. ..... George K. Porter, Church Rd., North Wales, Pa.

Kennedy, Frederick G. ..... Texas Instruments Inc., P. O. Box 5936 MS122, Dallas, Texas 75222

Kerr, Ian ..... Owens-Illinois Inc., 50 Belfield Rd., Rexdale, Ont., Canada

Kervitsky, Joseph ..... Night Vision Labs., Fort Belvoir, Va.

Kingsbury, Owen J. Jr. ..... Vanderbilt University, P. O. Box 1521, Station B, Nashville, Tenn. 37203

Kleemichen, Edward ..... The Machlett Labs. Inc., 1063 Hope St., Springdale, Conn. 06979

Kleinert, Richard A. ..... Bendix Research Labs., 10½ Mile at Northwestern, Southfield, Mich.

Knisely, Samuel E. ..... Mobil Oil, Paulsboro, N. J.

Kocsi, Andrew ..... American Standard Research, P. O. Box 2003, New Brunswick, N. J.

Korosi, Mihaly L. ..... State University of N. Y. at Buffalo, Buffalo, New York

Kraus, John R. ..... E. I. du Pont de Nemours & Co., Inc., Wilmington, Del. 19899

Kummer, Fred H. ..... Brookhaven National Lab., Upton, L. I., New York

Laderoute, Alfred G. ..... Olin Mathieson Chemical Corp., 275 Winchester Ave., New Haven, Conn 06504

Last, Homer C. S. ..... 290 Nelson St., Apt. 802, Ottawa 2, Canada

Lees, John ..... Dept. of Physics, University of British Columbia, Vancouver 8, B. C., Canada

Legge, John E. ..... University of Toronto, Physics Dept., Toronto 5, Ont., Canada

Lenzi, David J. ..... U. S. Army Medical Res. Lab., Ft. Knox, Ky.

Leuthner, Herman ..... Vactronic Res. Labs., 83 Main St., Mineola, N. Y. 11501

Lillie, Don ..... Georgia Tech., 225 North Ave., Atlanta, Ga. 30332

Litton, Charles V. ..... Litton Eng. Labs., P. O. Box 949, Grass Valley, Calif. 95945

Litz, Charles M. ..... Aberdeen Proving Ground, Aberdeen, Md.

Logsdon, E. C. ..... University of Florida Eng. College, Gainesville, Fla. 32603

Logsdon, William W. ..... University of Florida Eng. College, Gainesville, Fla. 32603

Lord, Edward E. ..... Thiokol Chemical Corp., 780 N. Clinton Ave., Trenton, N. J. 08638

Lorimer, Robert ..... Hewlett-Packard, 1501 Page Mill Rd., Palo Alto, Calif.

Lutter, Eugene ..... Granville-Phillips Co., P. O. Box 1290, Boulder, Colo. 80302

Mack, Arthur D. ..... Catholic University, Chemistry Dept., Washington, D. C.

Maiolatesi, Elmo ..... U. S. Edgewood Arsenal, Edgewood Arsenal, Md.

Malloy, F. Joseph ..... U. S. Steel Corp., Applied Res. Labs., Monroeville, Pa. 15146

Mateyka, Wilbur C. ..... University of Kentucky, Lexington, Ky.

Mattson, Elmer W. Jr. ..... Oglethorpe College, Box 23, Atlanta, Ga.

Mason, Austin ..... U.S.D.A. Southern Regional Lab., 1100 Robert E. Lee, New Orleans, La. 70124

Mead, Clinton E. ..... I.B.M., Box 218, Yorktown Heights, N. Y.

Merriam, Donald R. ..... Proctor & Gamble, P. O. Box 175, Cincinnati, Ohio 45239

Messick, George E. ..... Hercules Inc. Research Center, Wilmington, Del.

Mezynski, Stanley ..... North Carolina State University, Raleigh, N. C.

Michiel, William ..... Northern Electric Res. & Dev., Ottawa, Ont., Canada

Miller, Robert F. ..... Eli Lilly & Co., P. O. Box 618, Indianapolis, Ind. 46206

Mittelman, Richard ..... Atlas Chemical Industries, Chem. Res. & Dev. Lab., Wilmington, Del.

Moegenbier, Josef ..... The Rauland Corp., 5600 W. Jarvis Ave., Chicago, Ill. 60648

Moody, Donald P. ..... Ames Res. Ctr., N.A.S.A. n-213-7, Moffett Field, Calif. 94080

Moore, Edgar J. ..... Atomic Energy Comm., Pammell Dr., Ames, Iowa 50010

Morgenfruh, Lothar F. ..... Mobil Oil Corp., Central Res. Div. Labs., P. O. Box 1025, Princeton, N. J. 08540

Morris, James F. ..... Northwestern University Tech. Inst., Evanston, Ill. 60201

Nazzewski, Mathew ..... Sprague Electric Co., North Adams, Mass. 01247

Nelson, Eugene ..... Auburn University, Auburn, Ala. 36830

Nilsson, Per ..... Inst. of Marine Science, University of Miami, Rickenbacker C-Way, Miami, Fla. 33148

Norton, Peter ..... Nortel Manufacturing Ltd., 122 Howden Rd., Scarborough, Ont., Canada

O'Brien, Donald M. ..... University of Illinois, Dept. of Chemistry & Chem. Eng., Urbana, Ill.

Old, J. H. ..... University of South California, University Park, Los Angeles, Calif.

Palmaffy, Joseph ..... Westinghouse Electric Co., Bloomfield, N. J. 07003

Panczner, James ..... Owens Illinois Tech. Center, 1700 N. Westwood, Toledo, Ohio

Parillo, Edward V. ..... General Electric-Nela Park, Noble Rd., Cleveland, Ohio 44112

Parks, George E. ..... General Electric Co., P. O. Box 8555, Philadelphia, Pa.

Poole, Richard W. ..... Union Carbide Nuclear ORNL, P. O. Box X, Oak Ridge, Tenn.

Porter, George K. Jr. ..... George K. Porter Plant—Brooks Inst. Div., Church Rd., North Wales, Pa. 19454

Poulsen, Stephen ..... Air Reduction Co. Central Res. Labs., Mountain Ave., Murray Hill, N. J. 07971

Rak, Steve ..... U.B.C., Chemistry Dept., Vancouver 8, B. C., Canada

Reif, Joseph J. ..... W.R.W. Electron Corp., 10 Sagamore Hill Dr., Port Washington, N. Y.

Reynolds, Kevin W. ..... IBM, Bldg. 201-2, Dept. 575, P. O. Box 120, Kingston, N. Y. 12901

Robbins, Trueman Jr. ..... University of Florida, Gainesville, Fla.

Roensch, Arno P. ..... Los Alamos Scientific Lab., P. O. Box 1663, Los Alamos, N. Mex.

Roman, Paul W. ..... Brookhaven National Lab., Upton, L. I., N. Y.

Rosenbaum, Jacob ..... Technion-Israel Inst. of Tech., Haifa, Israel

Rothfels, John ..... U.S. Army, Dugway Proving Ground, Dugway, Utah

Russell, Robert L. ..... Proctor & Gamble, Cincinnati, Ohio

Russler, Ralph H. ..... The Johns Hopkins University, Dept. of Chemistry, Baltimore, Md.

Rybarczyk, John ..... Podbielniak Div. of Dresser, 3201 N. Wolf, Franklin Park, Ill.

Safferling, Ottmar A. ..... Brooklyn College Dept. of Chemistry, Bedfort Ave. & Ave. "H", Brooklyn, N. Y.

Saoner, Joseph L. ..... Wilmad Glass Co., Inc., Route 40 & Oak Rd., Buena, N. J.

Satterlee, Joseph ..... Saegertown Components Div. GTI Corp., Saegertown, Pa.

Schimmelpfennig, George A. . Universal Oil Products Co., 30 Algonquin Rd., Des Plaines, Ill. 60016

Schipmann, Robert H. ..... F.M.C. Corp., Rt. #1, Princeton, N. J.

Schlott, Rudolf W. ..... State University of N. Y. at StonyBrook, StonyBrook, L. I., N. Y.

Schultz, Elwood C. ..... University of North Carolina, Chapel Hill, N. C.

Schumann, Karl ..... Columbia University, Dept. of Chemistry, New York, N. Y.

Searle, Randolph H. ..... E. I. du Pont de Nemours & Co., Inc., Savannah River Lab., Aiken, S. C. 29801

Seckman, Jon W. ..... Lockheed M.S.D., 3251 Hanover, Palo Alto, Calif. 94304

Seer, Andrew E. Jr. ..... Michigan State University, East Lansing, Mich. 48823

Severn, Peter ..... University of Michigan, Ann Arbor, Mich.

Shott, Charles ..... University of Alberta, Edmonton, Alberta, Canada

Simpson, D. L. ..... Motorola Inc. Dept 89681, 5005 E. McDowell Rd., Phoenix, Ariz. 85008

Sites, George A. ..... Air Products & Chemicals Co., Hewes Avenue, Linwood, Pa.

Slominski, Harry J. ..... Union Carbide, Tarrytown, N. Y.

Smart, David R. ..... P. Lorillard Co., Res. Div., 2525 E. Market St., Greensboro, N. C.

Smith, Gordon A. ..... Mayo Clinic, 200 First St., S.W. Rochester, Minn.

Smith, Howe ..... Fischer & Porter Co., County Line Rd., Warminster, Pa.

Smulders, Johannes ..... University of Minnesota, Minneapolis, Minn. 55455

Souza, Raymond L. ..... Corning Glass Works, Medfield, Mass.

Spessard, Lewis ..... Melpar, Inc., 7700 Arlington Blvd., Falls Church, Va.

Squeo, Guy J. ..... American Oil Co., 2500 New York Ave., Whiting, Ind.

Stanley, Russell ..... Pennsylvania Optical Co., 2345 8th St., Reading, Pa.

Stone, Charles L. ..... University Research Glassware Inc., Box 51, Carrboro, N. C.

Stuart, Alexander ..... Simon Fraser University, Burnaby 2, B. C., Canada

Sward, John A. ..... McCoy Electronics, Mt. Holly Springs, Pa. 17065

Szalkowski, Bruno ..... H. S. Martin & Son, 1916 Greenleaf Ave., Evanston, Ill.

Terzich, Dennis ..... Penna. Industrial Chem. Corp., 120 N. State St., Clairton, Pa. 15025

Tobin, Robert B. ..... Mellon Institute, 4400 Fifth Ave., Pittsburgh, Pa.

Tudor, T. E. ..... Tudor Scientific Glass Co., 149 Palmetto Ave., Belvedere, S. C.

Uthman, Paul ..... Alcoa Research, New Kensington, Pa.

Valdna, Rein ..... West Virginia University, Chemistry Dept., Morgantown, W. V.

vanBragt, Herman E. ..... VanBragt Associates Inc., 989 Commercial St., Palo Alto, Calif.

Vandergouw, H. H. ..... Yale University, New Haven, Conn.

VanHespen, C. C. ..... University of Chicago, Kent Chemistry Dept., Chicago, Ill. 60637

Velluto, Anthony J. ..... Ryan, Velluto & Anderson, Inc., 103 First St., Cambridge, Mass. 02141

Villhauer, Kurt ..... Night Vision Lab., Fort Belvoir, Va.

Volk, Rudolph ..... Heights Lab. Glass, Inc., Box 604, Ardsley, N. Y. 10502

Wade, Melvin J. ..... U.S. Army E. Com., Ft. Monmouth, N. J.

Walrod, A. H. ..... Varian Associates, 611 Hansen Way, Palo Alto, Calif. 94303

Wanser, Roland ..... Harvard University, Cambridge, Mass.

Warsewich, Walter W. ..... West Virginia University Medical Ctr., Dept. of Biochem., Morgantown, W. Va.

Watson, Merrill B. ..... University of Alabama, Chemical Dept., Box H, University, Ala.

Weiss, Gunther ..... University of Oregon Medical School, Portland, Oregon

Wesanko, Johnny ..... A.E.C.L., Chalk River, Ontario, Canada

West, Joseph ..... Rosewell Park Memorial Inst., 666 Elm St., Buffalo, N. Y.

Wheaton, Edward C. ..... Wheaton Glass Co., Millville, N. J. 08322

White, Howard F. ..... George K. Porter Plant—Brooks Inst. Div., Church Rd., North Wales, Pa. 19454

Wier, Roy G. ..... Colorado State University, Fort Collins, Colo.

Wilson, Donald M. ..... Beckman, Inst., 2500 Harbor Blvd., Fullerton, Calif.

Wilson, Robert R. ..... National Lead Co. of Ohio, P. O. Box 39158, Cincinnati, Ohio

Wyse, Willard ..... Wyse Glass Specialties, 1722 Wyllys, Midland, Mich.

Younker, Waldo ..... University of Cincinnati, Kettering Lab., Eden & Bethesda Aves., Cincinnati, Ohio 45219

Zavoda, Oliver ..... Brigham Young University, E.S.C. 211, Provo, Utah 84601

Zurek, Tony ..... Chemstrand Research Center, Durham, N. C.

NON-MEMBERS

Anderson, Ron ..... Owens-Illinois, 50 Belfield Rd., Rexdale, Ont., Canada

Bate, William ..... IBM, East Fishkill, N. Y.

Cafferty, James ..... Atomic Energy of Canada, Ld., W.N.B.E., Pinawa, Manitoba, Canada

Celi, Hugo Ismael ..... Universidad De El Salvador C.A., C. Univeritaril Sn. Salvador, El Salvador, C.A.

Conger, Robert J. ..... National Bureau of Standards, Boulder, Colo. 80301

Cooper, Robert F. ..... General Electric Co., 24400 Highland, Cleveland, Ohio 44121

Cuanzon, Jaime B. ..... National Bureau of Stds. Shops Div. 145.06, Bldg. 304, Gaithersburg, Md. 20760

DeAngelis, William M. ..... Daran Products, Inc., 227 Westport Ave., Norwalk, Conn.

DeGroot, Jerry ..... Grand Valley State College, Allendale, Mich.

Dynes, Marvin W. ..... University of Minnesota, Rm. 43-S Physics, Minneapolis, Minn. 55006

Epp, George ..... University of Manitoba, Fort Garry, Winnipeg

Evans, B. ..... National Research Council, 100 Sussex Dr., Ottawa 2, Canada

Finkelstein, Howard ..... Philco-Ford, "C" & Tioga, Philadelphia, Pa.

Fleck, Horst ..... IMR, Princeton Div., P. O. Box 44, Princeton, N. J.

Fortier, W. L. ..... GTI Corporation, Saegertown Components Div., Saegertown, Pa.

Iovine, Michael ..... Louisiana State University of New Orleans, Lakefront, New Orleans, La.

Jones, Lloyd E. Jr. ..... Southwest Ctr. for Advanced Studies, P. O. Box 30365, Dallas, Texas 75230

Kidd, Robert S. ..... General Electric Co., Pinellas Park, Fla.

Kloess, Russel H. ..... Monsanto Co., 800 N. Lindbergh St., St. Louis, Mo.

Kresge, B. ..... National Vacuum Labs., 1125 Longwood Ave., New York, N. Y.

Langley, Russel W. ..... Continental Glass Co., Richland, N. J.

Lejeune, John P. ..... Philco-Ford, Ford Rd., Newport Beach, Calif.

Lowery, Robert M. ..... N.R.L., Washington, D. C.

Lozano, Jorge Alberto ..... Universidad De El Salvador, Ciucad Universidad, Sn. Salvador, C.A.

Luckhurst, Donald ..... Carler Products Corp., 119 Seeley Rd., Syracuse, N. Y.

McCann, Wayne L. ..... Beckman Instruments Inc., 5765 Peachtree Industrial, Chamblee, Ga. 30005

Maiolatesi, F. ..... Johns Hopkins University, Charles & 34th St., Baltimore, Md.

Mathias, Richard ..... Owens-Illinois Corp., 1700 N. Westwood, Toledo, Ohio

Meyer, J. C. ..... University of California, Chemistry Dept., Irvine, Calif. 92664

Meyers, George A. ..... E. G. & G., Inc., Crosby Dr., Bedford, Mass. 01730

O'Brien, Robert E. ..... Hercules Inc., Research Center, Wilmington, Del.

Osty, Julius ..... Argonne National, 9700 S. Cass Ave., Argonne, Ill.

Pelt, Randall ..... Florida State University, Tallahassee, Fla.

Pesce, Paul J. ..... A. A. Pesce Co., 216 Birch St., Kennett Square, Pa. 19348

Petrowski, Charles H. ..... General Electric Co., 2400 Highland Rd., Richmond Heights, Ohio

Ray, James D. ..... WPAF Base, Dayton, Ohio

Ryan, Lawrence W. ..... Mass. Inst. of Tech., 77 Mass. Ave., Cambridge Mass. 02139

Saepoff, G. M. ..... Dynasil Corp. of America, Berlin, N. J.

Sampson, Walter F. ..... MMM Co., 2301 Hudson Rd., St. Paul, Minn. 55119

Schamp, David E. ..... Beckman Instruments Inc., 2500 Harbor Blvd., Fullerton, Calif.

Schmidt, Franklin ..... Lab Glass, Vineland, N. J.

Shepherd, Jerry G. ..... U. S. Bureau of Standards, 28th St., Boulder, Colo.

Sheward, Orus A. Jr. ..... Florida State University, Tallahassee, Fla.

Snidow, Ronald D. ..... Sandia Corp., Dandia Base, Albuquerque, N. M.

Szilagyi, Imre ..... Case Institute of Tech., 10900 Euclid Ave., Cleveland, Ohio

Van Den Hoff, J. ..... National Res. Council, Div. of Pure Chem., 100 Sussex Dr., Ottawa, Canada

Vandenhoff, John M. ..... Brock University, Glenridge Ave., St. Cathrines, Ont., Canada

Wade, Robert E. ..... Avionics Labs.-AFAL-AVTL, Wright-Patterson A.F.B., Dayton, Ohio

Yates, Cleon ..... University of Texas, Physics Dept., Austin, Texas.